

STRATIGRAPHY OF PRE-VASHON QUATERNARY SEDIMENTS  
APPLIED TO THE EVALUATION OF A  
PROPOSED MAJOR TECTONIC STRUCTURE  
IN ISLAND COUNTY, WASHINGTON

Keith L. Stoffel

State of Washington  
Department of Natural Resources  
Division of Geology and Earth Resources  
Olympia, Washington 98504

USGS CONTRACT NO. 14-08-0001-17753  
Supported by the EARTHQUAKE HAZARDS REDUCTION PROGRAM

OPEN-FILE NO.81-292

U.S. Geological Survey  
OPEN FILE REPORT

This report was prepared under contract to the U.S. Geological Survey and has not been reviewed for conformity with USGS editorial standards and stratigraphic nomenclature. Opinions and conclusions expressed herein do not necessarily represent those of the USGS. Any use of trade names is for descriptive purposes only and does not imply endorsement by the USGS.

STRATIGRAPHY OF PRE-VASHON QUATERNARY SEDIMENTS  
APPLIED TO THE EVALUATION OF A  
PROPOSED MAJOR TECTONIC STRUCTURE  
IN ISLAND COUNTY, WASHINGTON

Final Technical Report; submitted April 22, 1980

USGS Grant No. 14-08-0001-17753

Contractor: State of Washington  
Department of Natural Resources  
Division of Geology and Earth Resources  
Olympia, Washington 98504

Principal Investigator: Keith L. Stoffel

USGS Technical Officer: Gordon W. Greene

Effective date of grant: January 9, 1979

Grant expiration date: January 9, 1980

Amount of grant: \$35,931.00

Sponsored by the U.S. Geological Survey

The views and conclusions contained in this document are those of the author and should not be interpreted as necessarily representing the official policies, either expressed or implied, by the U.S. Government.

## TABLE OF CONTENTS

	<u>PAGE</u>
SUMMARY	i
ACKNOWLEDGEMENTS	iv
INTRODUCTION	1
BACKGROUND AND OBJECTIVES	6
FIELD OBSERVATIONS	8
Double Bluff	8
Double Bluff West	10
Double Bluff East	12
Useless Bay East	14
Scatchet Head West	16
Possession Point	18
Conclusions	21
LABORATORY OBSERVATIONS	22
Grain Size Analyses	23
General Discussion	23
Methods Employed	23
Discussion of Results	24
Nonglacial Sediments	24
Glacial Sediments	34
Conclusions	34
Environmental Interpretation	35
Clay Mineralogy	37
General Discussion	37
Identification of Clay Minerals	37
mica	37
smectite	38
chlorite-kaolinite	38
mixed layer clay	38
quartz, feldspar and amphibole	38
Discussion of Results	39
Conclusions	46

	PAGE
Heavy Mineral Analysis	46
Procedure	46
Discussion of Results	47
Conclusions	49
Paleontology	50
REFERENCES CITED	52
APPENDIX A	
Field Observations	55
Geologic section: Double Bluff to Useless Bay	56
Section descriptions	
Double Bluff West (Section 1)	57
Double Bluff East (Section 2)	
Useless Bay East (Section 3)	66
Scatchet Head West (Section 4)	70
Possession Point (Section 5)	75
APPENDIX B	
Grain Size Analyses	78
Mechanical Method (Sieving)	78
Hydrometer Method	81
Grain Size Distribution Curves	85
APPENDIX C	
Clay Mineralogy	140
Procedure	140
Presentation of X-Ray Diffraction Patterns	141
APPENDIX D	
Heavy Mineral Analyses	153
Procedure	153
Presentation of Data	155



## LIST OF FIGURES

	<u>PAGE</u>
FIGURE 1. Map of Puget Sound region showing the locations of structural blocks suggested by Rogers (1970)	2
FIGURE 2. Schematic cross-section of suggested fault-bounded structural blocks	4
FIGURE 3. Pleistocene stratigraphic sequence in Island County, Washington	5
FIGURE 4. Index map of southern Whidbey Island, showing locations of sections	7
FIGURE 5. Plot of inclusive graphic skewness vs. inclusive graphic standard deviation	36
FIGURE 6. Composite X-ray diffraction pattern of sample DBW-D	42
FIGURE 7. Composite X-ray diffraction pattern of sample PP-4A.	44
FIGURE 8. Composite X-ray diffraction pattern of sample DBE-10	45

## LIST OF TABLES

	<u>PAGE</u>
TABLE 1. - Summary of the grain size properties of samples from the Double Bluff West section (Section 1).	25
TABLE 2. - Summary of the grain size properties of samples from the Double Bluff East section (Section 2).	26
TABLE 3. - Summary of the grain size properties of samples from the Useless Bay East section (Section 3).	28
TABLE 4. - Summary of the grain size properties of samples from the Scatchet Head West section (Section 4).	29
TABLE 5. - Summary of the grain size properties of samples from the Possession Point section (Section 5).	30
TABLE 6. - Summary of the grain size properties of non-glacial sand lithologies.	31
TABLE 7. - Summary of the grain size properties of non-glacial silt and clay lithologies.	32
TABLE 8. - Summary of the grain size properties of glacial sediments.	33
TABLE 9. - Summary of the relative abundance of clay mineral groups in Pleistocene sediments on southern Whidbey Island.	40

# LIST OF MAPS

	<u>PAGE</u>
MAP 1. Map showing location of Sections 1 (Double Bluff West) and 2 (Double Bluff East).	9
MAP 2. Map showing location of Section 3 (Useless Bay East).	15
MAP 3. Map showing location of Section 4 (Scatchet Head West).	17
MAP 4. Map showing location of Section 5 (Possession Point).	19

## SUMMARY

The main objective of this project was to conduct a careful stratigraphic study of Quaternary nonglacial sediments on southern Whidbey Island, Washington, in an attempt to "fingerprint" the Whidbey Formation. Once it was defined by sedimentary petrologic criteria, we hoped to be able to correlate outcrops of the Whidbey Formation on Whidbey Island. The ultimate goal was then to correlate stratigraphically equivalent units within the Whidbey Formation across a proposed major tectonic structure, and determine the amount of vertical tectonic movement (if any) along the structure.

Five representative outcrops on southern Whidbey Island, which contain thick sections of nonglacial sediments previously assigned to the Whidbey Formation, were described, measured, and sampled. Descriptions of lithology, texture and sedimentary structures were made. Representative samples of peat and wood fragments were collected and radiocarbon dated. Lab tests performed on the samples include grain size analyses by sieving and hydrometer methods, clay mineralogy by X-ray diffractometry, and heavy mineral analyses by heavy liquids and magnetic separation. The following conclusions were drawn:

1. Correlation of sedimentary units within the Whidbey Formation on southern Whidbey Island cannot be made using field criteria, for the following reasons:
  - a. Numerous erosional unconformities are present which eliminate layer-cake stratigraphy and produce complex stratigraphic relationships.
  - b. Horizontal facies changes are common, which increase the difficulty of characterizing and tracing Whidbey Formation sedimentary units, especially across covered areas.
  - c. There are few distinctive horizons in the Whidbey Formation sediments, and those which are present are only found in single outcrops.

- d. All radiocarbon age dates from the Whidbey Formation are infinite (greater than 40,000 years B.P.), prohibiting correlation of sedimentary units by their age.

Since identification of sedimentary units or sequences of units in the Whidbey Formation is not possible, correlation across the proposed tectonic structures of previous workers cannot be made.

2. Sedimentary units within the Whidbey Formation on southern Whidbey Island cannot be identified by grain-size properties, clay mineralogy, or heavy mineral composition. The sediments are characterized by homogeneous textural and mineralogic compositions, with variations within Whidbey Formation units just as great as between units, and variations within the Whidbey Formation nonglacial sediments just as great as between Whidbey Formation, younger(?) nonglacial, and glacial sediments. The similarity of the properties of nonglacial and glacial sediments on southern Whidbey Island even prohibits characterization of these depositional environments by sedimentary petrologic criteria. Apparently, the homogenization of Pleistocene sediments is the result of continual erosion and reworking of sediments prior to deposition. Since no distinctive units or beds have been identified by laboratory analyses, the horizontal tracing of sedimentary units within the Whidbey Formation over long distances is not possible, and correlation of Whidbey Formation sedimentary units across proposed tectonic structures cannot be made.
3. Three independent lines of evidence suggest that the nonglacial sediments in the Double Bluff East section are significantly younger than the nonglacial sediments at the type locality of the Whidbey Formation (Double Bluff West), and may record deposition during the Olympia Interglaciation:

- a. Double Bluff East nonglacial sediments are separated from Double Bluff West sediments by an erosional unconformity.
  - b. If peat clasts found in the Double Bluff East nonglacial sediments are reworked from Double Bluff West sediments, the Double Bluff East sediments should be substantially younger, since the peats would have to have been compacted and tough to survive reworking without disintegrating. Whether the sediments represent a younger Whidbey Interglaciation age or an Olympia Interglaciation age cannot be determined.
  - c. The Double Bluff East section apparently records an uninterrupted transition from nonglacial to glacial (Fraser glaciation) sedimentation, which suggests a finite age for the Double Bluff East nonglacial sediments. The lack of datable organic material in the nonglacial sediments prohibits verification.
4. Radiocarbon age dates from the base of the Esperance Sand suggest that outwash marking the beginning of the Fraser glaciation in the northern Puget Lowland had reached as far south as southern Whidbey Island by 22,000 to 23,000 years B.P., significantly earlier than previously reported.

### ACKNOWLEDGEMENTS

Thanks are extended to Dr. Dave Pevear of the Department of Geology, Western Washington University, for supplying the X-ray diffraction patterns used in figures 6, 7, and 8. Dr. Robert L. Carr of the Department of Biology, Eastern Washington University, identified the fossil plant seeds. The University of Washington (UW), Beta Analytic, Inc. (UM), and Teledyne Isotopes (I) radiocarbon laboratories provided the radiocarbon dates reported. Keith Kaler provided field and laboratory assistance.

## INTRODUCTION

Puget Sound is a seismically active area. In the last forty years, four damaging earthquakes (magnitudes 5.8 - 7.1) have shaken the region. These four quakes, plus scores of smaller ones, have raised interest in Puget Sound tectonics. Numerous organizations are presently involved in geologic research, attempting to better delineate the tectonic structures proposed by previous investigators. Ultimately, the verification and accurate location of these structures could lead to further studies concerning possible tectonically-induced landsliding, sediment liquefaction, alteration of ground water flow patterns, and sea level changes within Puget Sound.

Numerous investigators have provided evidence for differential crustal movement in the Puget Lowland, with movement continuing well into the Quaternary period. Rogers (1970) interpreted gravity and magnetic data to show the existence of five major structural blocks in the southern part of the Puget Lowland. He called these, from south to north, the Tacoma low, south Kitsap high, Seattle low, Port Gamble-Cathcart high, and Marysville low (figure 1). Rogers interprets these structural units as relatively uplifted and depressed crustal blocks that are bounded either by faults of considerable vertical displacement or by monoclinial folds with steep flexures.

Subsequent workers (personal communications: D. B. Braislin, 1973; D. D. Hastings, 1973; and H. D. Gower, 1978) have incorporated additional data, including seismic reflection, and have somewhat modified the interpretations of Rogers and other earlier investigators (Stuart, 1961; Danes and others, 1965). However, their data continue to support the concept of elevated and depressed structural blocks separated by faults (or possibly monoclinial folds), with major vertical displacements.



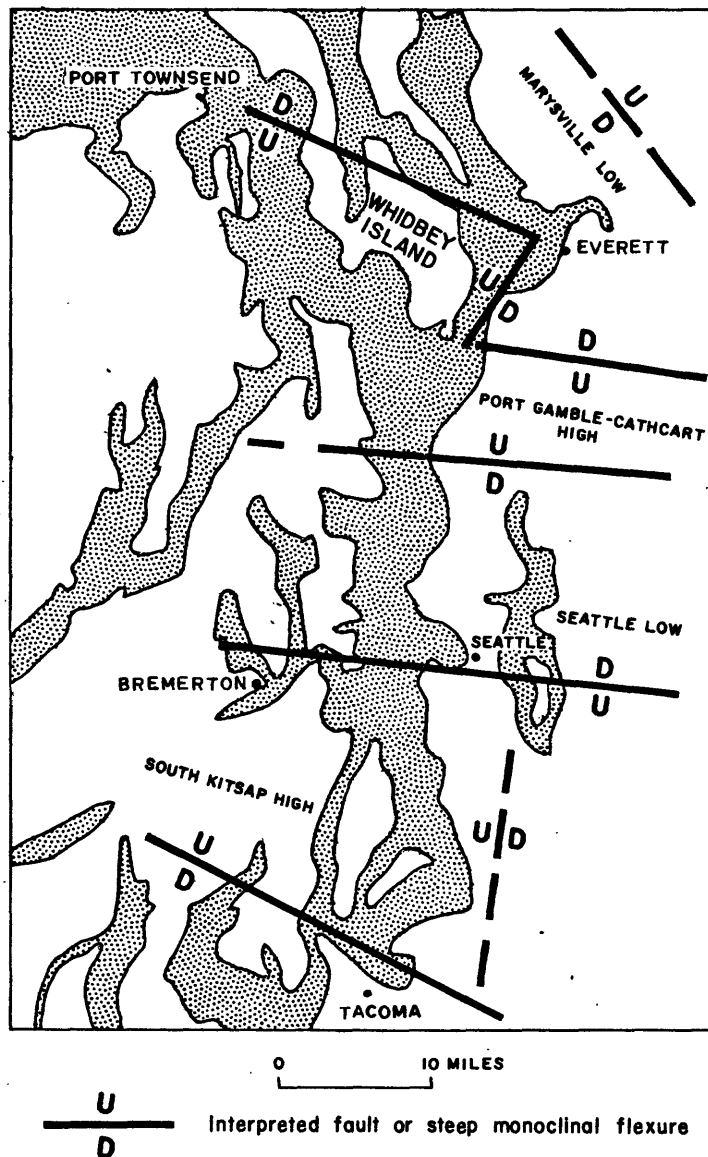


Figure 1. — Map of Puget Sound region showing the locations of structural blocks suggested by Rogers (1970).

Although these inferred structures are not clearly relatable to present seismic activity (Crosson, 1974, 1975; Crosson and Millard, 1975; Crosson and Noson, 1978a, 1978b), the structures have probably been active during the Quaternary period. This is suggested by the difference in thickness of unconsolidated sediments, which conforms in a general way to the inferred pattern of uplifted and downdropped structural blocks (Hall and Othberg, 1974). The uplifted blocks have a thinner cover of unconsolidated sediments than the downdropped blocks (figure 2). Since some, and perhaps most of these sediments are Quaternary, and since they vary in thickness from zero on upthrown blocks to 3,600 feet on downthrown blocks, the basins in which the sediments were deposited must have been subsiding or have subsided at the time of deposition.

When considered over a longer period of time, relative displacements between Puget Lowland crustal blocks may be very large. For example, between the Seattle low and south Kitsap high, one interpretation of gravity and magnetic data suggests relative subsidence of the Seattle low of as much as ten kilometers since the Oligocene (Othberg and Danes, 1975).

Although the Puget Lowland is a tectonically active region, few instances of surface ground breakage by faults are known. Reasons for the lack of recognizable faults may be: (1) vegetation is commonly dense, resulting in poor surface exposure of faults; (2) earthquake foci are usually rather deep (about 50 km) in the Puget Lowland; (3) the Puget Lowland is largely covered by a thick mantle of Quaternary sediments, which absorb movement along bedrock faults before such movement reaches the surface; and/or (4) most of the Lowland is covered by drift deposited during the latest (Fraser) glaciation (10,000 to 20,000 years B.P.), which suggests that evidence of any surface ground breakage that may have occurred prior to the Fraser glaciation has been obliterated by the glacier or covered by its deposits (figure 3).

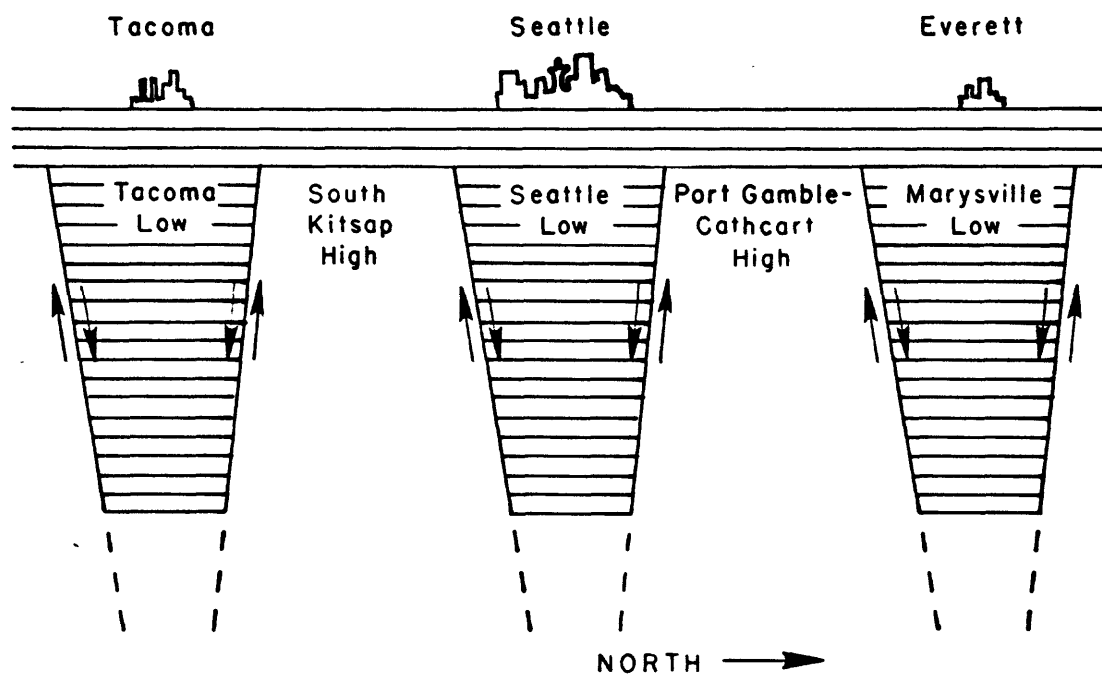


Figure 2. Schematic cross-section of suggested fault-bounded structural blocks. Note thickening of unconsolidated sediments in the structural lows, and thinning of sediments in the structural highs.

QUATERNARY Period	PLEISTOCENE Epoch	GEOLOGIC CLIMATE UNITS	ROCK STRATIGRAPHIC UNITS
		Fraser Glaciation	Sumas Drift Everson Glaciomarine Vashon Till Esperance Sand
		Olympia Interglaciation	Unnamed nonglacial sediments
		Possession Glaciation	Possession Drift
		Whidbey Interglaciation	Whidbey Formation
		Double Bluff Glaciation	Double Bluff Drift

Figure 3. — Pleistocene stratigraphic sequence in Island County, Washington (after Easterbrook, 1968).

## BACKGROUND AND OBJECTIVES

Large scale geologic mapping of Quaternary deposits in the Puget Lowland has been in progress for over fifteen years. Since this previous mapping led to the discovery of very few faults, and since the mapping concentrated on Fraser glaciation deposits, we chose to examine older Quaternary (pre-Fraser) deposits in search of evidence for Quaternary fault activity. If pre-Fraser deposits could be correlated so that thin sedimentary units of the same age could be identified at several localities, then an estimate of the relative uplift (if any) between the correlative sections could be made.

After considering all of the pre-Fraser stratigraphic units present in the area, the Whidbey Formation (figure 3) was chosen for study because it was considered to be the youngest and probably the most widespread nonglacial unit of pre-Fraser age in the northern Puget Lowland. Also, since Whidbey Formation sediments are presumed to have been deposited in a floodplain environment (Easterbrook, 1968), sediments of equivalent age should have been deposited at nearly the same elevation (elevation differences affected only by the stream gradient). Major relative offsets among correlative stratigraphic units could then be attributed to tectonic activity.

Examination of Whidbey Formation sediments was limited to southern Whidbey Island, Island County, Washington (figure 4). Whidbey Island was selected as the study area for the following reasons: (1) most earlier investigators have suggested a major fault(s) trending SE-NW across the island somewhere between Double Bluff and Lake Hancock (figure 4). This structure separates the Port Gamble-Cathcart high from the Marysville low of Rogers (1970) (figure 1); (2) the Whidbey Formation, the major pre-Fraser nonglacial unit found in the sea cliffs of the northern Puget Lowland, is well exposed at its type locality near Double Bluff (Easterbrook, 1968) and fairly well exposed at several other

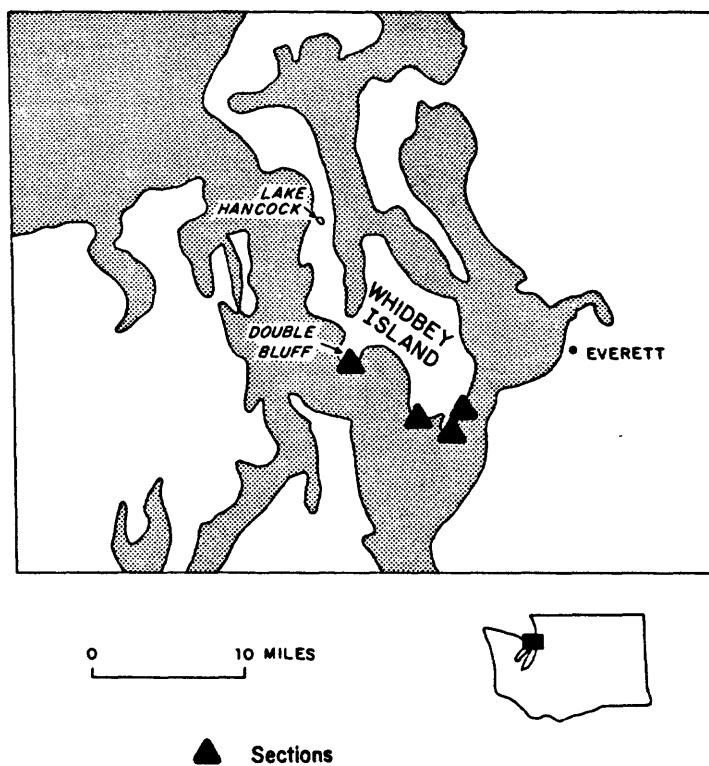


Figure 4. — Index map of southern Whidbey Island, showing locations of sections.

localities on Whidbey Island; and (3) a few outcrops of the Whidbey Formation on Whidbey Island are known to be faulted or folded, although the cause of deformation is unknown.

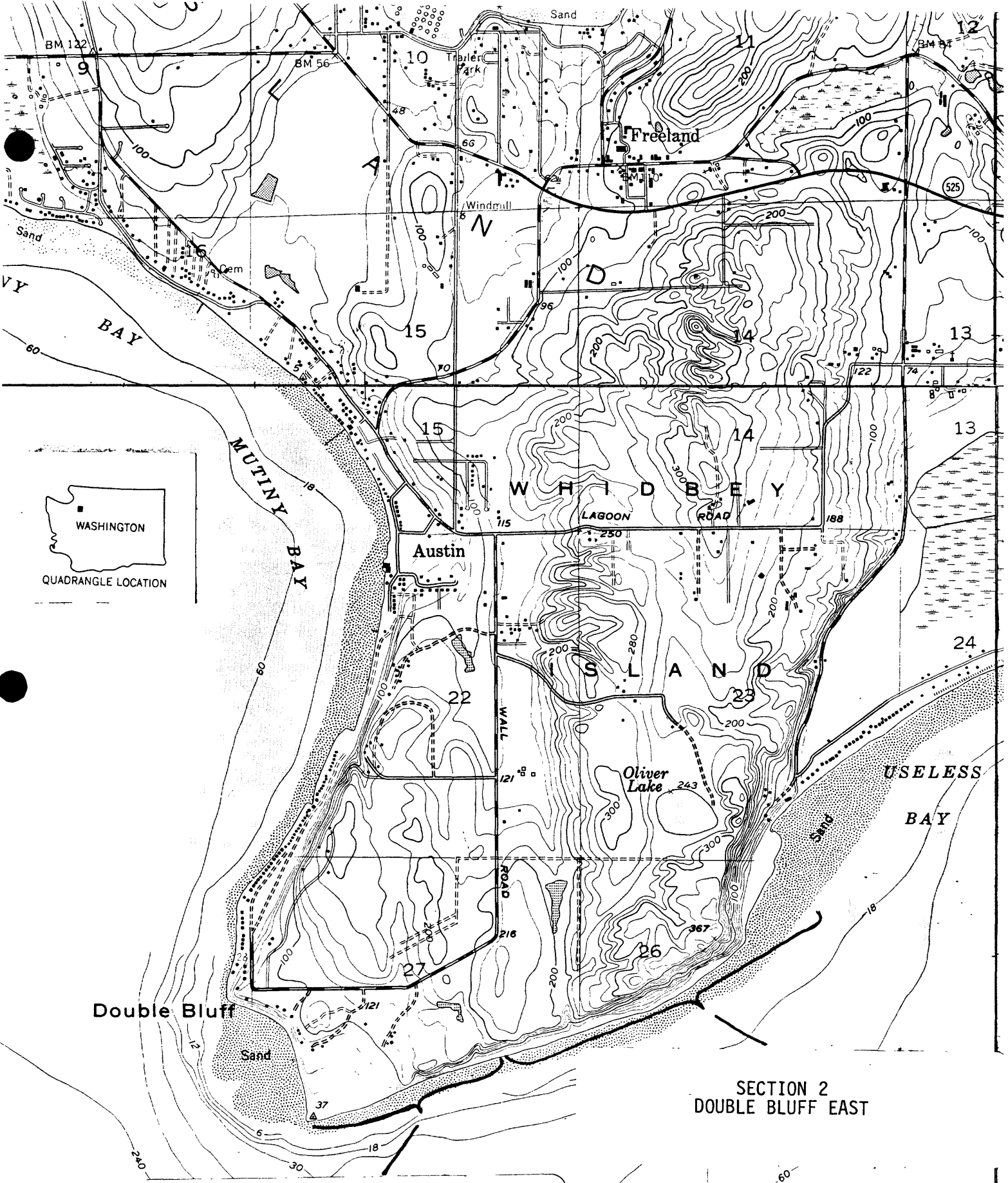
The main objective of this project was to conduct careful stratigraphic studies, in hopes of "fingerprinting" the Whidbey Formation. Once it was defined by sedimentary petrologic criteria, we hoped to be able to correlate outcrops of the Whidbey Formation on Whidbey Island. The ultimate goal of this project was to then correlate stratigraphically equivalent units within the Whidbey Formation across a proposed major tectonic structure and determine the amount of vertical tectonic movement (if any) along the structure.

#### FIELD OBSERVATIONS

Five representative outcrops on southern Whidbey Island, which contain thick sections of nonglacial sediments, were described, measured, and sampled. The nonglacial sediments in all five sections were previously assigned to the Whidbey Formation by Easterbrook (1968, 1969). The following is a summary of the geologic units present at each section. Individual section profiles and descriptions are given in Appendix A. Maps 1 through 4 show the locations of the five sections on southern Whidbey Island.

##### Double Bluff

Detailed field work at the type section of the Whidbey Formation (Double Bluff) has revealed complex relationships among the nonglacial sedimentary units. An erosional unconformity near the west end of the Double Bluff section separates, older, fine-grained nonglacial sediments from younger, coarser-grained sediments (see Geologic Section: Double Bluff to Useless Bay, in Appendix A). Detailed profiles and descriptions of the sections west (Section 1) and east (Section 2) of the unconformity are given in Appendix A, and are summarized here.



SECTION 1  
DOUBLE BLUFF WEST

SECTION 2  
DOUBLE BLUFF EAST



## Double Bluff West (Section 1)

The lower half of this section (units 0 through 7) is characterized by interbedded dark gray silts and a wide variety of oxidized sand and gravel lithologies. Many of the silt beds contain such an abundance of organic fragments within the silt matrix that they are fibrous in nature and highly resistant to weathering. Thin peat beds occur within units 3 and 5. Cross-beds indicative of deposition by westerly flowing water are common in the sand beds. A two foot thick peat bed approximately 60 feet above sea level separates the lower sand and silt units from the upper clay-rich unit 8. This upper unit is composed of massive to rhythmically bedded silty clays with very thin ( $\frac{1}{2}$  inch) fine-grained sand beds and a few thin peat beds.

As previously mentioned, the horizontal units of the Double Bluff West section are abruptly terminated by an erosional unconformity (Appendix A, Geologic Section). Sometime after deposition of the Double Bluff West sediments, the east end was eroded away, apparently by stream (or possibly ice?) activity. Erosion was probably the result of the lateral migration of a stream channel across a floodplain, either of Whidbey Interglaciation age or younger. Alternatively, the erosion could be the result of ice scouring during a glaciation (Possession) after the Whidbey Interglaciation, and before another nonglacial episode, but no evidence for glacial activity has yet been found. Angular blocks of silt, clay, peat and stone within a sand and gravel matrix provide evidence for colluvial activity along the unconformable surface following erosion. Deposition of younger horizontally-bedded silts and sands (Section 2) followed the colluvial activity.

A radiocarbon date of greater than 40,000 years B.P. (DBW #1 (UM-1753) was obtained from the thick peat bed between units 7 and 8, indicating that at

least the lower half of the section is beyond the limit of radiocarbon dating.<sup>1/</sup>

---

<sup>1/</sup>Six finite radiocarbon age dates\* reported in the semi-annual report (dated by the Beta Analytic lab) are apparently erroneous. Since the finite ages of these samples would have called for major revisions in the presently-accepted Pleistocene stratigraphy of the Puget Lowland, duplicate samples were sent to the University of Washington radiocarbon lab for verification. All dates reported by UW were infinite (greater than 40,000 years B.P.). In an attempt to resolve this dating conflict, additional organic material for radiocarbon dates UBE#1 and UBE#2 was sent to the Beta Analytic lab for redating. The results of the Beta Analytic lab dating of samples UBE#1 and UBE#2 are:

UBE#1

original reported date: 28,910 +690/-630 years B.P.  
recheck (weak acid pretreatment only): 35,750 +2030/-1620  
recheck (weak acid & alkali treatment): 26,840 +/- 1500 years B.P.

UBE#2

original reported date: 29,325 +550/-520 years B.P.  
recheck (weak acid pretreatment only): 40,545 +2420/-1860 years B.P.  
recheck (weak acid & alkali pretreatment): greater than 40,000 years B.P.

The Beta Analytic laboratory has not been able to reproduce any of their original reported finite dates. The dates they report vary, with no apparent connection to the type of pretreatment used.

Since the University of Washington radiocarbon lab has been able to reproduce their infinite age dates, they are assumed to be correct and are used in this report. John Erickson of the UW lab, and Jerry Stipp of the Beta Analytic lab, are presently working together in an attempt to resolve the remaining conflicting dates.

---

* <u>UBE#1</u>	28,910	+690/-630
<u>UBE#5</u>	39,210	+1730/-1420
<u>PP#1</u>	30,470	+1650/-1370

<u>UBE#2</u>	29,325	+550/-520
<u>SH#1</u>	29,130	+570/-530
<u>DBW#1</u>	43,250	+3200/-2280

## Double Bluff East (Section 2)

Deposition of the sediments composing the Double Bluff East section occurred after the erosional downcutting through the older Double Bluff West sediments. The sediments of the Double Bluff East section are dominated by grayish-brown, fine to medium-grained sands (Section 2, Appendix A). Occasional beds of dark gray silt and clay (Units F and H) are interbedded with the sands.

The nonglacial sediments of the Double Bluff East section (units G through K) differ from those of the Double Bluff West section by the dominance of sand lithologies and lack of peat horizons at Double Bluff East. Although numerous peat clasts are found in the Double Bluff East sediments (especially abundant in unit K), these clasts are detrital and record erosion and reworking of peat beds from older sediments. If these peat clasts are reworked from the Double Bluff West sediments, it would imply that the Double Bluff East sediments are significantly younger, since the peats would have to have been tough and compacted to survive reworking without disintegrating. Whether they would represent a younger Whidbey Interglaciation age or an Olympia Interglaciation age cannot be determined.

Cross-beds and ripple marks indicative of westerly flow are common in the grayish-brown medium-grained sands at the base of the section (unit K). All other nonglacial sand units in Section 2 are characterized by horizontal lamination, making reconstruction of flow direction impossible.

A unique, traceable horizon with the nonglacial sediments is located near the top of unit I. Approximately two feet below the contact with unit H, a 2 to 4 inch thick horizon of peat, wood, coal and pumice fragments is interbedded with moderately well sorted, horizontally laminated, medium-grained sand. This single thin bed is horizontally continuous for many hundreds of feet, while no

similar horizons occur above or below it. The significance of this association of low-density fragments is unknown, but apparently represents a single "geologic event", such as a flood.

Large-scale deformation features make two other units of the Double Bluff East section distinctive —units H and J. Deformation in unit H varies from broad, open folds to small diapiric structures, while flame structures up to 40 feet in height characterize unit J. When not deformed, these units are similar to other nonglacial sediments and are not distinctive. Although the causes of deformation are unknown, poorly sorted silty sand beds (probably deposited rapidly and containing abundant water) at the top of each unit could have resulted in the overloading of the sediments below, triggering deformation. Seismic liquefaction is an alternative explanation for the deformation in unit J, but sufficient evidence has not been found to support this hypothesis.

Units A through F of the Double Bluff East section record deposition during the Fraser glaciation (figure 3). Unit F is characterized by extremely fine rhythmic bedding of silt and clay (varves), which is the basis for interpreting the unit as glaciolacustrine in origin. Units C, D and E are outwash sands and gravels with cross-beds indicative of south-flowing streams. This Esperance Sand (figure 3) sequence coarsens upward, as the ice front approached from the north. Units A and B record deposition either by or in close proximity to Fraser ice.

No evidence of erosion or weathering is found between the nonglacial and glacial sediments of the Double Bluff East section. This apparent uninterrupted transition from nonglacial to glacial conditions implies that the nonglacial sediments are finite in age and may represent the Olympia Interglaciation (figure 3). If so, the nonglacial sediments in the Double Bluff East section would be significantly younger than those of the Double Bluff West section.

Radiocarbon dates of  $22,210 \pm 530$  years B.P. (I-10, 801) and  $23,600 \pm 275$  years B.P. (UM-1752) were obtained from wood fragments at the top of unit F (radiocarbon sample DBE #1). These dates represent the maximum age of the end of the glaciolacustrine conditions and the beginning of deposition of glacial outwash on southern Whidbey Island. Since the contact between units E and F is transitional, with no evidence of erosion or weathering, it is believed that a continuous deposition of sediments occurred. Therefore, unless the wood fragments are reworked from older sediments, these dates record earlier Fraser glaciation conditions in the Puget Lowland than has been previously reported.

#### Useless Bay East (Section 3)

Sediments of the Useless Bay East section are dominated by dark gray silts and clays interbedded with oxidized, medium-grained sands and gravels (Section 3, Appendix A). Cross-bedding in the coarse-grained horizons is generally indicative of west-northwesterly flowing streams. Cut-and-fill structures are also common, especially in the lower portion of unit 2.

The only distinctive horizon in the nonglacial sediments of the Useless Bay East section is the dark greenish-gray clay bed at the base of unit 3. However, exposures just south of the measured Useless Bay East section contain numerous similar greenish clay beds. The greenish beds are apparently the result of groundwater alteration of clay beds under reducing conditions.

The silt and clay-rich horizons in units 1, 4 and 5 contain abundant organic fragments and numerous peat beds. Four of the thicker beds in units 4 and 5 were radiocarbon dated: UBE #1 (UW-578), UBE #2 (UW-579), UBE #3 (UW-580), and UBE #5 (UM-1747). All four reported dates are  $> 40,000$  years B.P.



SECTION 3  
USELESS BAY EAST



QUADRANGLE LOCATION

The Double Bluff section illustrates one of the main obstacles to correlation of Quaternary sediments in the Puget Lowland—localized cut-and-fill, which eliminates layer-cake stratigraphy and produces complex stratigraphic relationships. The Useless Bay East section illustrates another major obstacle to Quaternary correlation—horizontal facies changes. Within only a few hundred feet, facies changes make recognition of Useless Bay East units 1 through 6 difficult. The presence of the peats as marker beds helps correlation attempts, but once the peat beds lens out, tracing of units becomes extremely difficult. Facies changes in covered areas between measured sections further complicates correlation attempts.

#### Scatchet Head West (Section 4)

Two hundred to two hundred fifty feet of nonglacial sediments are exposed at the Scatchet Head West section (Section 4, Appendix A). The lowermost 175 feet (units G through N) is composed of dark gray silt and clay interbedded with a wide variety of oxidized sand and gravel lithologies, similar to the sediments at the Double Bluff West and Useless Bay East sections. These lower nonglacial sediments also contain laterally-continuous peat beds. Cut-and-fill structures and cross-beds with east-southeast dips are common in the sands and gravels.

Approximately 175 feet above sea level, a recessed bench in the bluff marks a compositional change in the bluff material. Twenty-five to seventy-five feet of grayish-brown, horizontally-laminated, medium-grained sands are interbedded with thin beds of clayey silt (units A through F). The sediments composing this portion of the bluff are very similar to units G through I of the Double Bluff East section. However, their base is nearly 100 feet higher at Useless Bay East than at Double Bluff East.

P

U

G

E

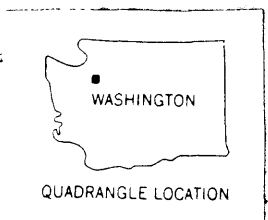
T

VANCOUVER - SEATTLE

FERRY

1ST AND C

SECTION 4  
SCATCHET HEAD WEST



S

O

#3

U  
-17-

Indian Point

Maxwelton

Dave Mackie  
County Park

Tide Gate

MUD

SEA LEVEL

4

9

16

Scal



At the top of the bluff, an erosional contact separates cross-bedded gravelly sands from the horizontally-laminated sands. These gray, cobbly and gravelly sands, which contain cross-beds indicative of south-flowing streams, are probably a glacial outwash unit associated with the Fraser glaciation (figure 3).

Three radiocarbon age dates have been obtained from organic material collected at the Scatchet Head West section. Two major peat beds were dated: SH #1 (UW-575) from unit J gave a greater than 40,000 year B.P. date, and a greater than 41,500 year B.P. date was obtained from SH #2 (UM-1742) in unit G. The third radiocarbon date ( $> 39,600$ ) is from tiny organic fragments dispersed in a sandy silt bed of unit F (SHW #3 (UM-1750)). The two dates from the peat beds indicate that the lowermost 175 feet (units G through N) of the Scatchet Head West section is older than the limit of conventional radiocarbon dating. The age of the upper sediments (units A through F) is less certain. If the tiny organic fragments which were dated are reworked from older peat beds, these upper units could be finite in age.

#### Possession Point (Section 5)

Seventy-five to one hundred feet of nonglacial sediments are sandwiched between two gray silty clay till units at the Possession Point Section (Section 5, Appendix A). The upper till has been assigned to the Possession glaciation and the lower drift unit to the Double Bluff glaciation by Easterbrook (1968).

Since the outcrop of the Whidbey Formation at the Possession Point section is largely covered with grass, which prohibits the horizontal tracing of units over long distances, Section 5 in Appendix A is a composite description of numerous small exposures at Possession Point. Dark brownish-gray clay and silt



beds, fine to medium-grained sands, and poorly sorted cobbly gravel are the dominant lithologies of the nonglacial sediments at Possession Point.

Massive to rhythmically bedded gray silty clays and thin sand beds in the upper portion of unit A are similar to those in unit 8 of the Whidbey Formation at the Double Bluff West section. Covered sections obscure stratigraphic relationships, but the rapid horizontal disappearance of the poorly sorted cobbly gravel of unit B suggests it is a channel deposit. Cross-bedding in many of the sand beds of unit C is indicative of east to southeasterly stream flow during deposition.

One unique lithologic horizon occurs in the Possession Point section near the top of unit C in the Whidbey Formation. Approximately one foot below the base of the gravel of unit B, a 1 to 2 inch thick pinkish-colored fine-grained silt is present, which can be traced horizontally for about one hundred feet before the section becomes covered. The combination of a floury texture and distinctive clay mineralogic composition (see discussion on clay mineralogy) indicate that it is, at least in part, a volcanic ash. No similar bed has been found in any of the other sections studied in this project, which eliminated the possibility of using it as a correlative tool.

Organic material from two units in the Possession Point section was collected for radiocarbon dating. PP #1 (UW-576), a portion of a peat clast incorporated into the base of the Possession drift, and PP #2 (UW-577), an organic silt near the top of the Whidbey Formation, both dated greater than 40,000 years B.P. The dates show that the Whidbey Formation nonglacial sediments at Possession Point are greater than 40,000 years old. They do not, however, provide evidence for the age of the overlying Possession drift, since the dated peat fragment was probably derived from older nonglacial sediments.

## Conclusions

1. Correlation of sedimentary units within the Whidbey Formation on southern Whidbey Island cannot be made using field criteria, for the following reasons:
  - A. Numerous erosional unconformities are present which eliminate layer-cake stratigraphy and produce complex stratigraphic relationships.
  - B. Horizontal facies changes are common, which increase the difficulty of characterizing and tracing Whidbey Formation sedimentary units, especially across covered areas.
  - C. There are few distinctive horizons in the Whidbey Formation sediments, and those which are present are only found in single outcrops.
  - D. All radiocarbon age dates from the Whidbey Formation are infinite (greater than 40,000 years B.P.), prohibiting correlation of sedimentary units by their age.

Since identification of sedimentary units or sequences of units in the Whidbey Formation is not possible, correlation across the proposed tectonic structures of previous workers cannot be made.

2. Three independent lines of evidence suggest that the nonglacial sediments in the Double Bluff East section are significantly younger than the nonglacial sediments at the type locality of the Whidbey Formation (Double Bluff West), and may record deposition during the Olympia Interglaciation (figure 3).
  - A. Double Bluff East nonglacial sediments are separated from Double Bluff West sediments by an erosional unconformity.

- B. If peat clasts found in the Double Bluff East nonglacial sediments are reworked from Double Bluff West sediments, the Double Bluff East sediments should be substantially younger, since the peats would have to have been compacted and tough to survive reworking without disintegrating. Whether the sediments represent a younger Whidbey Interglaciation age or an Olympia Interglaciation age cannot be determined.
- C. The Double Bluff East section apparently records an uninterrupted transition from nonglacial to glacial (Fraser glaciation) sedimentation, which suggests a finite age for the Double Bluff East nonglacial sediments. The lack of datable organic material in the nonglacial sediments prohibits verification.

Nonglacial sediments with sedimentary structures and textures similar to those in the Double Bluff East section also occur in the upper portion of the Scatchet Head West section (Section 4), but the lack of organic material there also prohibits age dating.

- 3. Radiocarbon age dates from the base of the Esperance Sand (figure 3) suggest that outwash marking the beginning of the Fraser glaciation in the northern Puget Lowland had reached as far south as southern Whidbey Island by 22,000 to 23,000 years B.P., significantly earlier than previously reported.

#### LABORATORY OBSERVATIONS

Sedimentary petrologic lab procedures were employed in this study, in an attempt to "fingerprint" Pleistocene stratigraphic units on southern Whidbey Island. Lab tests performed include grain-size analyses by sieving and hydrometer methods, clay mineralogy by X-ray diffractometry, and heavy mineral

analyses by heavy liquids and magnetic separation. In addition, laboratory treatment of numerous samples was performed to isolate microfossils for paleontological studies. A discussion of results for each lab method employed is offered in this chapter. The lab procedures employed, and the sample data produced, are given in the appendices.

## Grain-Size Analyses

### General Discussion

Grain-size analyses are performed to aid in reconstructing the geologic environment of deposition of sediments. By determining the relative abundance of the different grain sizes which compose the sample, values of mean grain size and sorting are obtained. Mean size of the constituent clastic particles reflects the amount of available energy imparted in the sediments, as well as the grain sizes of available clastic particles in the source material. The sorting of sediments also aids in environmental reconstruction, reflecting the size range of material supplied to the environment, the type of deposition of the particles (whether rapid dumping or continuous reworking), and the current characteristics of the transporting medium. Integration of mean grain size and sorting, along with stratigraphic relationships, the study of sedimentary structures, and detailed field mapping then permits an interpretation of the sedimentary environment of deposition of the sediments.

### Methods Employed

Fifty-two samples of Quaternary sediments were analyzed for their grain-size properties. Analyses were performed by sieve and hydrometer methods, as outlined in Appendix B. The sieve and hydrometer data produced were then used to draw a grain-size distribution curve for each sample. Sieve and hydro-

meter data and grain-size distribution curves for each sample are included in Appendix B.

Statistical measures are used to quantitatively describe certain features of grain-size distribution curves. In this way, sets of sediment samples can be evaluated and quantitatively compared. In this study, statistical parameters were calculated from each grain-size distribution curve. These parameters include texture, the relative proportions of gravel, sand, silt, and clay in a sample; graphic mean, the best graphic measure of the average grain size of a sediment sample; inclusive graphic standard deviation, a measure of the uniformity or sorting of a sediment; and inclusive graphic skewness, a measure of the amount of excess fine material (+ skewness) or excess coarse material (- skewness) present in the sediment sample. Equations used in the calculations of the statistical parameters are given in Appendix B.

## Discussion of Results

Statistical parameters calculated from the grain-size distribution curves are listed in Tables 1 through 5. The 52 samples for which statistical parameters are given represent both nonglacial and glacial environments of deposition in the Puget Lowland. Based upon field observations, 44 of the samples are believed to represent nonglacial sediment deposition, and 8 to represent glacial deposition. The following is a summary of the grain-size properties of the samples analyzed:

Nonglacial sediments — Representative samples from each measured section of Whidbey Formation nonglacial sediments were analyzed for their grain size properties. For comparison of their calculated statistical parameters, these nonglacial sediments are subdivided into two groups: sand lithologies (Table 6) and silt-clay lithologies (Table 7).

TABLE 1. - Summary of the grain size properties of samples from the Double Bluff West section (Section 1).

Environment	Sample	Texture	(Graphic mean) M <sub>Z</sub>	(sorting) σ <sub>I</sub> or σ <sub>G</sub>	S <sub>KI</sub> (skewness)
glaciolacustrine?	DBW-A	0/6-74-20	6.75φ (fine silt)	1.71φ (poorly sorted)	-0.03 (near symmetrical)
non-glacial	DBW-B	0/1-82-17	6.26φ (fine silt)	1.85φ (poorly sorted)	+0.44 (strongly fine skewed)
non-glacial	DBW-C	0/20-60-20	5.95φ (medium silt)	2.27φ (very poorly sorted)	+0.32 (strongly fine skewed)
non-glacial	DBW-D	0/10-57-33	7.06φ (very fine silt)	2.20φ (very poorly sorted)	+0.04 (near symmetrical)
non-glacial	DBW-E	0/0-40-60	8.43φ (clay)	1.13φ (poorly sorted)	+0.24 (fine skewed)
non-glacial	DBW-1	0/100-0-0	1.46φ (medium sand)	0.52φ, (moderately well sorted)	+0.15 (fine skewed)
non-glacial	DBW-2	0/99-1-0	2.00φ (medium-fine sand)	0.60φ (moderately well sorted)	0.00 (symmetrical)
non-glacial	DBW-3	0/99-1-0	1.25φ (medium sand)	0.56φ (moderately well sorted)	+0.007 (near symmetrical)
non-glacial	DBW-4	7/99-1-0	1.26φ (medium sand)	1.16φ (poorly sorted)	-0.25 (coarse skewed)



Table 2. - Summary of the grain size properties of samples from the Double Bluff West section (Section 1).

Environment	Sample	Texture	(Graphic mean) M <sub>Z</sub>	(Sorting) σ <sub>I</sub> or σ <sub>G</sub>	S <sub>KI</sub> (skewness)
glacial out-wash	DBE-6	0/99-1-0	1.95φ (medium sand)	0.45φ (well sorted)	+0.20 (fine skewed)
glacial out-wash	DBE-7	0/93-7-0	3.05φ (very fine sand)	0.52φ (moderately well sorted)	+0.29 (fine skewed)
glacial out-wash	DBE-8	0/7-90-3	5.73φ (medium silt)	1.20φ (poorly sorted)	-0.04 (near symmetrical)
glaciolacustrine?	DBE-10	0/11-41-48	7.93φ (very fine silt)	2.60φ (very poorly sorted)	+0.08 (near symmetrical)
glaciolacustrine?	DBE-11	0/15-28-57	7.93φ (very fine silt)	3.35φ (very poorly sorted)	-0.16 (coarse skewed)
non-glacial	DBE-12	0/99-1-0	1.35φ (medium sand)	0.51φ (moderately well sorted)	+0.12 (fine skewed)
non-glacial	DBE-13A	0/94-6-0	3.13φ (very fine sand)	0.50φ (moderately well sorted)	+0.06 (near symmetrical)
non-glacial	DBE-13B	0/0-54-46	8.13φ (clay)	2.30φ (very poorly sorted)	+0.22 (fine skewed)
non-glacial	DBE-13C	0/3-91-6	5.36φ (medium silt)	0.57φ (moderately well sorted)	+0.62 (strongly fine skewed)
glacial till?	DBE-13D	12/39-47-14	3.73φ (very fine sand)	3.90φ (very poorly sorted)	-0.18 (coarse skewed)
non-glacial	DBE-14	0/98-2-0	2.06φ (fine sand)	0.52φ (moderately well sorted)	+0.15 (fine skewed)

TABLE 2. - Continued

non-glacial	DBE-15	0/99-1-0	1.20 $\phi$ (medium sand)	0.79 $\phi$ (moderately sorted)	+0.04 (near symmetrical)
non-glacial	DBE-16	0/97-3-0	1.33 $\phi$ (medium sand)	0.85 $\phi$ (moderately sorted)	+0.29 (fine skewed)
non-glacial	DBE-18	0/99-1-0	1.73 $\phi$ (medium sand)	0.47 $\phi$ (well sorted)	+0.41 (strongly fine skewed)

TABLE 3. - Summary of the grain size properties of samples from the Useless Bay East section (Section 2).

Environment	Sample	Texture	(Graphic mean) $M_z$	(Sorting) $\sigma_1$ or $\sigma_g$	$S_{K_I}$ (skewness)
non-glacial	UBE-2	0/31-49-20	5.66 $\phi$ (medium silt)	2.45 $\phi$ (very poorly sorted)	+0.21 (fine skewed)
non-glacial	UBE-3	0/99-1-0	1.90 $\phi$ (medium sand)	0.61 $\phi$ (moderately well sorted)	-0.02 (near symmetrical)
non-glacial	UBE-4	0/99-1-0	2.06 $\phi$ (fine sand)	0.52 $\phi$ (moderately well sorted)	+0.15 (fine skewed)
non-glacial	UBE-5	0/16-68-16	5.96 $\phi$ (medium silt)	2.13 $\phi$ (very poorly sorted)	+0.06 (near symmetrical)
non-glacial	UBE-6	0/10-70-20	6.36 $\phi$ (fine silt)	2.15 $\phi$ (very poorly sorted)	+0.26 (fine skewed)
non-glacial	UBE-7	0/9-46-45	7.73 $\phi$ (very fine silt)	2.65 $\phi$ (very poorly sorted)	+0.02 (near symmetrical)
non-glacial	UBE-8	0/98-2-0	1.90 $\phi$ (medium sand)	0.76 $\phi$ (moderately sorted)	+0.02 (near symmetrical)
non-glacial	UBE-9	0/10-80-10	5.96 $\phi$ (medium silt)	1.50 $\phi$ (poorly sorted)	+0.06 (near symmetrical)
non-glacial	UBE-10	2/100-0-0	1.80 $\phi$ (medium sand)	0.65 $\phi$ (moderately well sorted)	-0.02 (near symmetrical)
non-glacial	UBE-11	0/2-60-38	7.76 $\phi$ (very fine silt)	1.61 $\phi$ (poorly sorted)	+0.19 (fine skewed)
non-glacial	UBE-12	0/98-2-0	2.43 $\phi$ (fine sand)	0.49 $\phi$ (well sorted)	+0.22 (fine skewed)

TABLE 4. - Summary of the grain size properties of samples from the Scatchet Head West section (Section 4).

Environment	Sample	Texture	(Graphic mean) M <sub>Z</sub>	(Sorting) σ <sub>I</sub> or σ <sub>G</sub>	S <sub>KI</sub> (skewness)
non-glacial	SHW-A	0/90-10-0	3.22φ (very fine sand)	0.63φ (moderately well sorted)	+0.40 (strongly fine skewed)
non-glacial	SHW-B	0/96-4-0	2.70φ (fine sand)	0.49φ (well sorted)	+0.24 (fine skewed)
non-glacial	SHW-C	0/2-50-48	8.33φ (clay)	2.30φ (very poorly sorted)	+0.28 (fine skewed)
non-glacial	SHW-0	0/100-0-0	1.73φ (medium sand)	0.54φ (moderately well sorted)	+0.04 (near symmetrical)
non-glacial	SHW-1	0/3-77-20	6.50φ (fine silt)	1.95φ (poorly sorted)	+0.35 (strongly fine skewed)
non-glacial	SHW-2	0/88-11-1	3.14φ (very fine sand)	0.87φ (moderately sorted)	+0.61 (strongly fine skewed)
non-glacial	SHW-3	0/0-29-71	9.03φ (clay)	1.65φ (poorly sorted)	+0.03 (near symmetrical)
non-glacial	SHW-4	0/3-71-26	7.22φ (very fine silt)	2.90φ (very poorly sorted)	+0.50 (strongly fine skewed)
non-glacial	SHW-5	0/97-3-0	2.20φ (fine sand)	0.50φ (well sorted)	+0.37 (strongly fine skewed)
non-glacial	SHW-6	0.95-5-0	2.80φ (fine sand)	0.52φ (moderately well sorted)	+0.07 (near symmetrical)

TABLE 5. - Summary of the grain size properties of samples from the Possession Point section (Section 5).

Environment	Sample	Texture	(Graphic mean) $M_z$	(Sorting) $\sigma_I$ or $\sigma_G$	$S_{K_I}$ (skewness)
non-glacial	PP-1	0/87-11-2	3.36 $\phi$ (very fine sand)	0.70 $\phi$ (moderately well sorted)	+0.43 (strongly fine skewed)
non-glacial	PP-2	0/20-69-11	5.73 $\phi$ (medium silt)	2.13 $\phi$ (very poorly sorted)	-0.05 (near symmetrical)
non-glacial	PP-2A	0/7-44-49	8.13 $\phi$ (clay)	1.75 $\phi$ (poorly sorted)	+0.20 (fine skewed)
non-glacial	PP-3	0/9-53-38	7.32 $\phi$ (very fine silt)	2.45 $\phi$ (very poorly sorted)	+0.04 (near symmetrical)
non-glacial	PP-4	0/90-8-2	3.23 $\phi$ (very fine sand)	0.53 $\phi$ (moderately well sorted)	+0.21 (fine skewed)
non-glacial	PP-4A	0/0-46-54	8.33 $\phi$ (clay)	1.67 $\phi$ (poorly sorted)	+0.11 (fine skewed)
non-glacial	PP-5	0/2-89-9	6.33 $\phi$ (fine silt)	1.16 $\phi$ (poorly sorted)	+0.12 (fine skewed)
non-glacial	pp-6A	27/57-29-14	1.93 $\phi$ (medium sand)	4.66 $\phi$ (extremely poorly sorted)	-0.22 (coarse skewed)

TABLE 6. - Summary of the grain size properties of non-glacial sand lithologies.

Section	Sample	Texture	(Graphic mean) $M_z$	(sorting) $\sigma_I$	$S_{K_I}$ (skewness)
1	DBW-1	0/100-0-0	1.460	0.520	+0.15
	DBW-2	0/99-1-0	2.000	0.600	0.00
	DBW-3	0/99-1-0	1.250	0.560	+0.07
	DBW-4	7/99-1-0	1.260	1.160	-0.25
2	DBE-12	0/99-1-0	1.350	0.510	+0.12
	DBE-13a	0/94-6-0	3.130	0.500	+0.06
	DBE-14	0/98-2-0	2.060	0.520	+0.15
	DBE-15	0/99-1-0	1.200	0.790	+0.04
	DBE-16	0/97-3-0	1.330	0.850	+0.29
	DBE-18	0/99-1-0	1.730	0.470	+0.41
3	UBE-3	0/99-1-0	1.900	0.610	-0.02
	UBE-4	0/99-1-0	2.060	0.520	+0.15
	UBE-8	0/98-2-0	1.900	0.760	+0.02
	UBE-10	2/100-0-0	1.800	0.650	-0.02
	UBE-12	0/98-2-0	2.430	0.490	+0.22
4	SHW-A	0/90-10-0	3.220	0.630	+0.40
	SHW-B	0/96-4-0	2.700	0.490	+0.24
	SHW-0	0/100-0-0	1.730	0.540	+0.04
	SHW-2	0/88-11-1	3.140	0.870	+0.61
	SHW-5	0/97-3-0	2.200	0.500	+0.37
	SHW-6	0/95-5-0	2.800	0.520	+0.07
5	PP-1	0/87-11-2	3.360	0.700	+0.43
	PP-4	0/90-8-2	3.230	0.530	+0.21

TABLE 7. - Summary of the grain size properties of non-glacial silt and clay lithologies.

Section	Sample	Texture	(Graphic mean) M <sub>Z</sub>	(Sorting) σ <sub>I</sub>	S <sub>KI</sub> (skewness)
1	DBW-B	0/1-32-17	6.260	1.350	+0.44
	DBW-C	0/20-60-20	5.950	2.270	+0.32
	DBW-D	0/10-57-33	7.060	2.200	+0.04
	DBW-E	0/1-40-60	8.430	1.130	+0.24
2	DBE-13b	0/0-54-46	3.130	2.300	+0.22
	DBE-13c	0/3-91-6	5.360	0.570	+0.62
3	UBE-2	0/31-49-20	5.660	2.450	+0.21
	UBE-5	0/16-63-16	5.960	2.130	+0.06
	UBE-6	0/10-70-20	6.360	2.150	+0.26
	UBE-7	0/9-46-45	7.730	2.650	+0.02
	UBE-9	0/10-80-10	5.960	1.500	+0.06
	UBE-11	0/2-60-38	7.760	1.610	+0.19
4	SHW-C	0/2-50-48	8.330	2.300	+0.28
	SHW-1	0/3-77-20	6.500	1.950	+0.35
	SHW-3	0/0-29-71	9.030	1.650	+0.03
	SHW-4	0/3-71-26	7.220	2.900	+0.50
5	PP-2	0/20-69-11	5.730	2.130	-0.05
	PP-2A	0/7-44-49	8.130	1.750	+0.20
	PP-3	0/9-53-38	7.320	2.450	+0.04
	PP-4A	0/0-46-54	8.330	1.670	+0.11
	PP-5	0/2-89-9	6.330	1.160	+0.12

TABLE 3. - Summary of the grain size properties of glacial sediments.

Section	Sample	Texture	(Graphic mean) $M_z$	(sorting) $\sigma_I$	$S_{K_I}$ (skewness)
<u>Sand Lithologies (glaciofluvial)</u>					
2	DBE-6	0/99-1-0	1.950	0.450	+0.20
	DBE-7	0/93-7-0	3.050	0.520	+0.29
<u>Silt-Clay Lithologies (glaciolacustrine)</u>					
1	DBW-A	0/6-74-20	6.750	1.710	-0.03
2	DBE-8	0/7-90-3	5.730	1.200	-0.04
	DBE-10	0/11-41-48	7.930	2.600	+0.08
	DBE-11	0/15-23-57	7.930	3.350	-0.16
<u>Glacial Till</u>					
5	PP-6A	27/57-29-14	1.930	4.660	-0.22
2	DBE-13D	12/39-47-14	3.730	3.900	-0.18



Texture of the nonglacial sands analyzed ranges from pure sand (0/100-0-0) to slightly silty sand (0/87-11-2), with the majority of the samples composed of 95-100% sand-size particles. Graphic means range from 1.20  $\phi$  (medium sand) to 3.36  $\phi$  (very fine sand), but the average grain size of the majority of the samples falls within the medium to fine-grained sand sizes. These nonglacial sands are characteristically moderately well-sorted, with the degree of sorting varying from moderate (0.79  $\phi$ ) to well (0.47  $\phi$ ). Positive skewness is also a characteristic of the nonglacial sands, reflecting excess fines in the sediment distribution.

Although the textures of the nonglacial silt-clay lithologies range from silt loam (0/21-49-20) to silty clay (0/0-29-71), most samples contain little to no sand and are mixtures of various proportions of silt and clay. Correspondingly, the measured graphic mean values range from 5.36  $\phi$  (medium silt) to 9.03  $\phi$  (clay).  $\sigma_1$  values indicate that all of the samples are poorly to very poorly sorted, and positive skewness values are generally indicative of excess fines present in these silt-clay lithologies.

Glacial sediments — The grain-size properties of the glacial sediments analyzed are given in Table 8. Comparison with Tables 6 and 7 illustrates the marked similarities of the glacial sands and silty clays with the nonglacial sediments. The properties of the glacial tills are quite obviously different from any of the sand and silty-clay lithologies. The tills are characterized by loamy textures, extremely poor sorting, and coarse skewness.

## Conclusions

The grain-size properties of sediments from each measured section illustrate the overall uniform composition of the Whidbey Formation nonglacial sediments.

Because of this homogeneity, lithologically distinct beds or units within the Whidbey Formation cannot be identified. The range of textural variation within a unit is just as great as the variation between units, and textural variation within a section of nonglacial sediments is just as great as between measured sections. Likewise, the marked similarity of glacial and nonglacial sediments on southern Whidbey Island prohibits characterization of these depositional environments by grain-size properties. Apparently, the homogenization of Pleistocene sediments is the result of continual erosion and reworking of sediments prior to deposition.

Since lithologic characterization of Pleistocene stratigraphic units cannot be made on southern Whidbey Island, grain-size analyses cannot be used as a correlative tool. Therefore, correlation of the Whidbey Formation across the proposed tectonic structure cannot be attempted.

### Environmental Interpretation

Friedman (1967) outlined textural criteria which can be used to reconstruct the depositional environment of sands. Since one of the goals of this study was to characterize the Whidbey Formation, reconstruction of the depositional environment of the Whidbey sediments was desirable. Previous workers (Easterbrook, 1968; Hansen and Mackin, 1949) have suggested that the Whidbey sediments were deposited in a fluvial environment.

A plot comparing statistical parameters for the purpose of distinguishing depositional environments is shown in figure 5. The graph plots inclusive graphic skewness ( $SK_I$ ) against inclusive graphic standard deviation ( $\sigma'_I$ ) to differentiate beach and river sands. The boundary separating river and beach sediments was adapted from Friedman (1967).

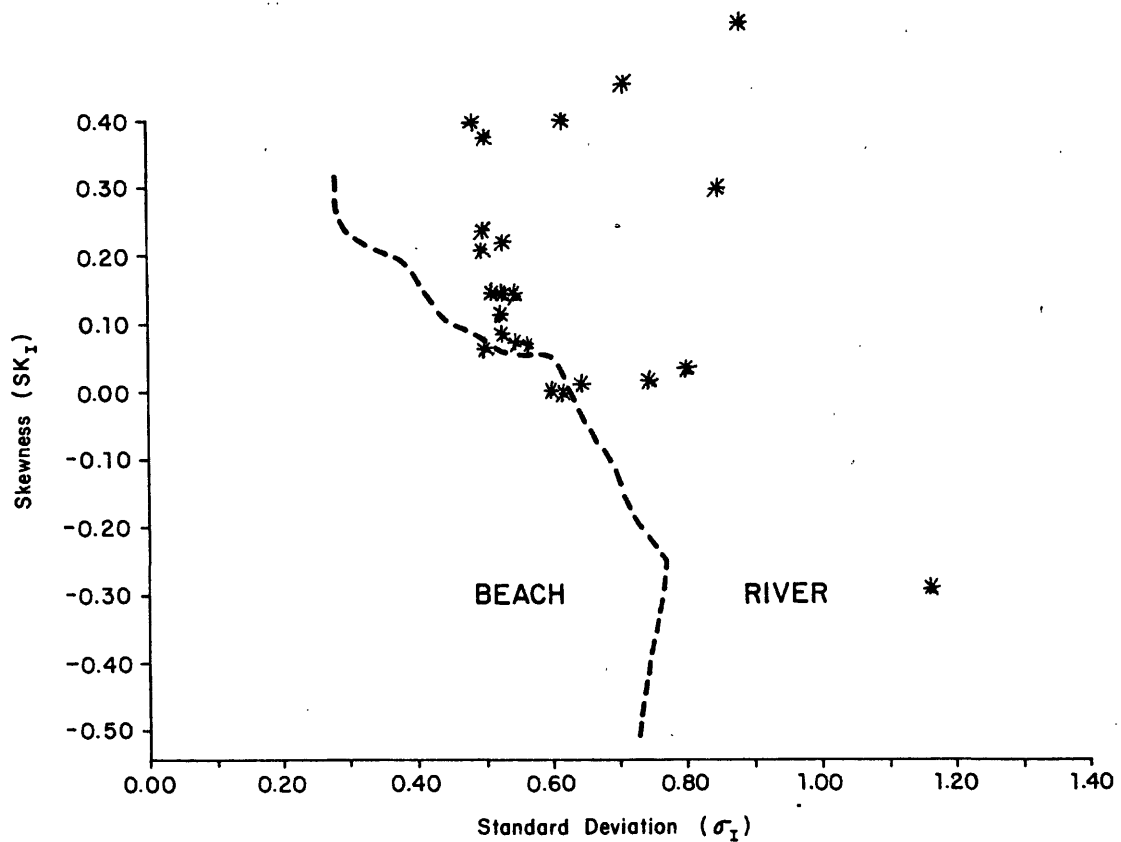


Figure 5. — Plot of Inclusive Graphic Skewness ( $SK_I$ ) vs. Inclusive Graphic Standard Deviation ( $\sigma_I$ ) for the samples listed in Table 1. The dashed line, which differentiates beach from river environments, is adapted from Friedman (1967).

The twenty-three samples listed in Table 6 are plotted in figure 5. The combination of positive skewness values and high standard deviation (sorting) values places the majority of the samples in Friedman's river category. The clustering of points in the river category substantiates previous workers' suggestions of a fluvial depositional environment for the Whidbey Formation sediments.

## Clay Mineralogy

### General Discussion

X-ray diffraction of clay minerals was used in an attempt to "fingerprint" Pleistocene stratigraphic units on southern Whidbey Island. It was anticipated that stratigraphic units of different ages or depositional environments might contain distinctive mineralogies, resulting from incorporation of unique sediments or bedrock types.

### Identification of Clay Minerals

Clay minerals present in the Quaternary sediments on southern Whidbey Island include mica, smectite, chlorite, kaolinite and mixed layer clay. Quartz, feldspar, and amphibole are also present in the diffraction patterns of the  $< 2$  micron clay fraction. The following criteria were used to identify the minerals (after Carroll, 1970):

Mica — Mica is characterized by an integral series of  $00l$  spacings, with the major peak, (001), at  $10\overset{0}{\text{\AA}}$ . The (002) peak at  $5\overset{0}{\text{\AA}}$  is less prominent, but easily recognizable. The (003) peak at  $3.33\overset{0}{\text{\AA}}$  merges with a quartz peak, making recognition difficult. Mica is used here as a general term for a mica-like clay of uncertain species and undetermined polymorph. Glycolation has no effect on the mica structure, thus diffraction peaks remain unchanged.

Smectite — Untreated smectite is characterized by an irrational sequence of reflections, with the (001) peak at approximately  $15\overset{\circ}{\text{\AA}}$ . Upon glycolation, the (001) peak swells to  $17\overset{\circ}{\text{\AA}}$ , and the reflections become rational and uniformly spaced. The (001) peak at  $17\overset{\circ}{\text{\AA}}$  is broad and the most intense. The (002) and (004) peaks are recognized by very broad and subdued peaks, around  $8.5\overset{\circ}{\text{\AA}}$  and  $4.25\overset{\circ}{\text{\AA}}$  respectively.

Chlorite-Kaolinite — Chlorite is characterized by diffraction peaks with an integral series of basal spacings from  $14\overset{\circ}{\text{\AA}}$  (001). The first five orders are recognized, with (002) at  $7\overset{\circ}{\text{\AA}}$ , (003) at  $4.72\overset{\circ}{\text{\AA}}$ , (004) at  $3.54\overset{\circ}{\text{\AA}}$ , and (005) at  $2.83\overset{\circ}{\text{\AA}}$ . Kaolinite is characterized by a series of diffraction peaks with (001) at  $7\overset{\circ}{\text{\AA}}$  and (002) at  $3.5\overset{\circ}{\text{\AA}}$ . Since the first and second order kaolinite peaks merge with the second and fourth order chlorite peaks, recognition of the presence of kaolinite is complicated. In this study, kaolinite peaks were not differentiated from chlorite peaks, and their presence is designated chlorite-kaolinite in the discussion which follows. Chlorite-kaolinite is not affected by glycolation and the diffraction pattern remains unchanged.

Mixed Layer Clay — The mixed layer clay in the sediments on southern Whidbey Island is characterized by a broad basal peak between  $10\overset{\circ}{\text{\AA}}$  and  $14\overset{\circ}{\text{\AA}}$  on the air dry-oriented diffraction patterns, where it is somewhat masked by first order peaks of both chlorite and mica. This broad peak disappears upon glycolation, and is presumably hidden behind the  $17\overset{\circ}{\text{\AA}}$  smectite peak. Heat treatment to  $550^{\circ}\text{C}$  results in the reappearance of the broad peak between  $10\overset{\circ}{\text{\AA}}$  and  $14\overset{\circ}{\text{\AA}}$ . These reactions to glycolation and heat treatment suggest a mixed-layer composition of chlorite-smectite.

Quartz, Feldspar, and Amphibole — Quartz is characterized by peaks at  $4.26\overset{\circ}{\text{\AA}}$  (100) and  $3.34\overset{\circ}{\text{\AA}}$  (101), the latter merging with the third order mica peak.

Feldspar is characterized by a peak at 3.19-3.23<sup>0</sup>A, dependent upon the variety of feldspar present. The largest amphibole peak occurs at 8.51<sup>0</sup>A.

## Discussion of Results

Twenty-four samples of Pleistocene sediments have been analyzed for their less than 2 micron clay mineralogic compositions (Table 9). Twenty-one of the samples are from nonglacial sediments of the Whidbey Formation, and three samples are from glacial sediments. Glycolated X-ray diffraction patterns for all samples are presented in Appendix C.

Clay minerals present in the nonglacial sediments include chlorite-kaolinite, mica, smectite and mixed-layer clay. Nonclay minerals present are quartz, feldspar, and amphibole. Figure 6 is a composite of the air dry-oriented, glycolated, 300<sup>0</sup>C, and 550<sup>0</sup>C diffraction patterns for nonglacial sample DBW-D, from which these interpretations were made.

Table 9 lists the relative abundance of each clay mineral group present. Letter symbols indicate the relative quantities; M, major; c, common; m, minor; N, none. Since the quantities were estimated from the glycolated diffraction patterns only (Appendix C), smectite and mixed-layer clay could not be differentiated and are grouped together, as are chlorite and kaolinite.

It is evident from Table 9 that the clay mineral composition of the Whidbey Formation nonglacial sediments is highly variable. These results agree with the conclusions reached by Mullineaux (1967). Within single exposures of nonglacial sedimentary units, compositional variations occur from bed to bed. The differences are apparently not related to other physical properties, such as texture or permeability.

These compositional differences appear to either represent variations in detrital materials supplied during deposition, or to record differences in post-

TABLE 9. - Summary of the relative abundance of clay mineral groups in Pleistocene sediments on southern Whidbey Island.

Environment	Sample	Chlorite- Kaolinite	Mica	Smectite- Mixed layer	Quartz	Feldspar	Amphibote
ng (nonglacial)	DBW-A	C	C	C	m	m	N
ng	DBW-B	C	C	M	m	m	m
ng	DBW-C	C	C	m	m	m	N
ng	DBW-D	C	M	m	m	m	N
ng	DBW-E	C	C	C	m	m	N
*glaciolacustrine	DBE-10	C	C	C	m	m	m
ng	DBE-13b	C	C	M	m	m	N
ng	DBE-13C	C	C	C	m	m	N
ng	DBE-17	C	C	M	m	m	m
ng	UBE-2	C	C	C	m	m	m
ng	UBE-5	C	C	C	m	m	m
ng	UBE-7	C	N	M	m	m	m
ng	UBE-9	N	N	M	N	N	N
ng	UBE-11	C	m	C	m	m	m
ng	SHW-0	C	C	C	m	m	N
ng	SHW-1	C	N	C	m	m	m
ng	SHW-3	C	C	C	m	m	N
ng	SHW-4A	C	C	C	m	m	m
ng	PP-2	C	m	C	m	m	N
ng	PP-2A	m	m	M	m	m	N
ng	PP-3	C	C	C	m	m	N
volcanic ash	PP-4A	N	m	m	m	M	m

TABLE 9. - Continued

*glacial till	PP-6	c	c	c	m	m	m
*glacial till	PP-6A	c	c	c	m	m	m

c = common

m = minor

M = major

N = none



depositional alteration. The clay minerals which compose the Pleistocene sediments on southern Whidbey Island are also common bedrock constituents in the Cascade Range to the east and north. Chlorite, kaolinite, and mica are especially common in the bedrock, and their presence in the Puget Lowland sediments undoubtedly records mechanical weathering and transport prior to deposition. While smectite and mixed-layer clay are also reported as detrital components from Cascade bedrock, they probably also record chemical alteration during or after deposition of the Pleistocene sediments. The degree of mineralogical variation attributable to mechanical vs. chemical weathering is ill-defined.

Only one bed with a unique mineralogic composition was found in the non-glacial sediments. Sample PP-4A, from a pinkish-colored silt horizon near the top of Unit C at Possession Point, is composed chiefly of plagioclase feldspar, with minor amounts of amphibole, mica, smectite, and mixed-layer clay (figure 7). This composition is similar to the mineralogic composition of volcanic ash deposits in the Cascade Range (Pevear, personal communication, 1979), and combined with its floury texture suggest this horizon is at least in part, volcanic ash. No other similar horizon was found in any of the five sections studied.

The clay mineralogic compositions of the three glacial clays analyzed (DBE-10, PP-6, PP-6A) are not distinguishable from the Whidbey Formation non-glacial sediments. Figure 8 is a composite of the air dry-oriented, glycolated 300°C, and 550°C diffraction patterns for glaciolacustrine sample DBE-10. The composition of the glacial clays is similar to that of some of the nonglacial clays, and variation of the glacial clays fall within the range of clay mineralogic variation of the nonglacial sediments. Apparently, ice overrode, incorporated and reworked bedrock and nonglacial sediments, accounting for the

similar clay mineralogic compositions of glacial and nonglacial sediments.

## Conclusions

Distinct units within the Whidbey Formation cannot be differentiated by clay mineral composition. Mineralogic variation within units is just as great as between units, and differences within single outcrops are as great as between outcrops. Glacial and nonglacial sediments apparently cannot be distinguished by their clay mineralogic compositions either, since their ranges of compositional variations overlap.

Since clay mineralogic characterization of Pleistocene stratigraphic units cannot be made on southern Whidbey Island, X-ray diffraction methods cannot be used as a correlative tool, and correlation of the Whidbey Formation across the proposed tectonic structure cannot be attempted.

## Heavy Mineral Analysis

Heavy mineral analysis is the technique used to study the heavy mineral suites of sediments, which commonly compose a fraction of the sand-size grains. It was anticipated that stratigraphic units of different ages or origin might contain distinctive heavy mineral compositions, resulting from the incorporation of unique sediments or bedrock types.

Procedure — The heavy mineral analyses performed in this study consisted of two phases: separation of the heavy minerals from light minerals, and magnetic separation of the heavy mineral fraction into fractions of similar magnetic susceptibilities. A detailed procedure of the heavy mineral analysis used in this study is given in Appendix D.

In this study, bromoform (S.G. 2.85) was the heavy liquid used to separate the heavy and light minerals. Magnetic separations were performed on a Franz Isodynamic separator, using six settings of varying amperage. This separated the heavy mineral grains into seven groups for study under the binocular and petrographic microscopes. These separations were performed for the #120 and #170 mesh (U.S. Standard) sieve fractions of eighteen samples.

Discussion of Results — The heavy mineral composition of a sediment sample is a function of numerous complex variables, such as grain size and shape, hardness, chemical stability, and source area lithology. The goal of heavy mineral analyses is to eliminate all variables except the source area lithology. In this study, in order to eliminate some of the variables, ten samples of similar size fractions (#120 mesh) from sediments with similar graphic means (1.73 $\phi$  to 2.06 $\phi$ , medium to fine-grained sands) were examined under the microscope. Percentage estimates of the individual heavy minerals present were made for each of the seven magnetic fractions. Data for each of the fractions studied are given in Appendix D.

The 0.10A+ magnet fraction of the samples studied is dominated by the black, opaque heavy minerals: magnetite, ilmenite and hematite. Nine of the ten samples studied contain at least 50% black opaques, while sample DBW-2 only contains 10%. Idocrase is the other main constituent of this fraction, varying from 5 to 40% in abundance. With the exception of DBW-2, there are always more black opaque minerals than idocrase present in this fraction. Over half of the samples also contain a minor amount of an undetermined member of the clinopyroxene family. Minor proportions of the amphiboles hornblende and actinolite (green) occur in some samples.

Idocrase becomes the principal heavy mineral constituent of the 0.25A fraction, varying from 30 to 90% in abundance. Hornblende is the second most abundant constituent, while clinopyroxene and green actinolite are also present

in almost every sample. Black opaque mineral grains occur in only three samples, but compose over 50% of sample DBE-18.

The 0.50A magnetic fraction is composed of four main constituents in variable proportions--hornblende, idocrase, almandine (garnet), and green actinolite. Hornblende is the most abundant mineral in over half of the samples, and either idocrase or actinolite (green) is dominant in the remaining ones. Up to 20% brown actinolite, a distinctive variety readily distinguishable from the green actinolite, is also present in half of the samples, while minor (less than 10%) amounts of epidote, biotite + chlorite, and clinopyroxene are less common.

Epidote and actinolite are the dominant minerals present in the 0.75A magnetic fraction. Epidote constitutes 30 to 65% of every sample, while brown and green actinolite compose from 10 to 60%. The ratio of brown to green actinolite in the 0.75A fraction is much greater than in the more magnetic fractions. Hornblende still composes up to 30% of some samples, but is absent in five others. Idocrase, biotite + chlorite, clinopyroxene and kyanite are minor constituents of some samples, but absent in others. Rounded dark blue-green satiny grains, of an undetermined mineral, are also present in minor (less than 10%) amounts. Limited optical properties suggest these grains may be nephrite.

Fifty to eighty percent of every sample (except UBE-4) in the 1.0A magnetic fraction is composed of epidote. Green actinolite, clear actinolite (distinctive and readily distinguishable from the other actinolite varieties), clinopyroxene and rounded blue-green grains (nephrite?) compose up to 30% of some samples, but each is also absent in at least half of the samples. Per-

centage estimates from sample UBE-4 could not be made, since a large light mineral population obscures the heavy minerals present. The presence of heavy minerals in this sample are simply identified by an X on the data sheet in Appendix D.

The combination of the presence of abundant light minerals and a wide variety of heavy minerals makes characterization of the 1.30A magnetic fraction difficult. Heavy minerals present include epidote, green actinolite, clear actinolite, rounded blue-green grains (nephrite?), rutile (yellow-brown and red-brown), and zircon. An X on the data sheet in Appendix D indicates the presence of undetermined amounts of the individual minerals. When the ratio of heavy to light minerals was high enough, percentage estimates of individual heavy minerals could still be made, and are given.

The > 1.30A magnetic fraction contains only three heavy mineral varieties: kyanite, rutile and zircon. Ratios of the three minerals vary from sample to sample, with no obvious pattern. Light minerals constitute a large portion of some of the samples.

Conclusions — Microscopic examination of seventy heavy mineral fractions from ten samples indicates that there are significant quantitative variations in the heavy mineral composition of the Quaternary sediments on southern Whidbey Island. However, variations within sections are just as great as between sections, and variations within the Whidbey Formation nonglacial sediments are just as great as between Whidbey Formation, younger(?) nonglacial, and glacial sediments.

Since no distinctive units or beds have been identified by heavy mineral analyses, correlation of sedimentary units within the Whidbey Formation cannot be made. Therefore, correlation of the Whidbey Formation sediments across the

proposed tectonic structure is not feasible.

## Paleontology

At the outset of the project, it was thought that some paleontological work might aid us in our work to characterize the Whidbey Formation. Field work resulted in no macrofossil discoveries. Seventeen samples<sup>1/</sup> of Whidbey sediments, which were suspected to possibly contain fossils, were treated in the following manner to isolate any fossils for microscopic inspection:

- 1) 0.5 to 1.0 kg of sample was dried to remove water.
- 2) The sample was placed in kerosene, to permit thorough soaking.
- 3) The kerosene was poured off and water added to the sample.
- 4) The sample was allowed to stand until it was the texture of fine silt to clay.
- 5) The sample was washed on #14 and #100 mesh screens (U.S. Standard Mesh), to isolate fossils for inspection.

No invertebrate fossils were found in any of the seventeen samples. However, three nonglacial samples (DBW-E, DBE-13b, SHW-3) did contain scattered seeds. A single seed from a plant of the Family Umbelliferae ("the Parsley family") was found in sample DBE-13b, and three seeds from plants of the Family Cruciferae ("the Mustard family") were extracted from sample SHW-3. These seeds represent small herbaceous weedy plants of undetermined genus. Sample DBW-E contained numerous "oogonia" (female sexual reproductive organs) from fresh or brackish water algae of the Family Characeae, genus Chara or Nitella. This association

---

<sup>1/</sup>

I	1) DBW-A	2) DBW-B	3) DBW-C	4) DBW-D	5) DBW-E
II	6) DBE-11	7) DBE-13b	8) DBE-17		
III	9) UBE-7	10) UBE-11			
IV	11) SHW-C	12) SHW-0	13) SHW-2	14) SHW-3	15) SHW-4A
V	16) PP-2A	17) PP-5			

of fresh to brackish water algae and herbaceous weedy plants is further evidence for deposition of Whidbey Formation sediments on open, flat terrain with fresh or brackish water subenvironments. This model fits the suggested floodplain environment rather well.

## REFERENCES CITED

- Bowles, J.E., 1970, Engineering properties of soils and their measurement: McGraw-Hill Book Co., New York, 187 p.
- Carroll, Dorothy, 1970, Clay minerals: a guide to their X-ray identification: Geological Society of America Special Paper 126, 80 p.
- Crosson, R.S., 1974, Compilation of earthquake hypocenters in western Washington: Washington Division of Geology and Earth Resources Information Circular 53, 25 p.
- Crosson, R.S., 1975a, Compilation of earthquake hypocenters in western Washington - 1973: Washington Division of Geology and Earth Resources Information Circular 55, 14 p.
- Crosson, R.S., 1975b, Compilation of earthquake hypocenters in western Washington - 1974: Washington Division of Geology and Earth Resources Information Circular 56, 14 p.
- Crosson, R.S.; and Millard, R.C., 1975, Compilation of earthquake hypocenters in western Washington - 1974: Washington Division of Geology and Earth Resources Information Circular 56, 14 p.
- Crosson, R.S.; and Noson, L.J., 1978a, Compilation of earthquake hypocenters in western Washington - 1975: Washington Division of Geology and Earth Resources Information Circular 64, 12 p.
- Crosson, R.S.; and Noson, L.J., 1978b, Compilation of earthquake hypocenters in western Washington - 1976: Washington Division of Geology and Earth Resources Information Circular 65, 13 p.
- Crosson, R.S., and Noson, L.J., 1979, Compilation of earthquake hypocenters in western Washington - 1977: Washington Division of Geology and Earth Resources Information Circular 66, 12 p.
- Danes, Z.F.; and others, 1965, Geophysical investigations of the Southern Puget Sound area: Journal of Geophysical Research, Vol. 70, no. 22, p. 5573-5580.
- Easterbrook, D.J., 1968, Pleistocene stratigraphy of Island County: Washington Department of Water Resources Water Supply Bulletin 25, Part I, 317 p., 4 plates.
- Easterbrook, D.J., 1969, Pleistocene chronology of the Puget Lowland and San Juan Islands, Washington: Geological Society of America Bulletin, Vol. 80, p. 2273-2286.
- Folk, R.L., 1978, Petrology of sedimentary rocks: Hemphill Book Company Austin, Texas, 170 p.



- Friedman, G.M., 1967, Dynamic processes and statistical parameters compared for size frequency distribution of beach and river sands: *Journal of Sedimentary Petrology*, Vol. 37, No. 2, p. 327-354, figs. 1-19.
- Hall, J.B.; and Othberg, K.L., 1974, Thickness of unconsolidated sediments, Puget Lowland, Washington: Washington Division of Geology and Earth Resources Geologic Map GM-12.
- Hansen, H.P.; and Mackin, J.H., 1949, A pre-Wisconsinan forest succession in the Puget Lowland, Washington: *American Journal of Science*, Vol. 247, p. 833-855.
- Mullineaux, D.R., 1967, Gross composition of Pleistocene clays in Seattle, Washington: U.S. Geological Survey Professional Paper 575-B, p. B69-B76.
- Othberg, K.L.; and Danes, Z.F., 1975, Delimitation of a buried structure across the Puget Lowland, Washington: *Geological Society of America, Abstracts with Programs*, Vol. 7, no. 3, March 25-27, 1975.
- Rogers, W.P., 1970, A geological and geophysical study of the central Puget Sound Lowland: unpublished University of Washington Ph.D. thesis, 123 p.
- Schultz, L.G., 1964, Quantitative interpretation of mineralogical composition from X-ray and chemical data for the Pierre shale: Geological Survey Professional Paper 391-C, 31 p.
- Stuart, D.J., 1961, Gravity study of crustal structure in western Washington: U.S. Geological Survey Professional Paper 424-C, p. C273-C276.

## APPENDIX A

### Field Observations

Geologic section: Double Bluff to Useless Bay

#### Section description

Double Bluff West (Section 1)

Double Bluff East (Section 2)

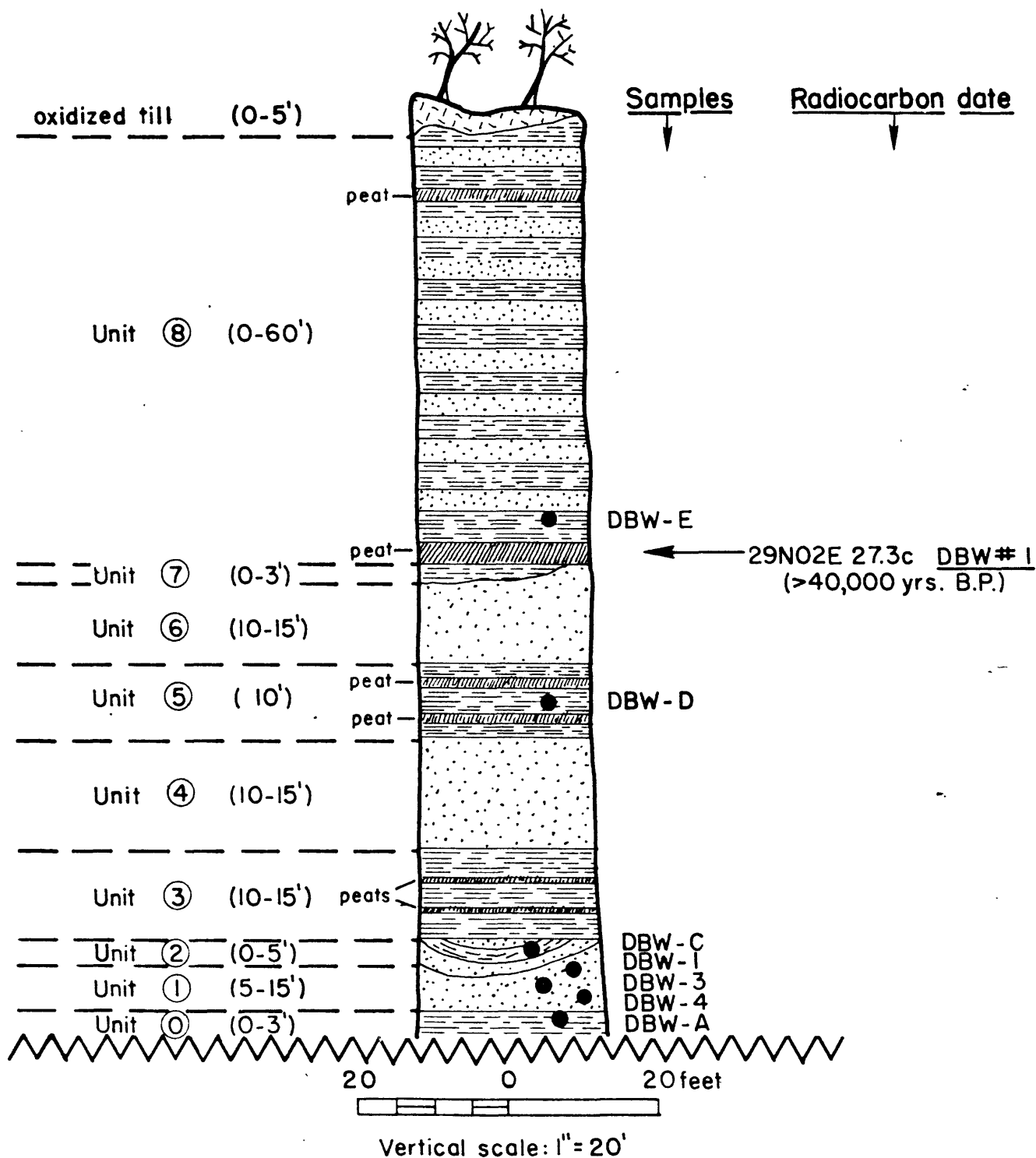
Useless Bay East (Section 3)

Scatchet Head West (Section 4)

Possession Point (Section 5)

# SECTION 1: DOUBLE BLUFF WEST (DBW)

NW 1/4 SE 1/4 Section 27, Twp 29N,  
Rge 2E



Double Bluff West (Section 1) (DBW) — NW $\frac{1}{4}$  SE $\frac{1}{4}$  section 27, T. 29 N., R. 2 E.

Unit 8 — Gray silty clay with thin very fine sand lenses; bedding alternates between massive and rhythmically-bedded horizons; maximum individual bed thickness is two feet; massive silty clay is distinctly bluish-gray and unoxidized; rhythmically-bedded horizons are gray when unoxidized, but are commonly oxidized orange-brown along the very thin layers of sand; Unit 8 contains at least one peat bed near its top, and is separated from Unit 7 by a two-foot thick peat bed, which was radiocarbon dated (radiocarbon date DBW #1); Unit 8 also contains small organic fragments scattered throughout the matrix, some of which has been replaced by vivianite.

Sample DBW-E from silty clay horizon.

Unit 7 — Light tan silt; massive; maximum thickness of unit is approximately three feet, but it thins laterally and disappears.

Unit 6 — Yellow-brown fine to medium-grained sand; slightly oxidized; horizontally laminated.

Unit 5 — Grayish-brown clayey silt, massive to thin-bedded; contains scattered organic fragments in the matrix; also contains two peat beds (less than six inches thick).

Sample DBW-D

Unit 4 — Yellow-brown fine to medium-grained sand; horizontally laminated; slightly oxidized; interbedded with thin gray silt lenses near the top.

Unit 3 — Thin-bedded organic silt, with the abundant organic fragments giving a fibrous nature to the unit, which results in the formation of a very resistant bed. The organic silt becomes interbedded with Unit 4 sand near the east end of Section 1, and is not easily recognizable; Unit 3 contains numerous thin peat beds in the eastern half of the section.

Unit 2 — Interbedded gray, micaceous clayey silt and grayish-brown fine-grained sand; the unit is folded gently, with the individual folds measuring less than 100 feet across; the top of the folds have been planed off and are flat.

Sample DBW-C from silt horizon.

Unit 1 — Sand and gravel; characterized by great lateral and vertical variation in lithologies; alternating lithologies in tabular beds, generally two to four feet thick. Base of Unit 1 is below sea level and is not observable; upper contact with other units of the Whidbey Formation is broadly undulating. Many of the beds contain abundant cross-beds, with most dipping W-SW; another component of cross-beds dip in the opposite direction (E-NE), but this direction of dip is much less common; some beds within Unit 1 contain numerous wood, peat, organic, and organic silt fragments - all rounded to some degree. The following are the lithologic types found in Unit 1 — fine-grained sand, medium-grained sand, coarse sand with gravel, gravelly sand, and fine to coarse gravel. Samples DBW-1, DBW-3, and DBW-4 from sand and gravel beds.

Unit 0 — Dark gray silty clay, contains scattered pebbles, massive. Unit 0 is probably glacial in origin — either glacial till or glaciomarine, and probably belongs to the Double Bluff Formation.

Double Bluff East (Section 2) (DBE) — NW¼ section 26, T. 29 N., R. 2 E.

Unit A — Orange-brown to gray cobbly till and cobbly gravel; oxidized; discontinuous; thin veneer along bluff top.

Unit B — Interbedded sand and silt; sand beds are thin and few near the base of the unit, but become thicker and dominant near the top; silt beds are brownish-gray and massive and contain numerous very small and thin sand lenses; silts are also weakly oxidized (orange); sand beds are gray and mostly very fine-grained, with some beds horizontally laminated and others cross-bedded (with dips to the SW) and ripple marked; sand beds are well sorted, micaceous, and predominantly fresh. All of Unit B is inclined inwardly toward the bluff, at an angle of 30-40°. Since the unit appears to be in place and not slumped, the deformation is probably related to glacial activity, and may represent ice shove or ice collapse phenomenon.

Sample DBE-1 from sand and Sample DBE-2 from silt.

Angular unconformity between Units B and C.

Unit C — Grayish-brown sand and gravel with minor cobbles; cobbles and gravel are sub-rounded to rounded and are matrix-supported; Unit C is characterized by both horizontal lamination and cross-bedding, with cross-beds dipping toward the south; Unit C is planar bedded, with beds generally less than two feet thick; a few beds are virtually gravel-free, and are very similar to Unit D beds below; maximum cobble size in Unit C is approximately 12" in diameter, but few cobbles exceed six inches.

Sample DBE-3 from gravelly sand, and Sample DBE-4 from gravel-free sand. Sharp contact between Units C and D.

Unit D — Brownish-gray fine-grained sand; thin to thick planar beds; sand is well sorted, loose and friable and contains only scattered gravel; some beds contain a concentration of gravel along their base; gravel is rounded when present; sand is horizontally laminated to cross-bedded in nature, with the abundant trough cross-beds dipping to the south; a few brownish-gray laminated silt lenses occur in Unit D, but they are generally thin (3-12" thick) when present.

Sample DBE-5 from sand near top of Unit D; Sample DBE-6 from sand near the base of Unit D.

The contact between Units D and E is a transitional contact.

Unit E — Interbedded silt and very fine-grained sand; thin to thick beds; sand beds are very fine-grained, otherwise are similar to Unit D sand beds; sand is moderately well sorted and generally contains no gravel; horizontal lamination dominates the sand beds, but cross-beds present dip to the SW; some sand horizons are strongly oxidized, while others remain fresh; silt beds are characteristically brownish-gray and massive; some silt beds are slightly sandy and most contain very fine interlaminae of sand; a few silt beds are very finely rhythmically bedded and may represent varves; Unit E also contains angular blocks of sandstone (as large as 6 feet in diameter) which probably represent ice-rafted material; thin pockets of laterally-discontinuous, unsorted debris piles probably record similar depositional conditions; Unit E appears to simply be a finer-grained equivalent of Unit D, and must represent deposition under

less energetic conditions.

Sample DBE-7 from sand, and Sample DBE-8 from silt.

Unit F — Transitional contact between Units E and F. This slightly oxidized, four foot thick transition zone consists of thin-bedded ( $< 1"$  thick) brown silt, dark gray clay, and gray, very fine-grained sand; the base of the transition zone is sharp, with compact dark gray silty clay below it; this silty clay is massive near the top, but becomes distinctly rhythmically bedded, with dark gray clay and lighter gray silt components, which are believed to be varves of a glaciolacustrine deposit. This silty clay also contains a few thin, discontinuous lenses of brown, horizontally-laminated sand. An accumulation of wood fragments (stems, twigs, etc.) occurs along the base of the transitional zone (surface of the compact clay). These wood fragments were collected for radio-carbon date DBE#1.

Sample DBE-9 from massive gray clay near the transitional contact with Unit E, Samples DBE-10 and DBE-11 from rhythmically-bedded silt and clay. Contact with Unit G is sharp, with a thin ( $< \frac{1}{2}"$ ) layer of hard iron oxide along the contact.

Unit G — Gray-brown, moderately well-sorted, medium to coarse sand; horizontally laminated; beds are 2-4 feet thick; rounded to partially flattened re-worked silt fragments are concentrated along the base of beds. These silt pebbles are reworked from Unit H below; elsewhere, silt pebbles are scattered throughout the sand matrix, in varying degrees of concentration.

Sample DBE-12 taken 4 feet below contact with Unit F.



Unit H — When undeformed, the following subunits are found in Unit H:

1 foot to 3 feet -- dark gray silty fine sand; horizontally-laminated; thin-bedded; contains a trace of scattered organic material; some beds are siltier than others, with the sandy layers more oxidized.

1 foot to 3 feet -- massive dark gray clay; very hard; structureless.

6 inches to 2 feet -- dark gray massive silt; faintly laminated

While Unit H is flat-lying and undeformed on the western end of Section 2, it is deformed into diapiric structures on the eastern end. The deformation consists of diapirs of mixed silt and clay, intruded into a matrix of silty sand. In many places, the diapiric fines have become detached from the silt and clay body and are floating in the silty sand matrix. The underlying unit (Unit I) is only moderately deformed in a few places, where it protrudes up toward the diapirs. This relative lack of deformation of Unit I may be due to the fact that its coarser-grained and better sorted nature resulted in it containing much less water than the sediments of Unit H. The truncation of diapirs and the abundance of reworked silt and clay fragments in Unit G, suggest that Unit H was the surficial unit at the time of deformation. Unit G was deposited later. The author believes that the deformation of Unit H is a result of sediment overloading. The excess weight (and/or rapid deposition) of the silty sand appears to have overloaded the water-saturated silts and clays, initiating deformation.

Sample 13a from the upper silty fine sand subunit; Sample 13b from the middle gray clay subunit; Sample 13c from the lower massive silt subunit.

Unit I — Grayish-brown horizontally-laminated sand; medium to coarse-grained near the base of the unit, becoming finer-grained near the top. Contains scattered concentrations of rounded to flattened silt and clay pebbles; these matrix-supported pebbles increase in abundance toward the base of the unit, implying that they are reworked fragments from Unit J; concentration of the pebbles occur along the base of beds six inches to two feet below the contact with Unit H, a 2-4" thick detrital layer of low density fragments occurs, sandwiched between fine to medium-grained sands. The detritus is composed of wood, peat, coal, and dacitic pumice fragments, with the coal being very finely disseminated. While this thin horizon is very continuous laterally (over hundreds of feet), no organic detritus occurs in the sands above or below it. In one place along this horizon, a block of diamicton (brown silty clay with pebbles and cobbles) three feet long and one foot thick was found. The sand above it is depressed toward the diamicton, as if it collapsed in response to some action by the diamicton block.

Sample 13d from the diamicton; Sample 14 from two feet below contact with Unit H; Sample 15 from 15 feet below contact with Unit H.

Unit J — Brownish-gray, medium-grained silty sand; with tan sand and silt injected into sand from below; Unit J is dominated by flame structures composed of a jumbled mixture of silt and sand; some of the sand from in the flame structures appears to have originated from Unit K below. Unit J is a prominent cliff-former.

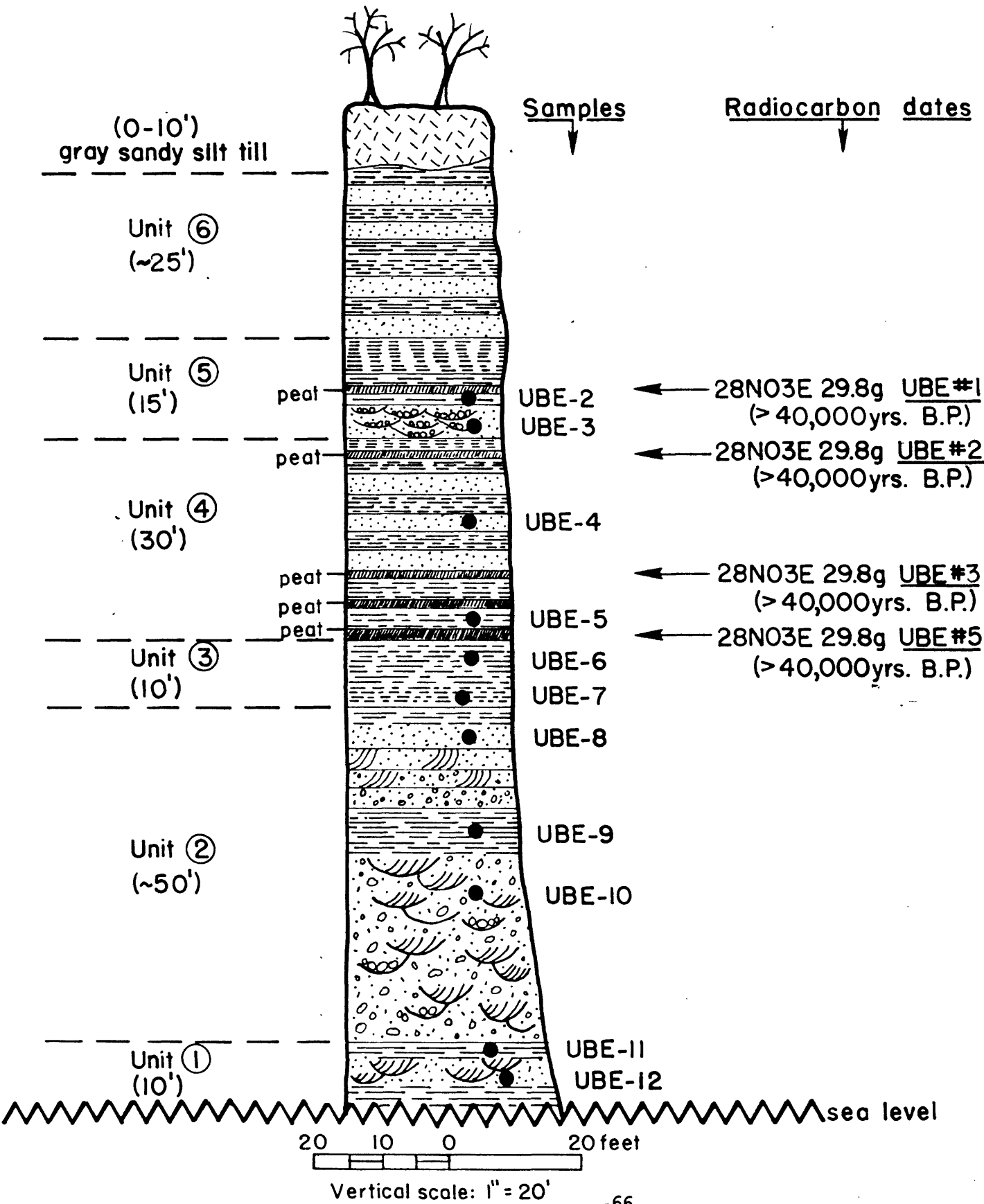
Sample DBE-16 from silty sand; Sample DBE-17 from deformed silt and sand mixture from within a flame structure. Sharp contact between Units J and K, but some Unit K sand has been deformed and protrudes upward into Unit J.

Unit K — Brownish-gray, planar-bedded, medium to coarse-grained sand; contains scattered matrix-supported pebbles and trace cobbles, which are commonly coated with manganese staining; abundant cut-and-fill structures with gravel concentrated along the base of the fills; numerous asymmetric ripples are also indicative of westerly flow. Unit K also contains some silt and silty fine sand beds, up to 12 inches thick; some are laterally continuous, but others are lenticular and discontinuous. Organic fragments are abundant, with many large pieces scattered throughout, and finer organic fragments concentrated along cross-beds; all of the organic fragments found are rounded peat fragments, which are apparently reworked from older sediments.

Sample DBE-18 from fine sand (with no gravel).

SECTION 3: USELESS BAY EAST (UBE)

SW1/4 ~ NW1/4 NW1/4 Section 29,  
Twp 29N, Rge 3E



Useless Bay East (Section 3) (UBE) — SW $\frac{1}{4}$  NW $\frac{1}{4}$  NW $\frac{1}{4}$  section 29, T. 29 N., R. 3 E.

Surficial till — Gray sandy silt till; occurs only as a thin veneer at the UBE section, but thickens rapidly to the north and eventually composes the entire bluff.

Unit 6 — Interbedded dark gray clay, grayish-brown silt, and light gray sand. No peat beds observed. No detailed description or sampling of Unit 6 could be made, since the cliff-forming Unit 5 prevented access.

Unit 5 — Upper 5 feet: thinly laminated, dark gray silty clay.

Middle 4 feet: massive light gray clayey silt; contains scattered wood and organic fragments; contains a couple very thin (< 2") peat lenses and a 6" thick peat bed (radiocarbon date UBE #1).

Sample UBE-2 from clayey silt.

Lower 6 feet: gray fine to medium-grained sand; with minor thin (< 2" thick) brown silt lenses; numerous cut-and-fill structures; sand fines upward; sand contains numerous wood and organic fragments; cross-beds and ripple marks indicative of NW flow; sharp contact with Unit 4 -- rounded pebble concentration at contact, with its lower portion very strongly oxidized (orange).

Sample UBE-3 from lower sand.

Unit 4 — Interbedded gray silty clay beds with gray medium-grained sand; clay beds average about three feet thick and sand beds about 1½ feet thick; sands are fine to medium-grained and mostly structureless (a few cross-beds dip westerly); silty clays are dense and dark gray when unoxidized, but are commonly oxidized along contacts with sand beds; Unit 4 contains

numerous scattered organic fragments, four major (>6" thick) peat beds and a few other minor (< 2" thick) peat lenses. Radiocarbon dates UBE#2, UBE#3, UBE#4, and UBE#5 are from the four major peat beds (from top to bottom). Interbedded with the peats are greenish-gray silts and gray fine sands; the silts are massive; the sands are fine-grained sand to silty sand.

Sample UBE-4 is from fine sand near the top of Unit 4; Sample UBE-5 is from clayey silt near the base of Unit 4.

Unit 3 — Upper 6 feet: grayish-brown clayey silt; massive; micaceous; structureless; scattered organics.

Sample UBE-6.

Lower 4 feet: dark greenish-gray clay; dense; weathers to a distinct green color; horizontally continuous and traceable.

Sample UBE-7.

Unit 2 — Upper 2 feet: brown silt and strongly oxidized (orange) silt and fine sand.  
12 feet: wide variety of sands and gravels; characterized by great lateral and vertical variation; lithologies alternate in tabular beds from 2-4' thick; sands contain numerous crossbeds dipping W-NW and also contain numerous rounded silt balls; no organic fragments were found in the sands; this portion of Unit 2 is characterized by a fining upward sequence — from gravelly sand near the base to fine sand at the top; all sands are oxidized.

Sample UBE-8 from medium-grained sand.

6 feet: grayish-brown massive clayey silt; contains a few thin interbeds of medium-grained sand; this portion of Unit 2 thickens to the north, where sand interbeds become thicker and dominant.

Sample UBE-9 from silt.

Lower 30 feet: poorly sorted mixture of fine to coarse sand with some gravel scattered throughout; oxidized to a light yellowish-brown color; horizontally laminated to cross-bedded (with dips to the NW; gravel and pebbles dominantly rounded and coated with a purple (Mn oxide?) coating; contains scattered rounded silt fragments; cut-and-fill structures abundant; contact with Unit 1 is sharp.

Sample UBE-10 from sand.

Unit 1 — Interbedded grayish-brown massive silt, gray fine to very fine sand, and a few very thin (~1" thick) peat beds; organic fragments scattered throughout the unit; many of the silt beds contain thin lenses of very fine-grained sand which pinches out laterally; sands are slightly oxidized to fresh; cross-beds dip both W-NW and S-SE; cut-and-fill structures are common; Unit 1 dips to the south and rapidly disappears below sea level.

Sample UBE-11 from silt, and Sample UBE-12 from sand.

Scatchet Head West (Section 4) (SHW) —  $W\frac{1}{2}$   $SW\frac{1}{4}$   $NE\frac{1}{4}$  section 16, T. 28 N., R. 3 E.

Unit A — Gray sandy silt till; massive; occurs as a thin veneer along the top of the bluff; thickens to the north, where it eventually composes the whole bluff.

Unit B — Grayish-brown fine to medium-grained sand; gravel is commonly scattered throughout the sand matrix and concentrated along the bases of beds; sand coarsens upward; numerous thin silt beds occur in the lower portion of the unit, with the thickest approximately 2 feet thick; cross-beds indicative of S-SE flow are common; subrounded to rounded gravel increases in abundance toward the top of Unit B; scour-and-fill features are common; reworked(?) organic fragments are abundant; base of Unit B is a scour surface, with detrital material concentrated along that surface.

Unit C — Grayish-brown fine to medium-grained sand; only scattered gravel present; brown silt lenses (< 6" thick) are occasionally interbedded with the sand; sand is horizontally laminated; Unit C is a massive cliff former.

Unit D — Upper 2-3 feet: massive light brown silt.

Middle 4 feet: horizontally laminated and cross-bedded fine-grained sand.

Lower 4 feet: horizontally laminated, light brown micaceous silty sand.

Base of Unit D is a scour surface.

Sample SHW-A from the fine-grained sand in the middle of the unit.

Unit E — Grayish-brown fine to medium-grained sand similar to Unit C; dominantly horizontally laminated, but near the base of the unit cross-beds dip S-SE; Unit E contains virtually no gravel or silt beds; organic fragments are



scattered throughout the sand.

Sample SHW-B from fine-grained sand. Radiocarbon date SHW#3 from the scattered organic fragments.

Unit F — Interbedded gray and gray-brown silt, dark gray clay, and light gray fine sand; individual beds vary from 6 inches to 2 feet thick; sands contain cross-beds indicative of S-SE flow; silts are massive to thinly laminated; clays are massive; base of Unit F is covered by talus which produces a bench above Unit G; Units F and G are apparently conformable, with no evidence of erosion or weathering.

Sample SHW-C from a very fine-grained sand horizon.

Unit G — Interbedded fine-grained brown sand, light gray organic silt, and dark gray clay; contains wavy horizons of dark brown organic-rich material and a 1 foot thick peat horizon near the top of the unit; interfingering of the above lithologies is common; oxidation along lithologic contacts give a bright orange color to many sand beds; in places the sand, silt, clay, and organics have been deformed and mixed together.

Sample SHW-D from fine-grained brown sand immediately below the peat bed. Radiocarbon date SHW#2 from the 1 foot thick peat bed.

Unit H — Brown, horizontally laminated fine-grained sand; forms a small bench which is mostly covered by talus and debris.

Unit I — Dark gray clay and gray-brown silt; organic fragments common; a few sandy silt horizons are oxidized to bright orange and stand out in appearance; lower 10 feet of Unit I contains numerous very thin (< 2" thick) peat beds.

Sample SHW-1 from grayish-brown silt.

Unit J — Interbedded dark gray clay, gray-brown silt, light gray fine-grained sand, and peat; most beds are < 1 foot thick; peat and organic beds are 6-9 inches thick and scattered throughout the unit.

Sample SHW-2 from sand, Sample SHW-3 from clay, Sample SHW-4 from clay.  
Radiocarbon date SHW #1 from the uppermost peat bed in the unit.

Unit K — Greenish-gray massive silt; pebbly near the base of the unit, especially in a channel-like depression in the top of Unit L which is filled with deformed silt and peat beds.

Sample SHW-4 from pebble-free silt.

Unit L — Strongly oxidized (orange) gravel; subrounded to well-rounded; gravel is supported by a coarse sand matrix; gravel is interbedded with fine to medium-grained sand beds; fine sand is pebble-free while the coarser sand contains scattered gravel; cross-beds in Unit L dip S-SE; the gravel in Unit L is commonly coated with a purple (Mn) coating.

Sample SHW-5 from medium-grained sand.

Unit M — Thin interbeds of grayish-brown silt, gray clay, and light gray fine sand; sand beds contain abundant cross-beds dipping E-SE.

Unit N — Upper 10 feet: brown medium to coarse-grained sand with gravel concentrated in pockets and horizons; reworked flat silt fragments common. Thin gray silt broken into pieces along an undulating surface separates the upper and lower sands.

Lower 15 feet: light brown fine-grained sand; dominantly horizontally laminated, but some cross-beds dip E-SE; cut-and-fill structures are abundant; organic fragments are common; this lower sand is virtually gravel-free.

Sample SHW-6 is from fine-grained sand.

Possession Point (Section 5) (PP) — N $\frac{1}{2}$  NW $\frac{1}{4}$  NE $\frac{1}{4}$  section 23, T. 28 N., R. 3 E.

Possession (?) — Gray silty clay till; massive cliff-former; contains glaciofluvial  
Point  
sediments near the top; contains organic debris in the base of  
the till, apparently reworked from older sediments (collected for  
radiocarbon date PP#1).

Unit A — Upper 0-20 feet: rhythmically-bedded dark and light gray clay and silt,  
with some sand lenses; pinches out to the north and east.  
Lower 30-50 feet: dark gray silty clay interbedded with brown, hori-  
zontally laminated fine sand beds; beds vary from 1-4 feet in thickness;  
a few dark brown organic silt beds occur near the top - radiocarbon date  
PP#2 is from the thickest organic bed in the unit; Sample PP-1 from very  
fine sand; Sample PP-2 from medium silt; Sample PP-2A from clay.

Unit B — Gravelly cobbles with a coarse sand matrix; cobbles and gravel are matrix-  
supported; most gravel and cobbles are rounded to well-rounded; numerous  
silt lenses are interbedded with the gravelly cobbles, some contain gravel;  
cobble lithologies are highly variable; small organic fragments dispersed  
throughout unit; contact with Unit C is irregular; Unit B pinches out to  
the north and east.

Unit C — Interbedded dark gray massive silty clay, gray sand, and grayish-brown  
silt; organics scattered throughout; numerous cross-beds in sand beds  
indicative of E-SE flow; individual bed thickness varies from 6" to 4';  
sands oxidized along cross-beds, giving them a salmon-color; much inter-  
stratification of lithologies occurs on a small scale, reflecting large-  
scale relationships; Sample PP-3 from a 1-2" thick distinct pinkish-

colored floury silt (volcanic ash?) bed occurs near the top of Unit C; Sample PP-4 from very fine sand; Sample PP-4A from clay; Sample PP-5 from medium silt.

Double Bluff Drift — Gray silty clay till; interbedded with deformed layered silt beds and gravelly horizons; boulder concentration along contact with the nonglacial sediments above; the upper 2-5' is gleyed (green) in places, suggesting a soil-forming interval prior to nonglacial sediment deposition; Sample PP-6 and Sample PP-6A both from glacial till.

## APPENDIX B

### Grain Size Analyses

#### Mechanical Method (Sieving)

The sieving method is used to determine the presence of relative proportions of clastic particles greater than  $4\phi$  (.0625 mm) in diameter. As the determination of individual particle sizes is impractical, the sieving process is used merely to bracket the ranges of clastic particle sizes. Since the #200 sieve (U.S. Standard mesh) is constructed of the finest mesh which permits the free passage of sediment, it was the finest screen used.

The following sieving process was employed in this study, since it is an accurate, easily reproducible, and reliable method. This procedure is a modification of those suggested by Bowles (1970) and Folk (1968): 1) The sediment sample was oven-dried, pulverized (with mortar and pestle), and weighed to obtain the exact sample weight. Five hundred to eight hundred grams were used if the sample was predominantly sand and gravel. 2) The sample was placed on a #200 sieve (U.S. Standard mesh) and carefully washed until the water cleared, so that most of the material finer than  $3.75\phi$  (.074 mm) was washed out of the sample. 3) The residue was carefully poured into a large weighed porcelain evaporating dish and left to set until the top of the suspension was clear. The clear top water was then poured off. The dish and remaining soil-water suspension were placed in the oven for drying. 4) After drying, the oven-dry residue was weighed. Then it was passed through a stack of sieves for 15 minutes. Since the objective was to produce a grain-size distribution curve, it was necessary to obtain a good distribution of points across the range of sieve sizes. The number of sieves

used in the sieving process varied according to the amount of sample coarser than 3.75 $\phi$ . 5) The sieve stack was removed from the shaker, and the weights of material remaining on each sieve were obtained. The weights were summed and compared with the sample weight (after wet sieving) in order to detect any loss of sample in the sieving operation. A loss of more than 2% by weight was not acceptable. 6) The percent retained (by weight) on each sieve was computed by dividing the weight retained on each sieve by the original sample weight. 7) The percent finer (or percent passing) was then computed by starting with 100% and subtracting the percent retained on each sieve as a cumulative procedure. The results were recorded on the data sheet for mechanical grain-size analysis (a representative data sheet follows this discussion). 8) The data was plotted on the grain-size distribution curve. When more than 15% of the sample passed the #200 sieve a hydrometer analysis was performed on the sample, in order to determine the relative proportions of grain sizes finer than 3.75 $\phi$  in diameter.

## GRAIN SIZE ANALYSIS - MECHANICAL

Data Sheet

Sample No. DBW-1Location Double Bluff West sectionDate of testing 3-19-79Weight of dry sample 493.83 gWeight of sample after wet sieving 492.12 gWeight loss from wet sieving 1.71 g

Sieve no.	Diam., Ø	Wt. retained	% retained	% passing
7	-1.5	0.00	0.00	100.00
10	-1.0	0.28	0.06	99.94
14	-0.5	1.50	0.30	99.64
18	0.0	3.69	0.75	98.89
25	0.5	10.55	2.14	96.75
35	1.0	92.18	18.67	78.08
45	1.5	188.83	38.24	39.84
60	2.0	141.42	28.64	11.20
80	2.5	34.30	6.95	4.25
120	3.0	15.45	3.13	1.12
170	3.5	2.68	0.54	0.58
200	3.75	0.99	0.20	0.38

$$\% \text{ passing} = 100 - \sum \% \text{ retained}$$

$$\begin{aligned}
 \text{pan} &= 0.80 \\
 + \text{wash} &= 1.71 \\
 \hline
 < 200 \text{ mesh} &= 2.51
 \end{aligned}$$

$$\text{TOTAL} = 494.38 \text{ g}$$

$$\begin{aligned}
 \text{Wt. gain} &= 0.55 \text{ g} \\
 &= 0.11 \% \text{ error}
 \end{aligned}$$



## Hydrometer Method

The hydrometer method utilizes differential settling rates in water to analyze the grain sizes of particles finer than  $4\phi$  (.0625 mm) in diameter. The hydrometer method is used to measure the settling velocity of particles. If the density of soil grains is  $2.65 \text{ g/cm}^3$  and the density of water is 1.000, the soil hydrometer directly measures the number of grams of soil in suspension. Unfortunately, these conditions are seldom met. In reality then, the hydrometer only estimates the number of grams of soil in suspension, by directly measuring the density of the soil-water suspension.

Procedure - The following procedure was used for the hydrometer analysis of the samples in this project. It is a slight modification of that outlined by Bowles (1970):

- 1) 50-60 grams of sample were well pulverized (with mortar and pestle), oven-dried, and then weighed for exact weight.
- 2) The sample was mixed with 125 ml of 4% sodium hexametaphosphate solution (dispersing agent), and allowed to set overnight. The dispersing agent was added to neutralize the electrical charges on the clay particles, which cause the grains to be attracted to each other and stick together, forming larger particles.
- 3) The mixture was diluted with water and mechanically disaggregated in a mixer for 3 to 5 minutes, for complete disaggregation.
- 4) This mixture was transferred to the sedimentation cylinder, and tap water was added to fill the cylinder to the 1,000 ml mark.
- 5) The solution was stirred thoroughly, and upon completion of stirring, timing began for the hydrometer readings.
- 6) Hydrometer readings were made at 1, 2, 4, 8, 15, and 30 minutes, and at 1, 2, 4, 8, 24, and 48 hours.
- 7) Temperature of the solution was taken at the time of each hydrometer reading.
- 8) The data was recorded on the data sheet for the hydrometer method of grain-size analysis (a representative data sheet follows this discussion). Calculations of particle diameter,  $D$ , and % finer were completed, using the

equations given on the explanation sheet which follows. 9) This data was then plotted on the grain-size distribution curve, and the curve was drawn.

#### Explanation Sheet for Hydrometer Data Computation

Time of Reading (from Start)

Elapsed time (t), in minutes

Temperature (T), centigrade

$R_a$  Actual hydrometer reading (read from the top of the meniscus)

$R$  Hydrometer reading corrected for meniscus only

$R_c$  Corrected hydrometer reading ( $R_c = R_a - \text{zero correction} + C_T$ )

This correction is made to obtain the effect of water and dispersant on the hydrometer reading. This correction factor can be calculated by preparing a clear water standard, in which the same quantity of dispersing agent is used as was used in the soil suspension (4%). This solution calibrates the water to a zero reading (zero correction value). The standard is also prepared using water of the same temperature as that used in the soil suspension. Since a 4% solution of sodium hexametaphosphate (dispersing agent) was used in all hydrometer analyses, the zero correction factor was plus 6 units. The correction for temperature ( $C_T$ ) was then obtained from Tables and added to that value to produce the corrected hydrometer reading.

Percent Finer (% finer =  $R_c a/W_s \times 100$ )

$R_c$  = corrected hydrometer reading, measure of grams of soil in suspension at elapsed time t

$W_s$  = Weight of original soil sample placed in suspension, in grams

a = correction factor for density of the solids (obtained from Tables.)

## GRAIN SIZE ANALYSIS - HYDROMETER METHOD

Data Sheet

Sample No. DBW-ELocation Double Bluff West sectionDate of testing 3-22-79Hydrometer no. 152H  $G_s$  of solids 2.65  $a =$  1.00Dispersing agent CALGON (4%) Amount 125 mlZero correction +6 units Meniscus correction +1 unitWeight of soil,  $W_s$  50.29 g

Date	Time of reading	Elapsed time, min	Temp., °C	Actual Hyd. reading $R_a$	Corr. Hyd. reading $R_c$	% Finer	Hyd. Corr. only for meniscus, $R$	$L$	$\frac{L}{t}$	$K$	$D, \text{mm}$	$D, \phi$
3-22-79	2:09	START	—	—	—	—	—	—	—	—	—	—
"	2:11	2	23	55	49.7	98.8	56	7.1	3.55	0.0132	0.0249	5.33
"	2:13	4	23	53.5	48.2	95.8	54.5	7.35	1.838	0.0132	0.0179	5.80
"	2:17	8	23	52.5	47.2	93.9	53.5	7.5	0.938	0.0132	0.0128	6.29
"	2:24	15	23	51	45.7	90.9	52	7.8	0.520	0.0132	0.0095	6.71
"	2:39	30	23	49	43.7	86.9	50	8.1	0.270	0.0132	0.0069	7.19
"	3:09	60	23	43.5	38.2	76.0	44.5	9.0	0.150	0.0132	0.0051	7.61
"	4:09	120	23	35.5	30.2	60.1	36.5	10.3	0.0858	0.0132	0.0039	8.01
"	6:09	240	23	28	22.7	45.1	29	11.5	0.0479	0.0132	0.0029	8.43
"	10:09	480	22	20	14.4	28.6	21	12.9	0.0269	0.0133	0.0022	8.84
3-23-79	2:09	1440	22	14	8.4	16.7	15	13.8	0.0095	0.0133	0.0013	9.59
3-24-79	2:09	2880	18	12	5.5	10.9	13	14.2	0.0049	0.0140	0.0010	9.99

$$R_c = R_{\text{actual}} - \text{zero correction} + C_T$$

$$\% \text{ finer} = R_c(a)/W_s$$

$$D = K\sqrt{L/t}$$

L Effective Depth, in cm, of the hydrometer in the soil suspension

L is the distance, in cm, between the center of the volume of the hydrometer bulb and the suspension surface. L can be readily calculated if R is known.

L values are obtained from Tables.

Settling velocity  $L/t = v$

L = effective depth

t = time elapsed, in minutes

K

K is a function of the temperature (T), specific gravity ( $G_s$ ), and viscosity ( $\gamma$ ) of the soil solution. It is obtained by using Tables.

Particle diameter (D), in mm and  $\phi$

$$D = K\sqrt{L/t}$$

## Grain-size Distribution Curves

Explanation—Sieve and hydrometer data were used to produce a grain-size distribution curve for each sample. In order to facilitate the reading of statistical parameters, the data was plotted as a cumulative curve. Grain diameters were plotted on the abscissa (arithmetic scale) in  $\phi$  units. Cumulative percent frequency (or percent finer) was plotted on the ordinate (probability scale).

Percentages of gravel, sand, silt, and clay were calculated from each curve, and recorded as texture. The gravel percentage given is the percent of the entire sample. Sand, silt, and clay percentages given are exclusive of the gravel-size material present; they total 100% when added together.

Statistical parameters have been calculated for each grain-size distribution curve. Following is a short discussion of each parameter used, including graphic mean ( $M_z$ ), graphic standard deviation ( $\sigma'_G$  or  $\sigma'_I$ ), and graphic skewness ( $S_{K_G}$  or  $S_{K_I}$ ). Equations and tables are from Folk (1968).

Graphic Mean ( $M_z$ ) — The graphic mean is the best graphic measure of the average grain size of a sediment sample. It is superior to the median ( $\phi_{50}$ ), because it is calculated from three points on the grain size curve, rather than just one. Thus, calculations of mean size by measuring the median are not very satisfactory in strongly skewed curves. The graphic mean is a standard measure of grain size used in sedimentary petrologic studies

$$M_z = (\phi_{16} + \phi_{50} + \phi_{84}) / 3$$

Graphic Standard Deviation ( $\sigma'_G$ ) or Inclusive Graphic Standard Deviation ( $\sigma'_I$ )

The standard deviation is a measure of the uniformity or sorting of a sediment. The inclusive graphic standard deviation ( $\sigma'_I$ ) is the best measure of sorting, because it embraces 90% of the distribution curve.

$$\sigma'_I = (\phi_{16} - \phi_{84})/4 + (\phi_5 - \phi_{95})/6.6$$

It was calculated whenever possible. However, most of the fine-grained samples analyzed in this project contained so much clay that the  $\phi_5$  value could not be obtained. Therefore, it was necessary to use the graphic standard deviation ( $\sigma'_G$ ), which covers only 68% of the curve.

$$\sigma'_G = (\phi_{16} - \phi_{84})/2$$

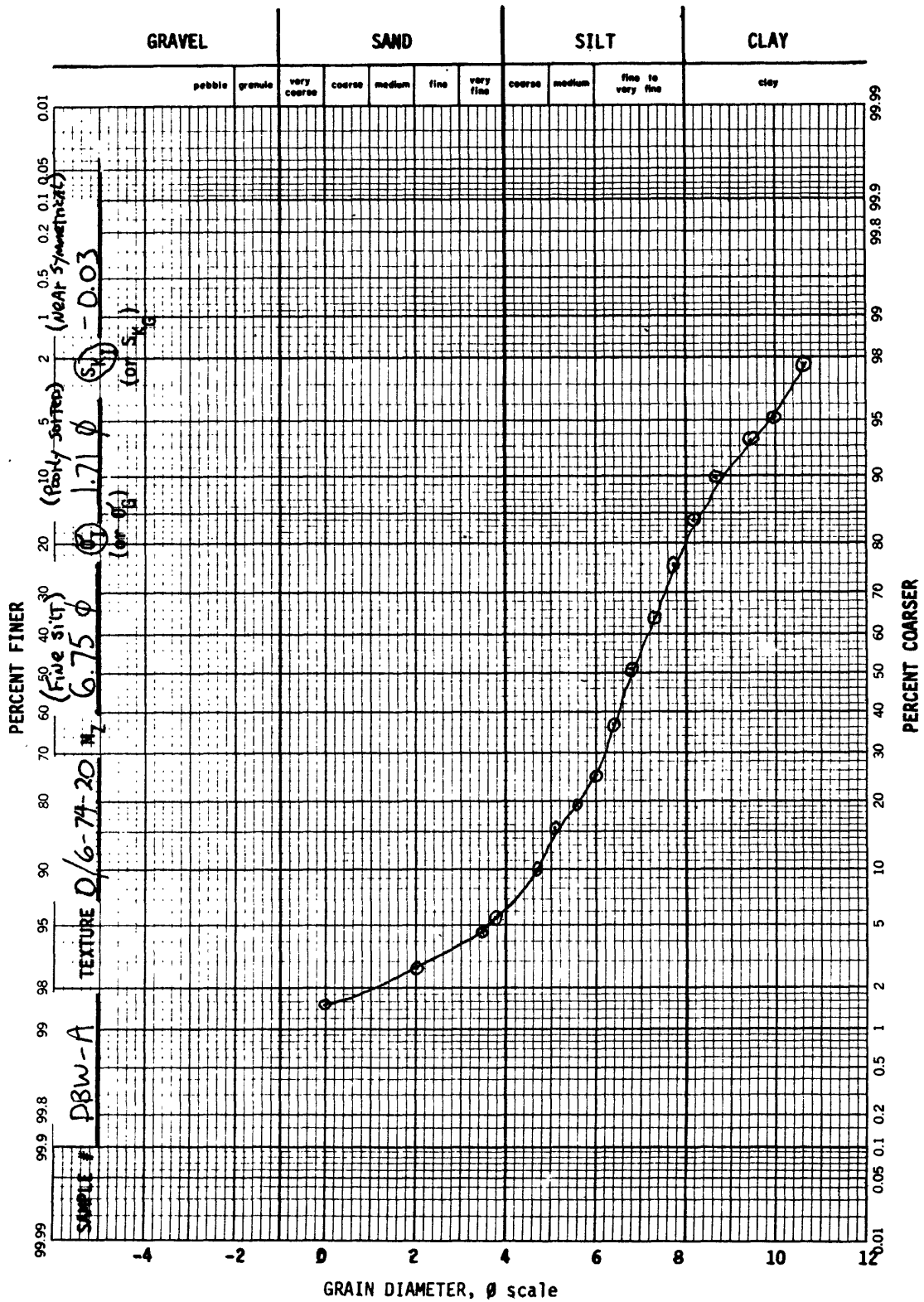
It is still a good measure of sorting, which is commonly used in sedimentological analyses. A classification of sediment sorting devised by Folk (1968) is given below.

$\sigma'_I$ (or $\sigma'_G$ )	under .35 $\phi$ , very well sorted
	.35 - .50 $\phi$ , well sorted
	.50 - .71 $\phi$ , moderately well sorted
	.71 - 1.0 $\phi$ , moderately sorted
	1.0 - 2.0 $\phi$ , poorly sorted
	2.0 - 4.0 $\phi$ , very poorly sorted
	over 4.0 $\phi$ , extremely poorly sorted

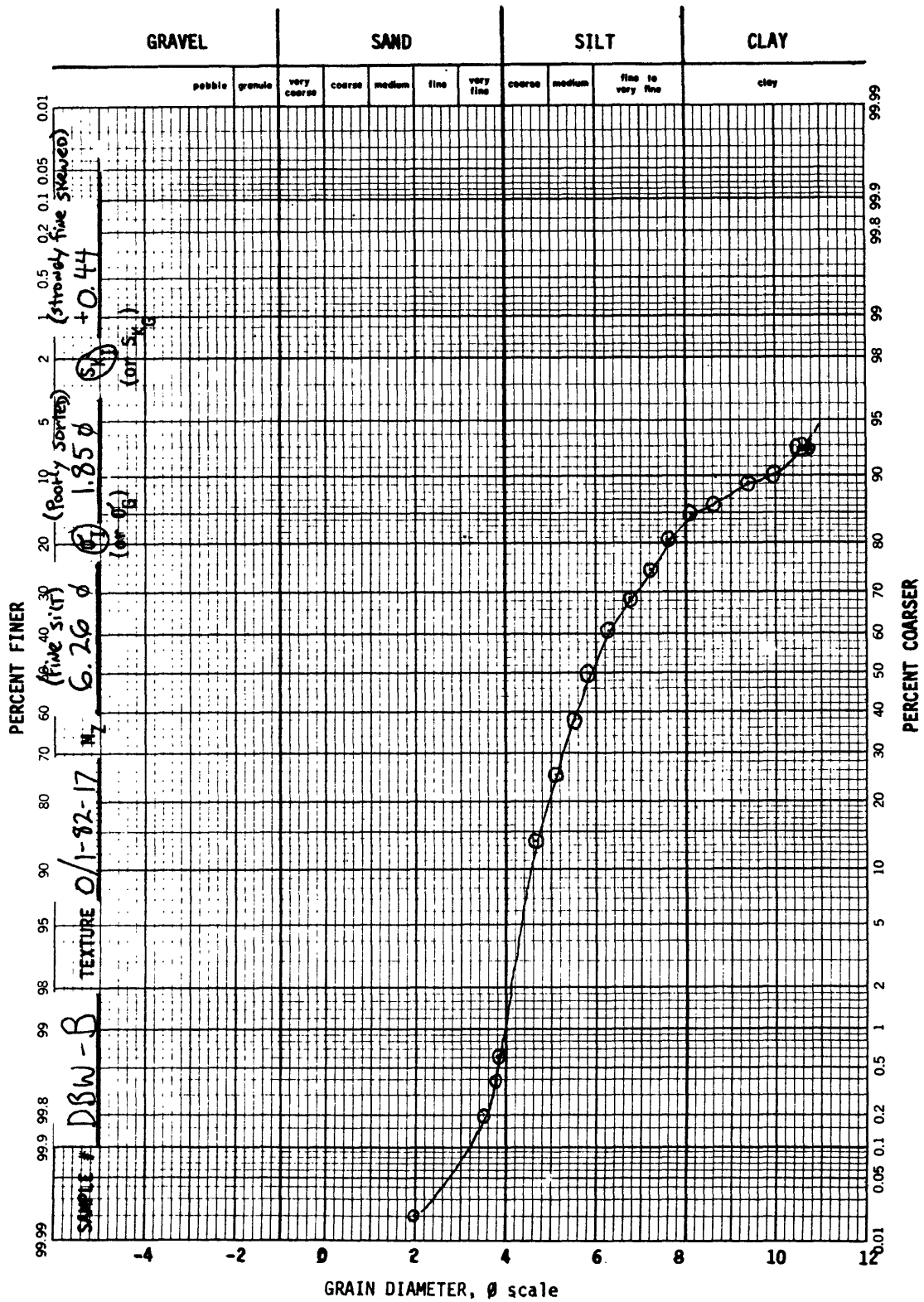
Graphic Skewness ( $S_{K_G}$ ) or Inclusive Graphic Skewness ( $S_{K_I}$ )

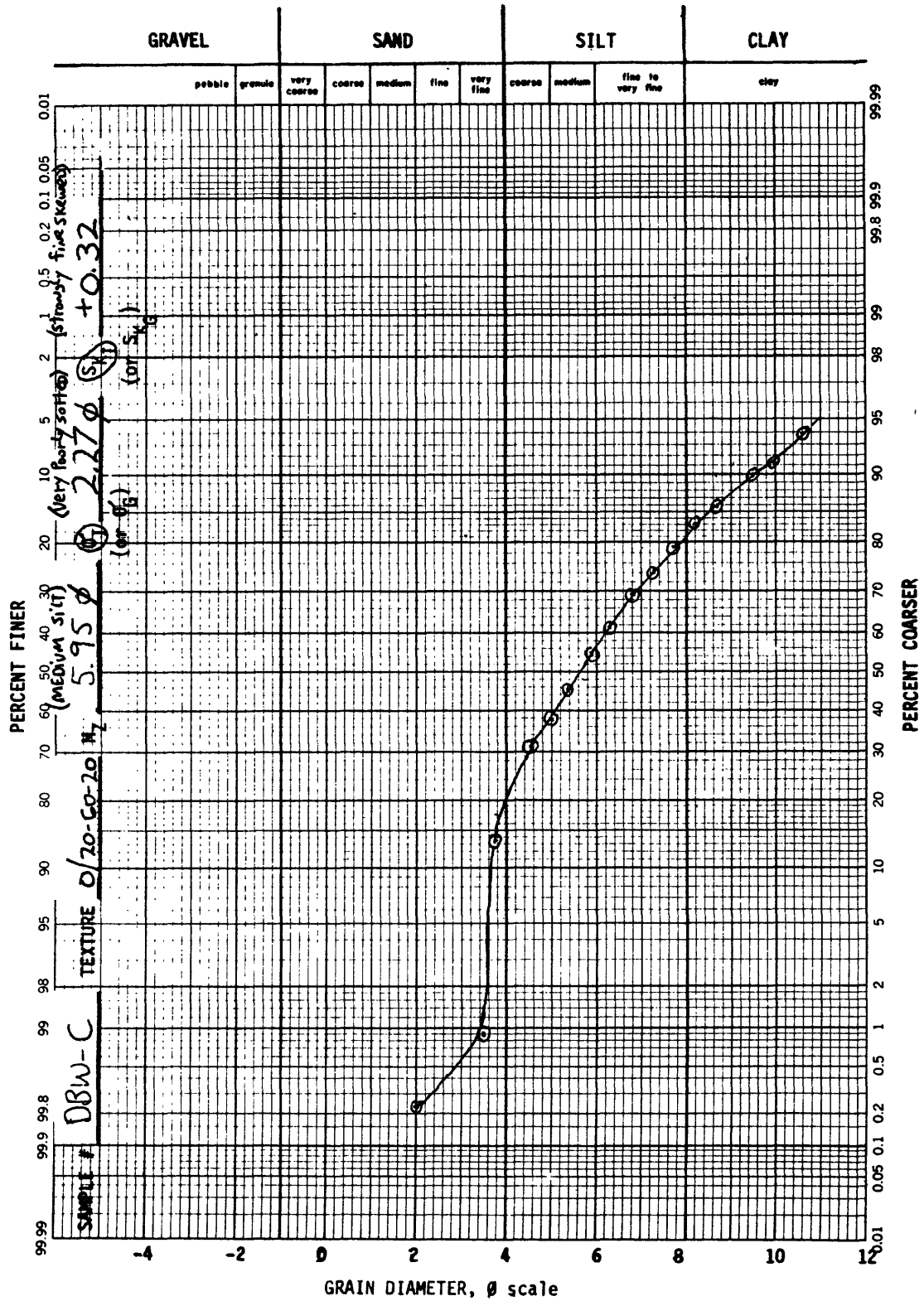
The graphic skewness is an indicator of the amount of asymmetry of the distribution curve. In essence, it is a measure of the amount of displacement of the median ( $\phi_{50}$ ) from the graphic mean ( $M_Z$ ). Thus, graphic skewness is a

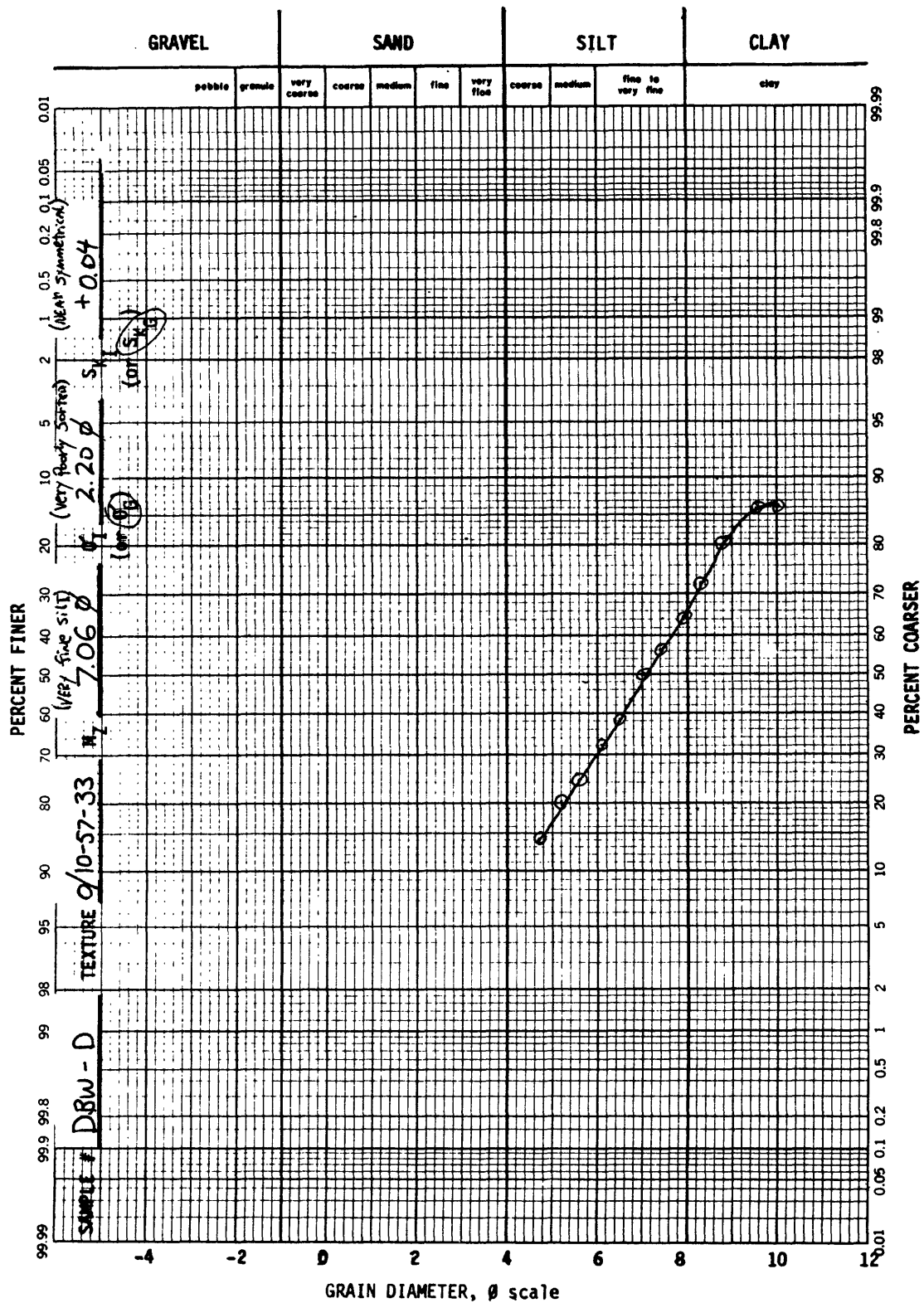


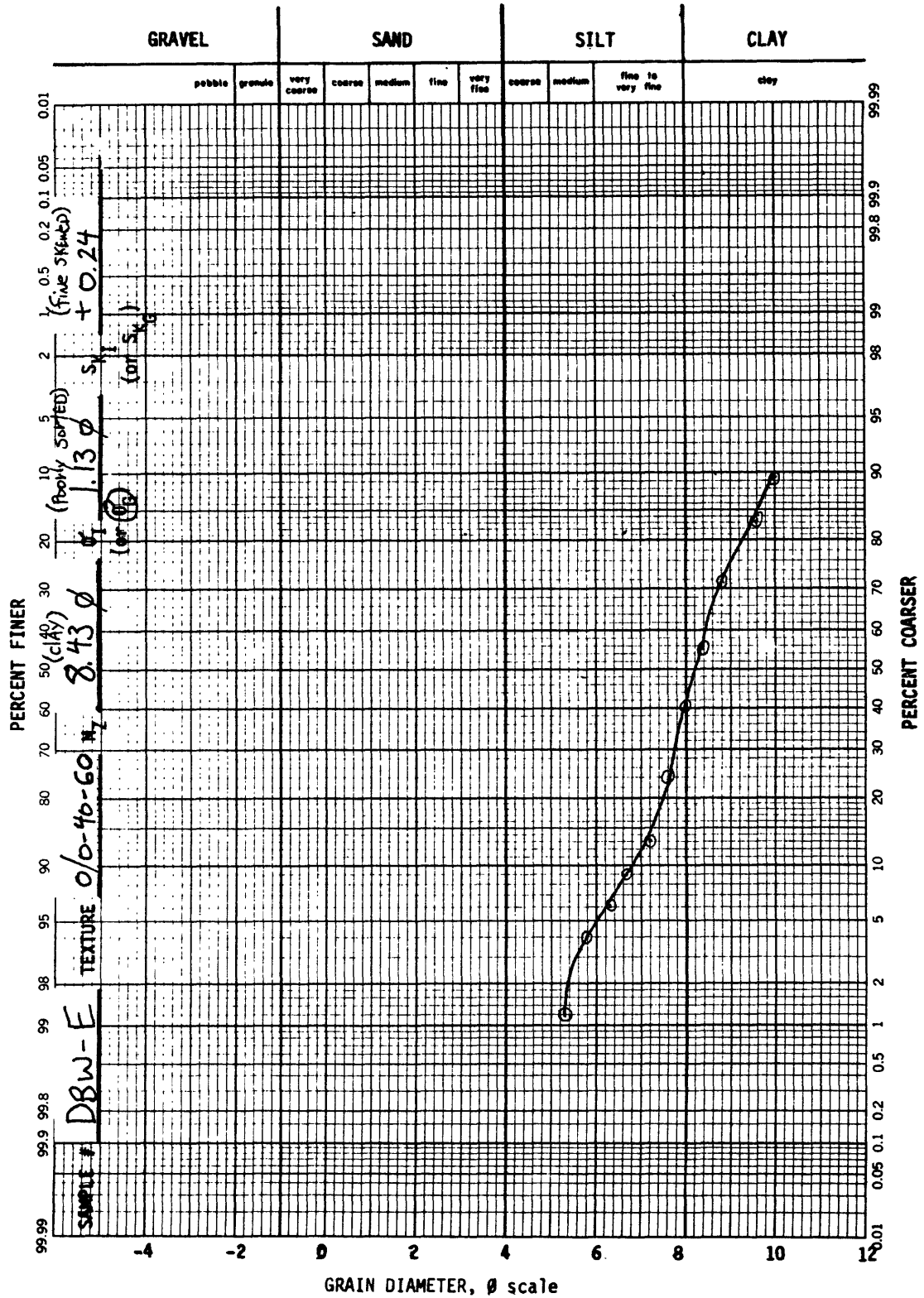




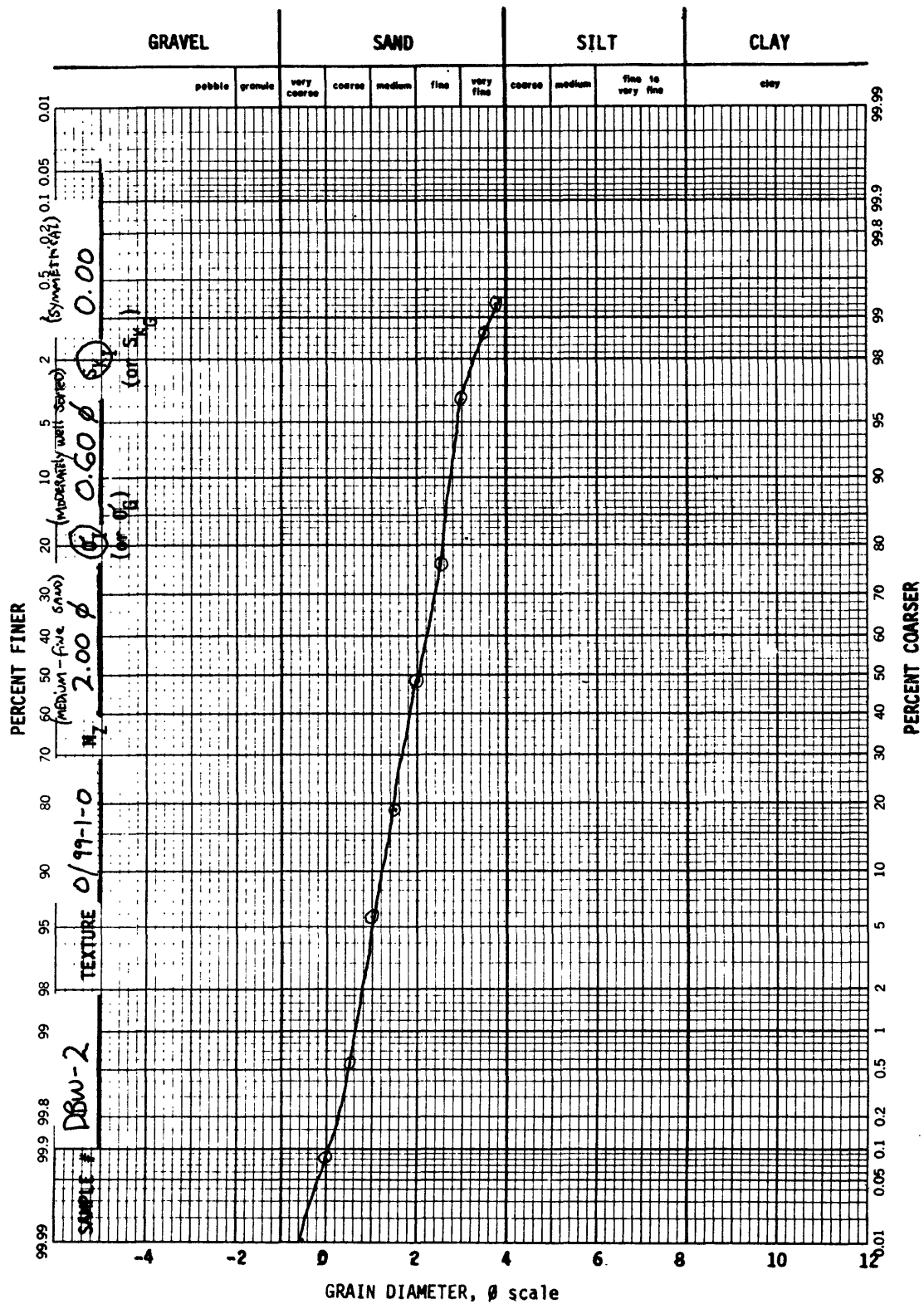




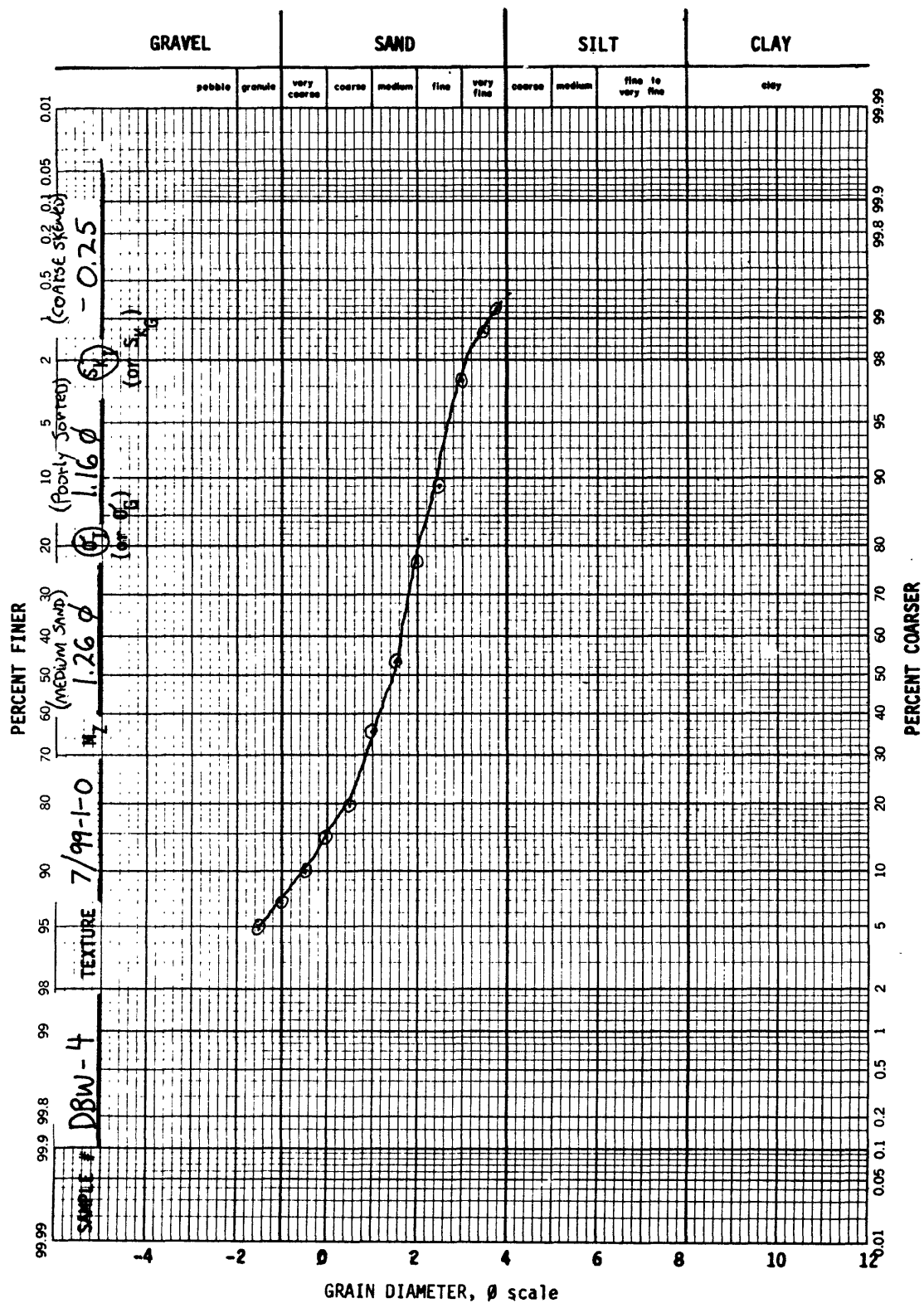




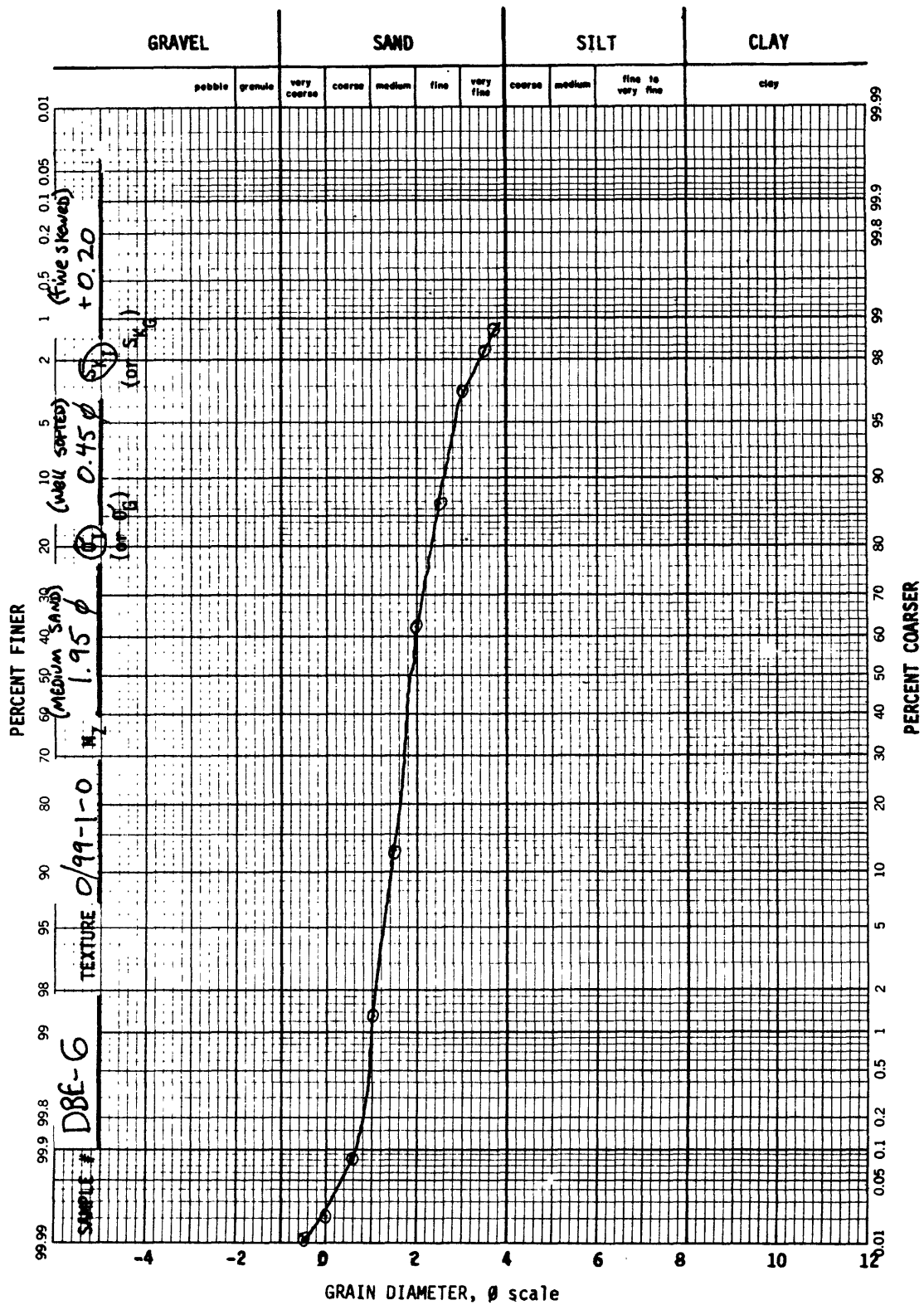




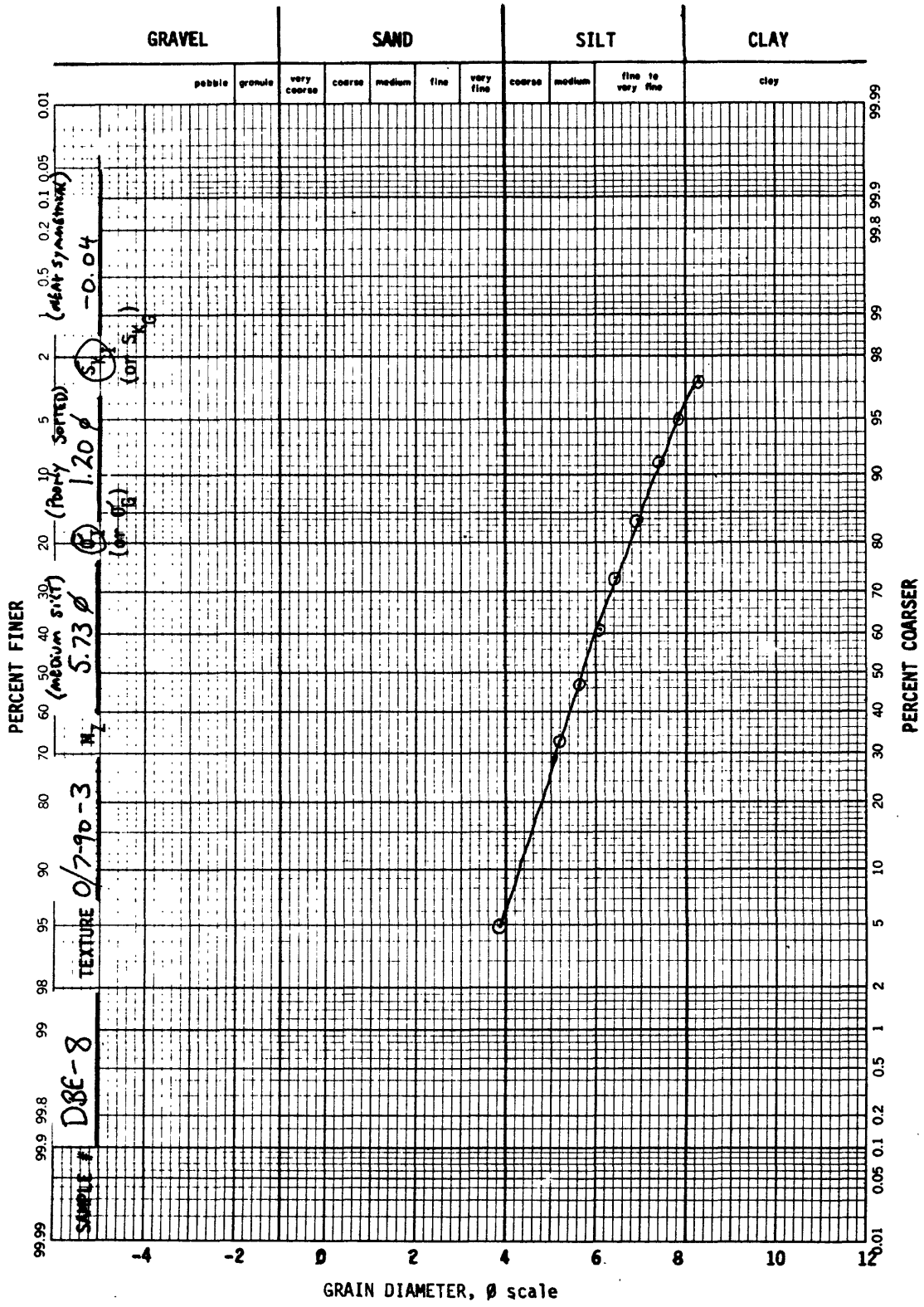


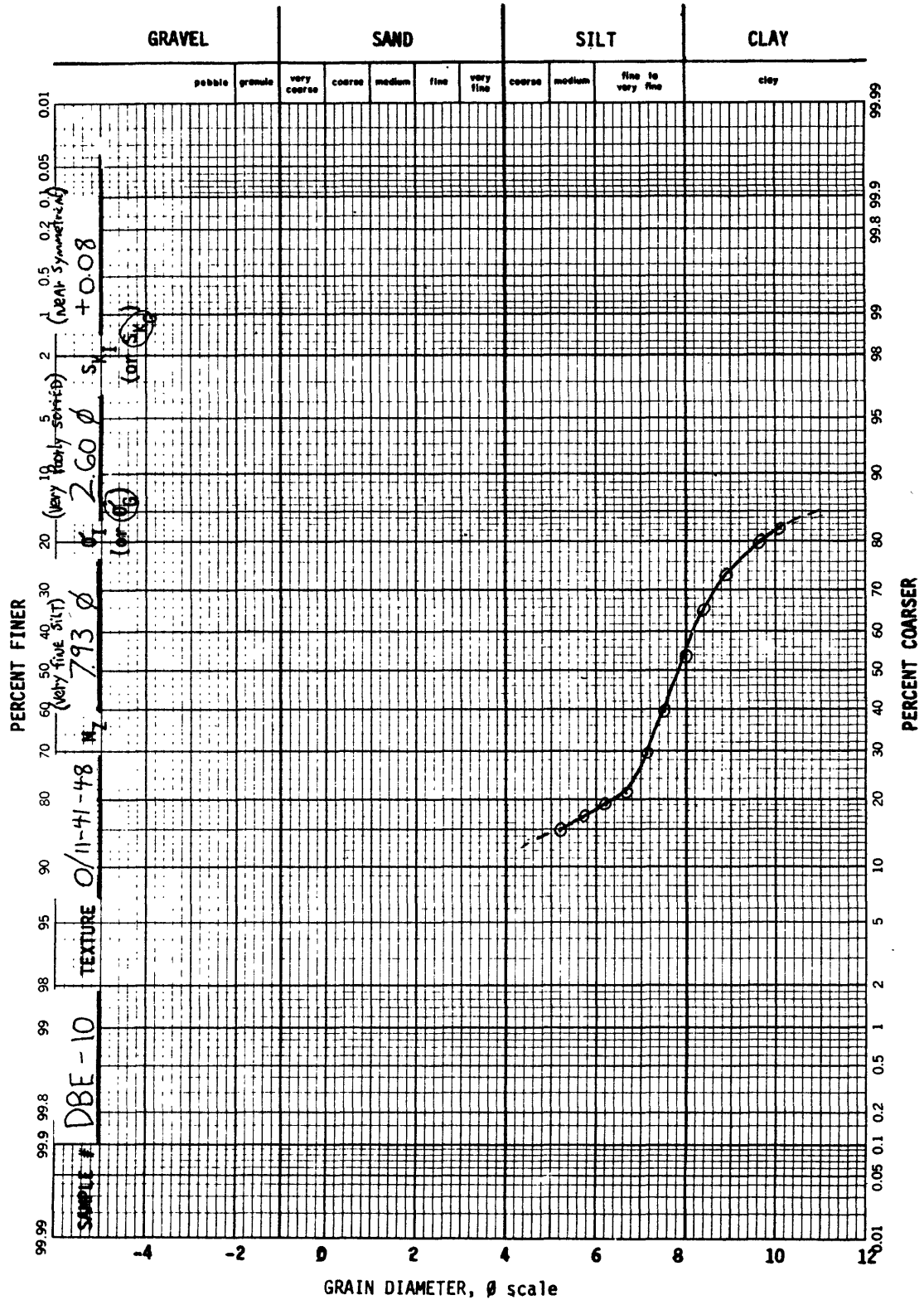


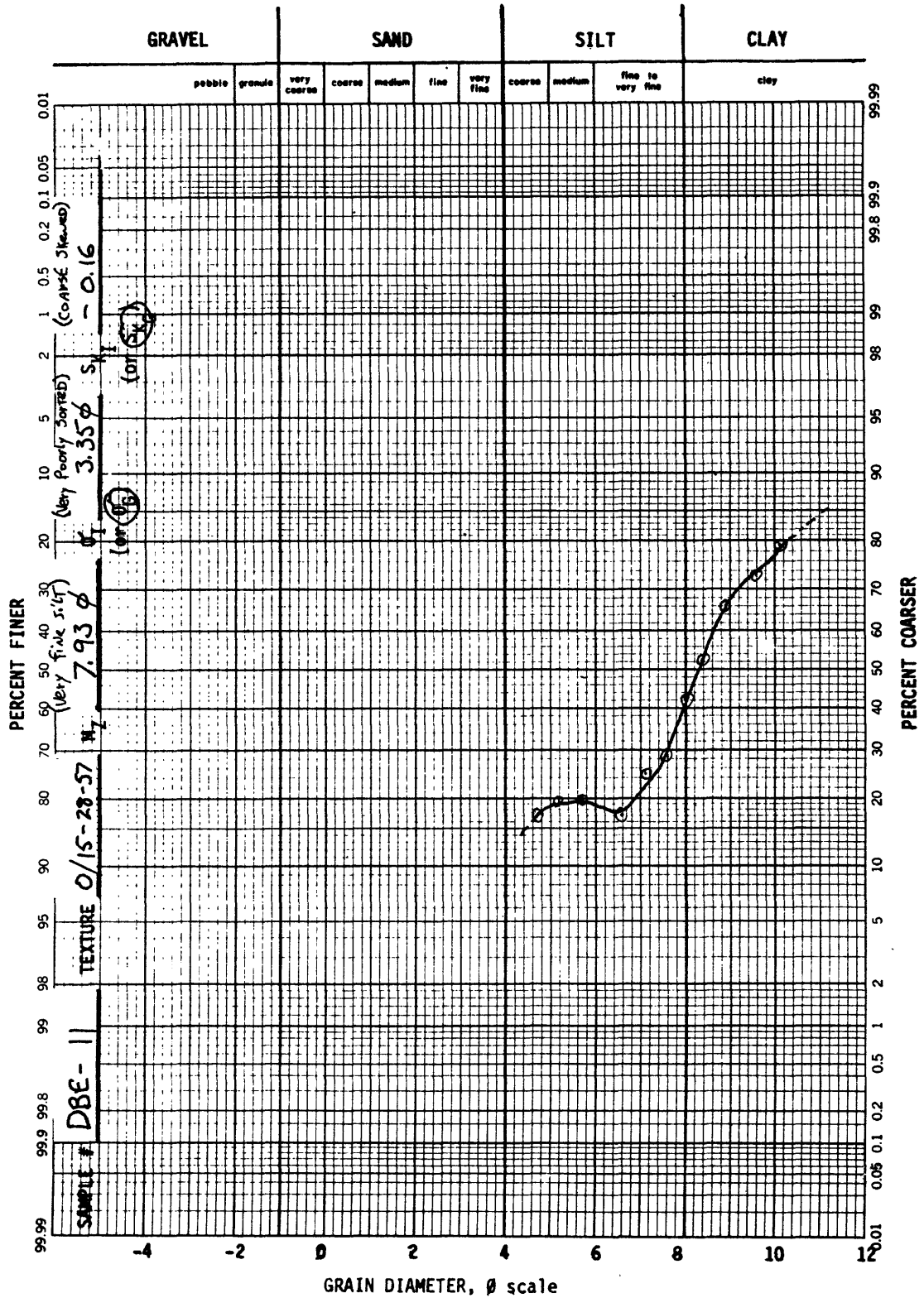


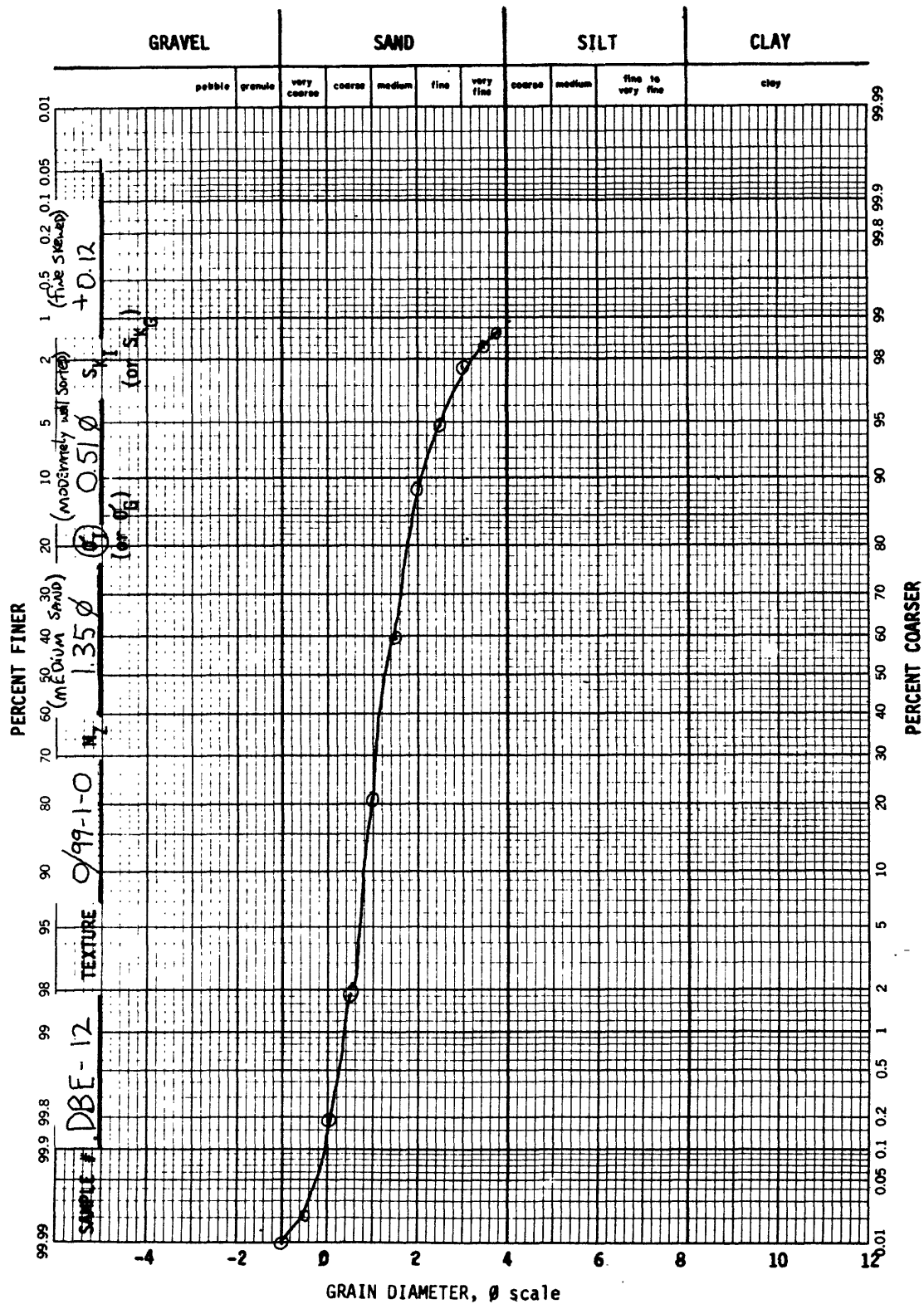


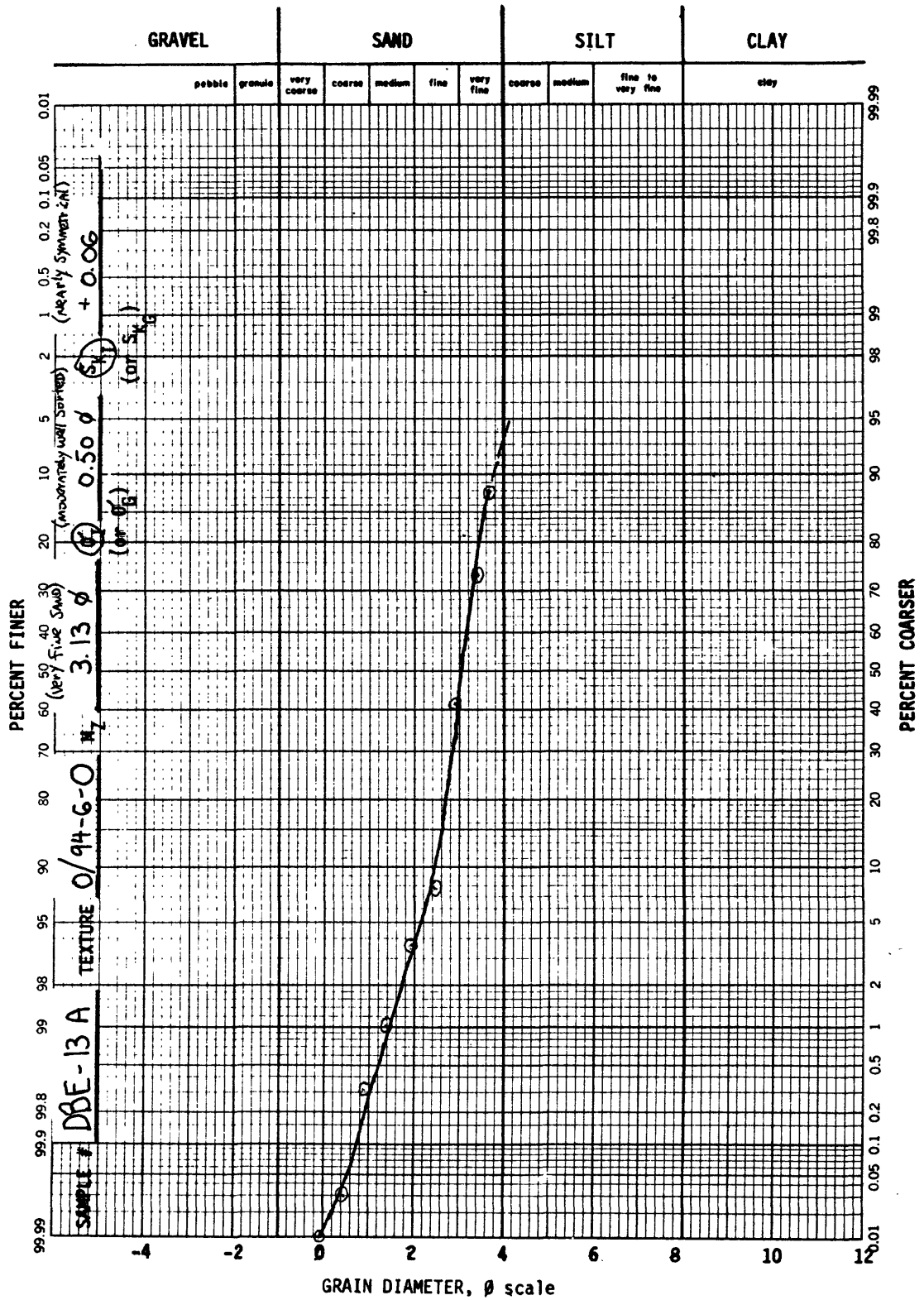


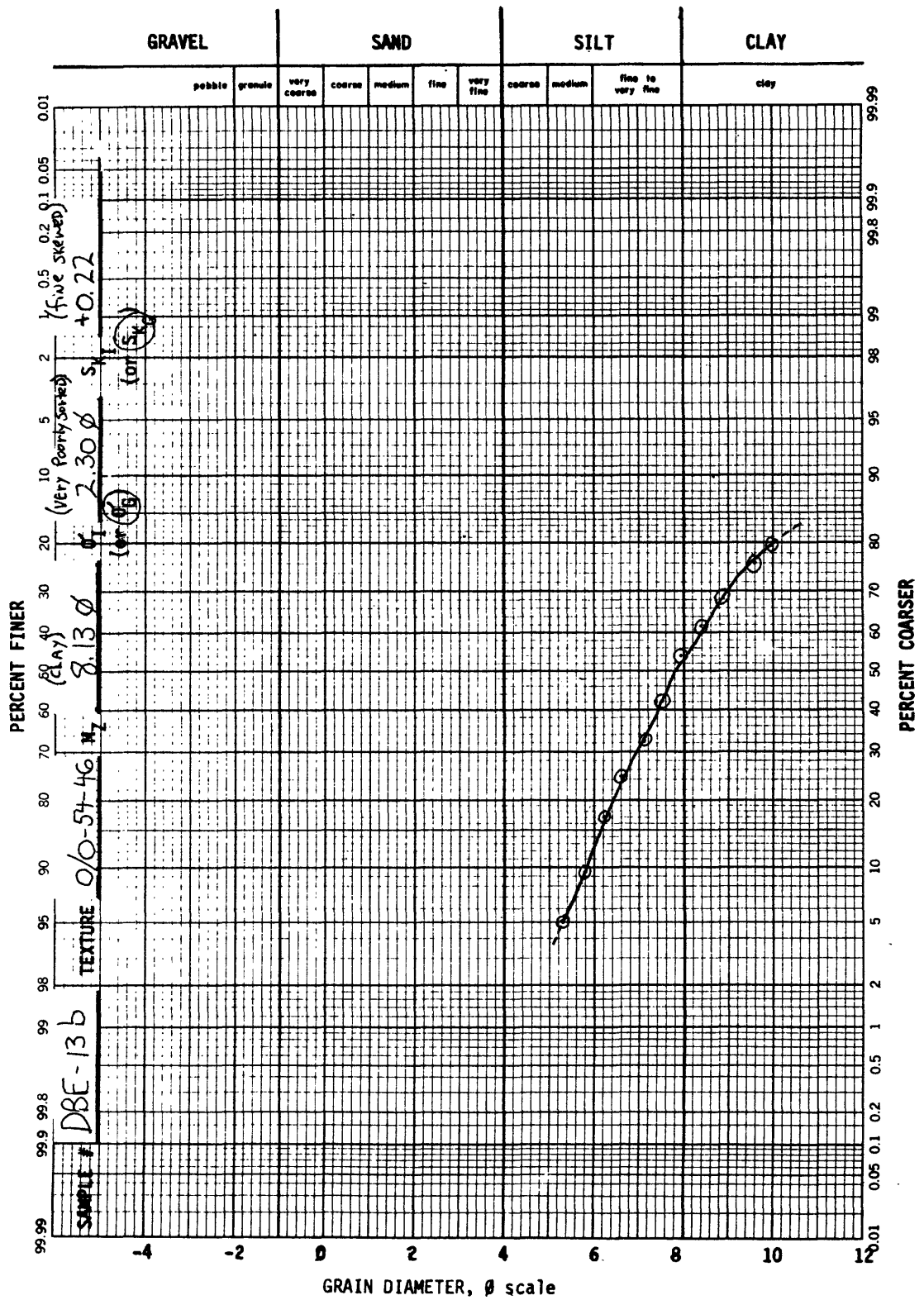




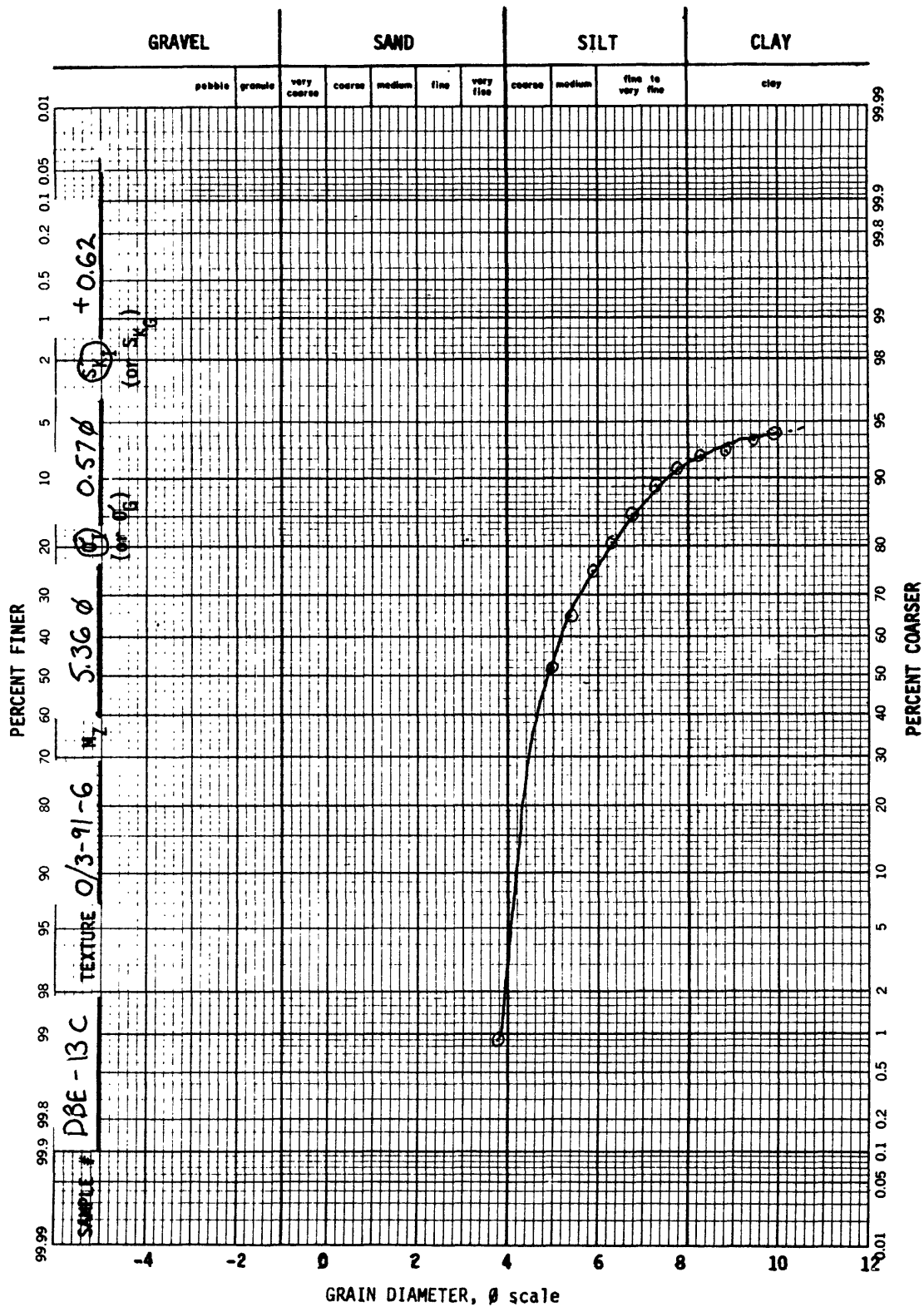




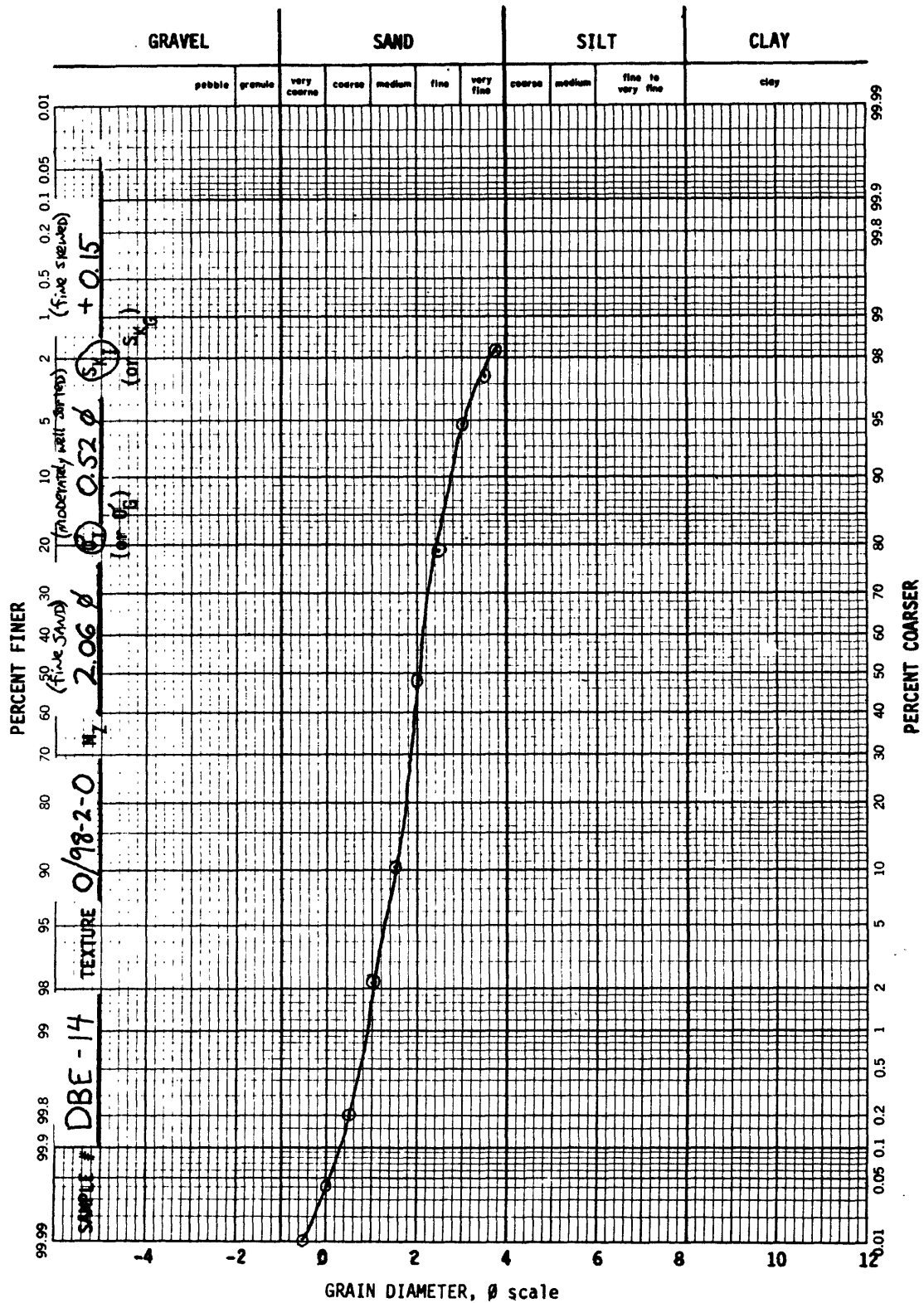


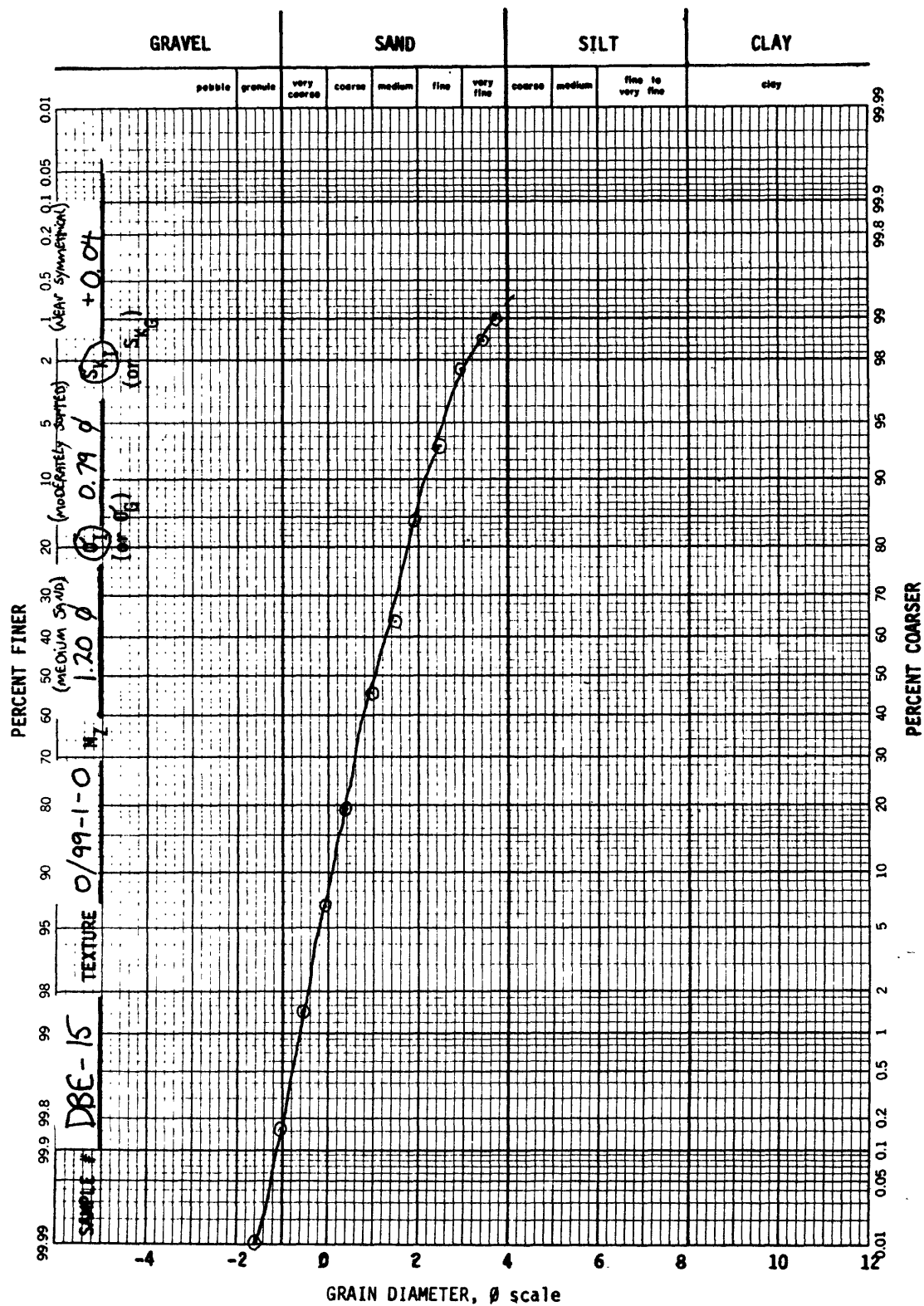






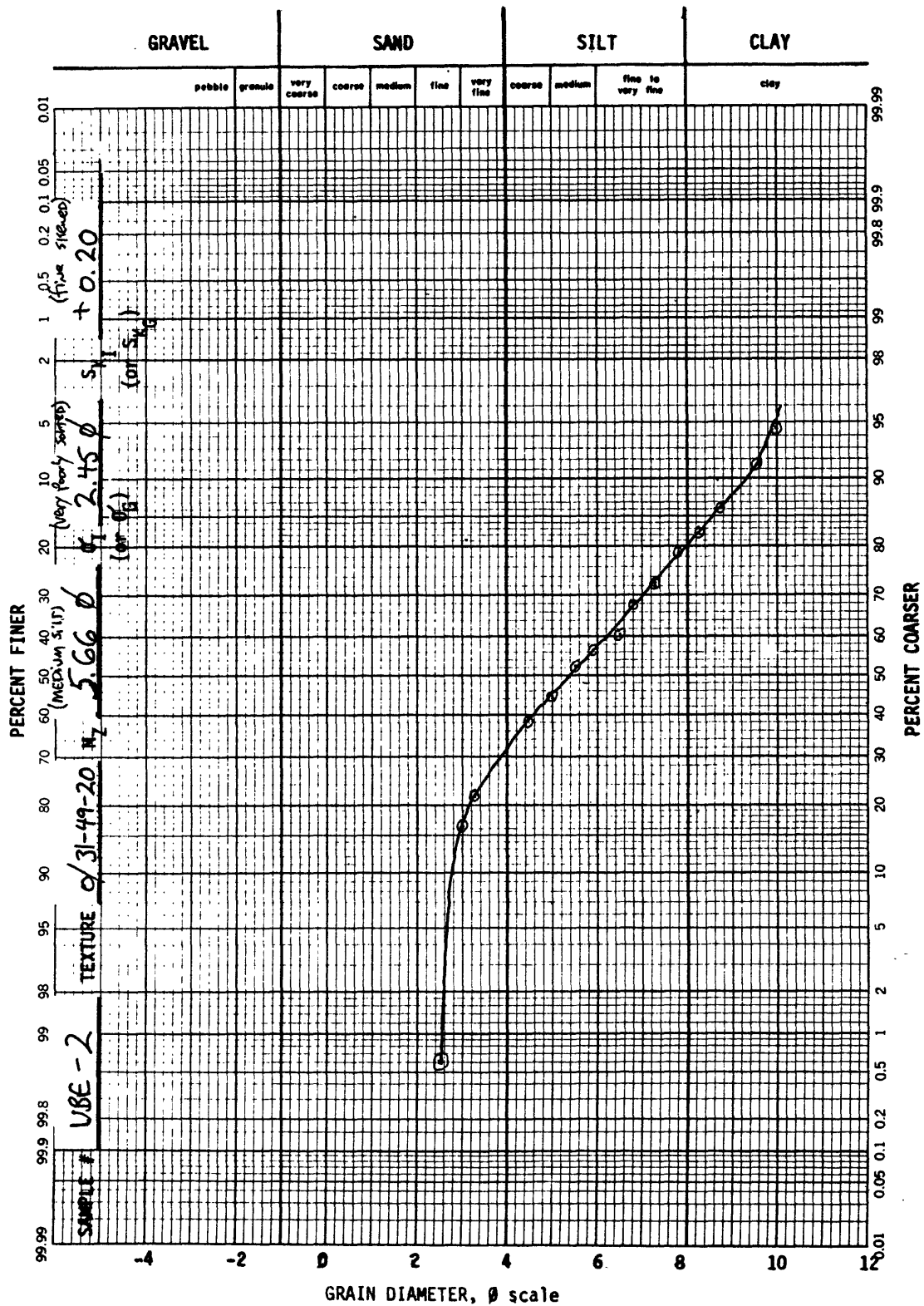


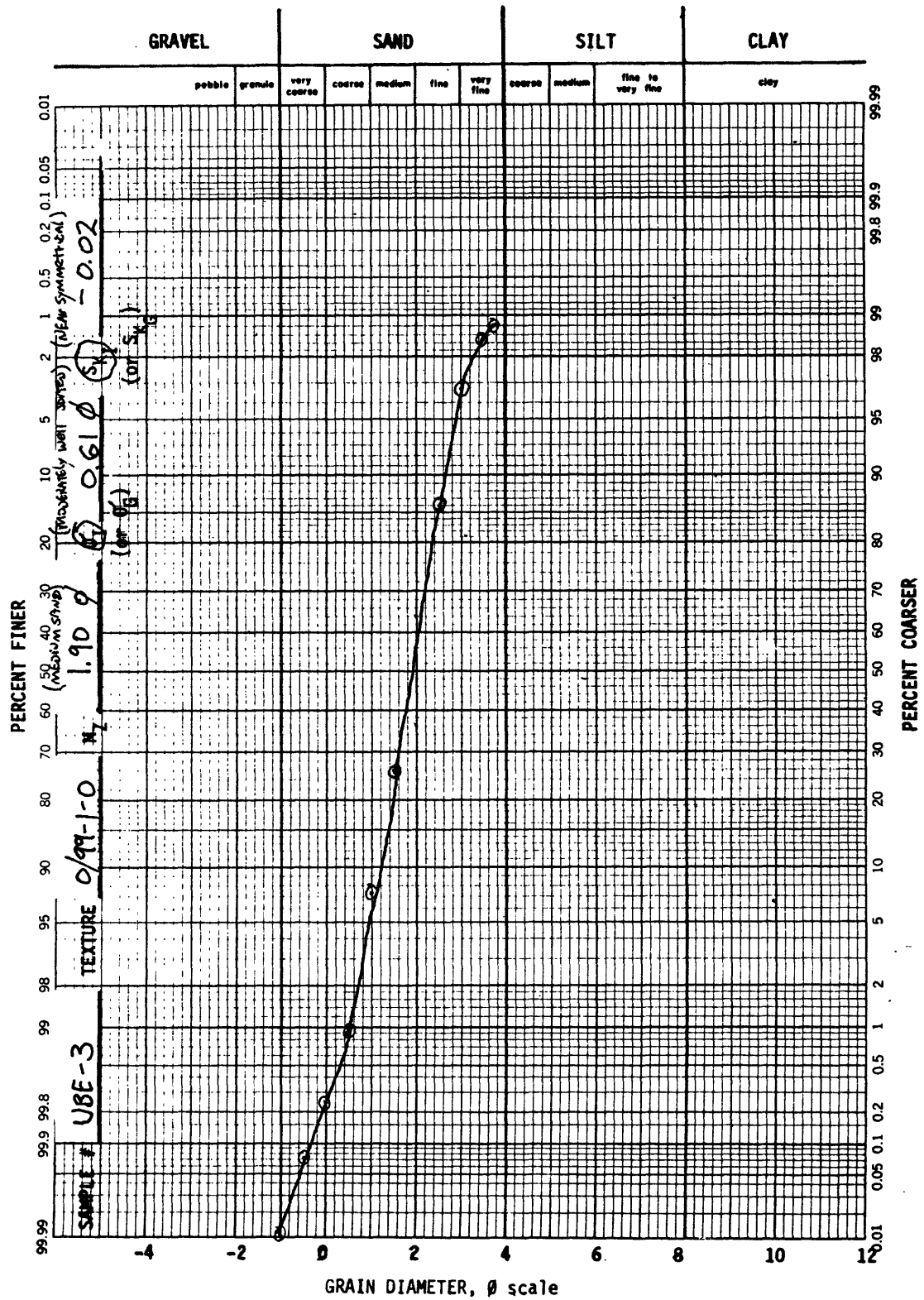




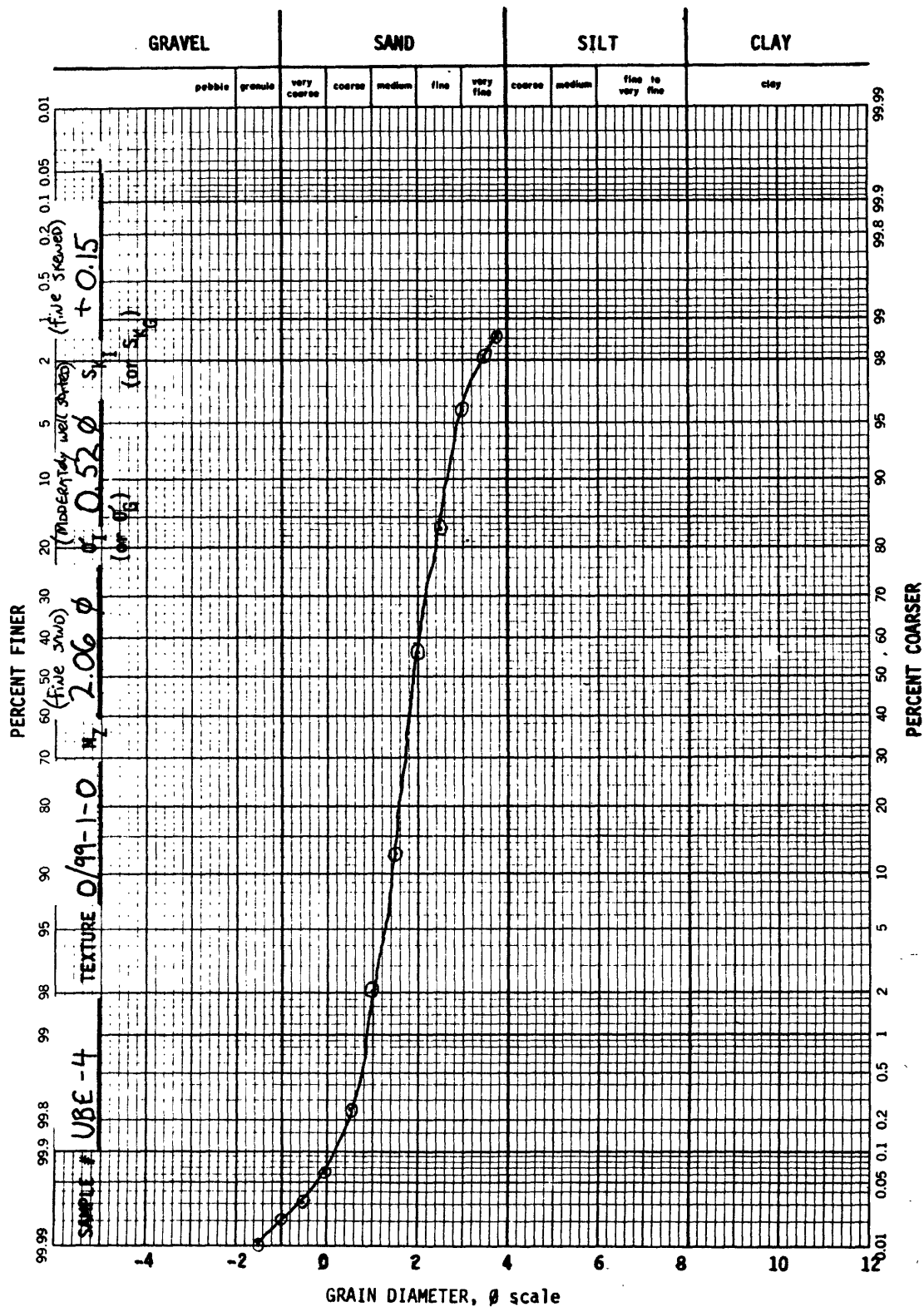


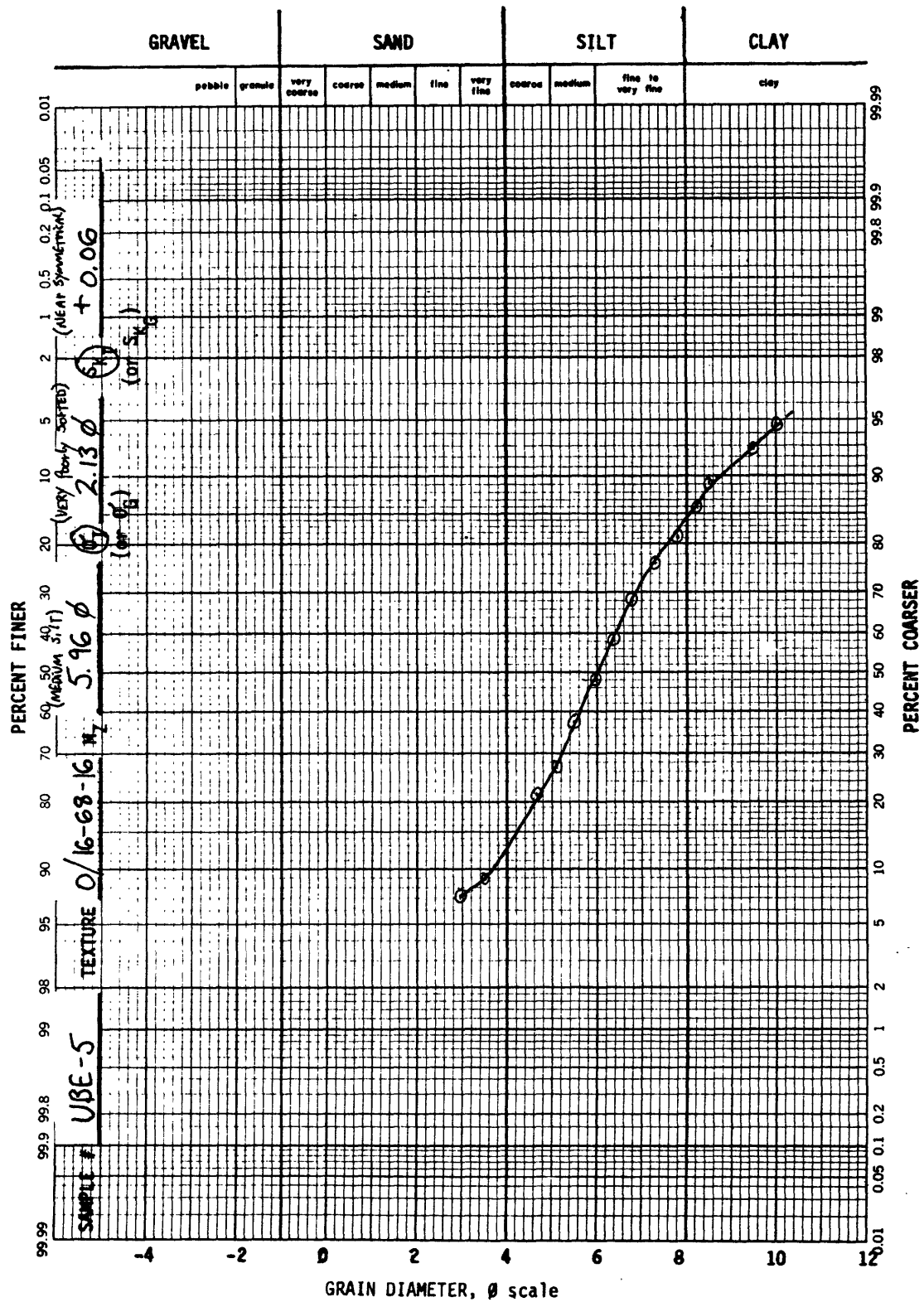




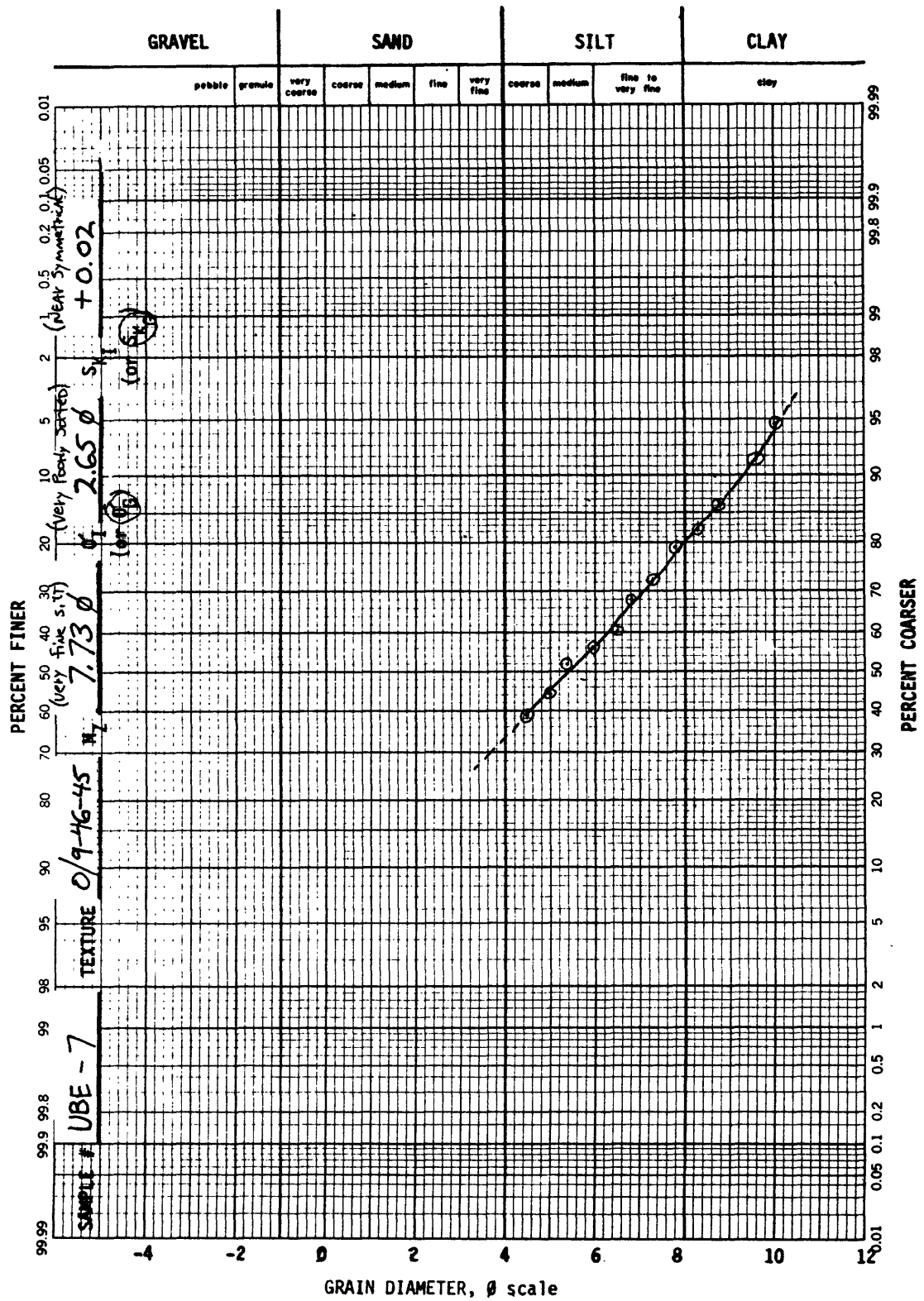


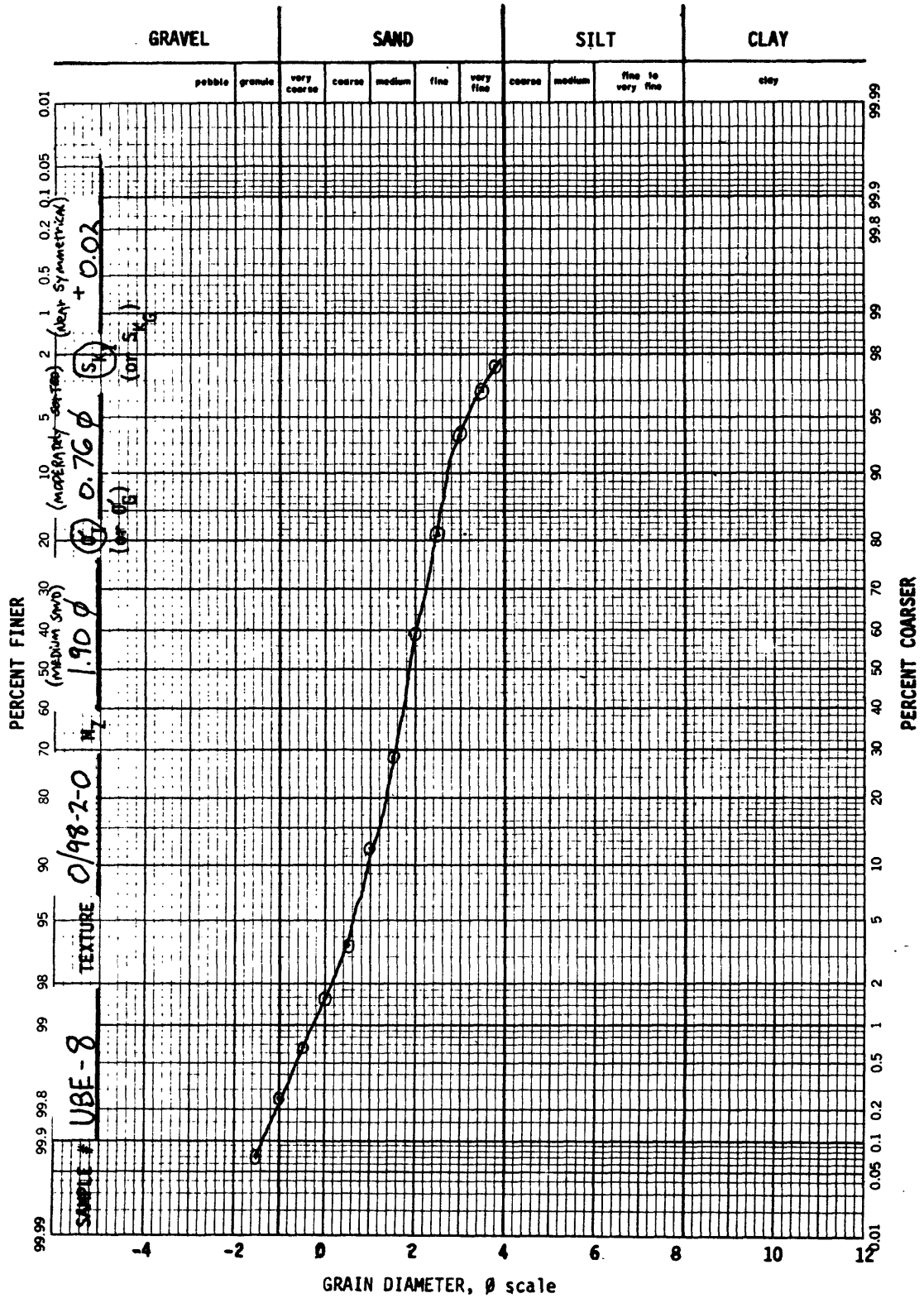


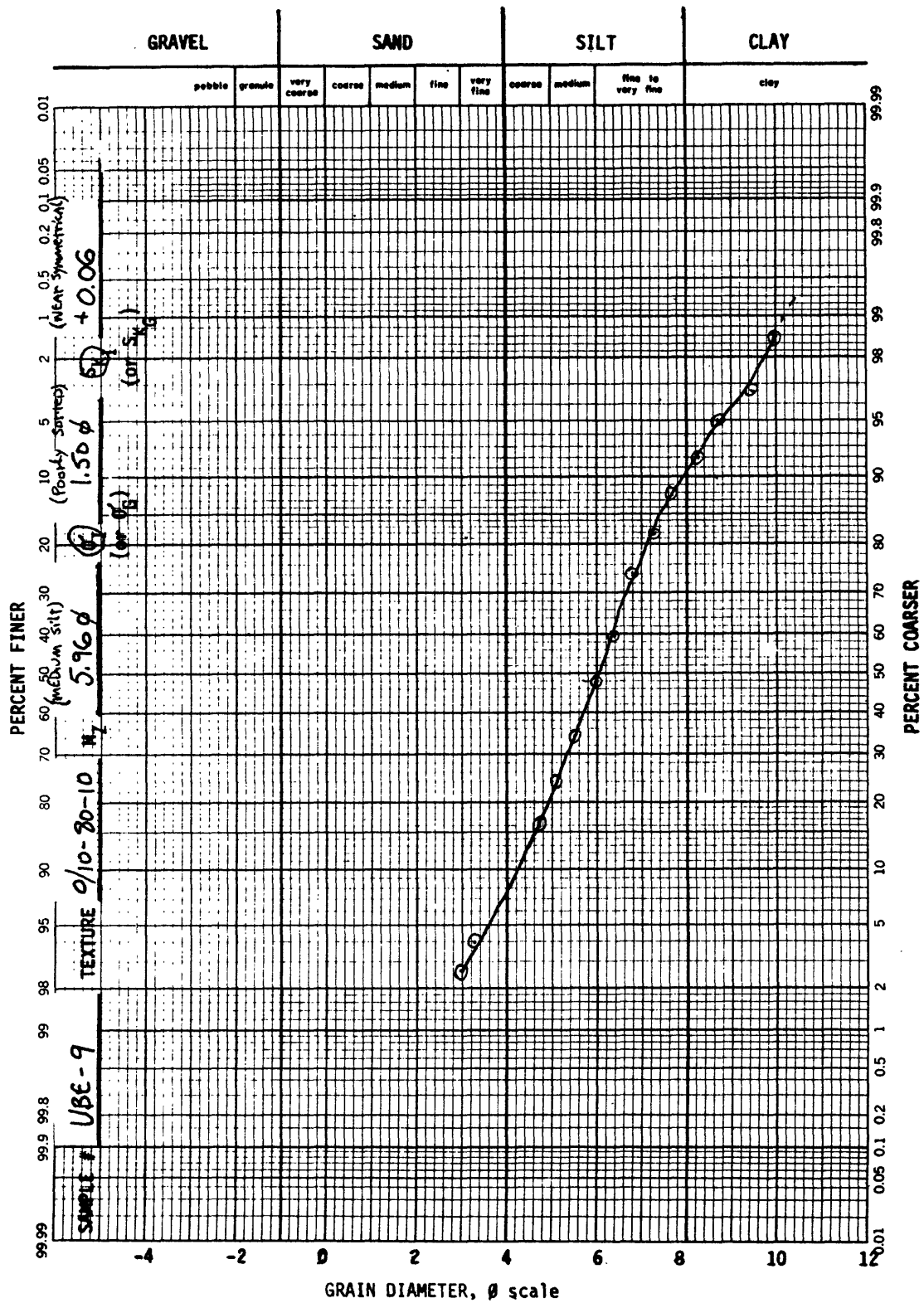


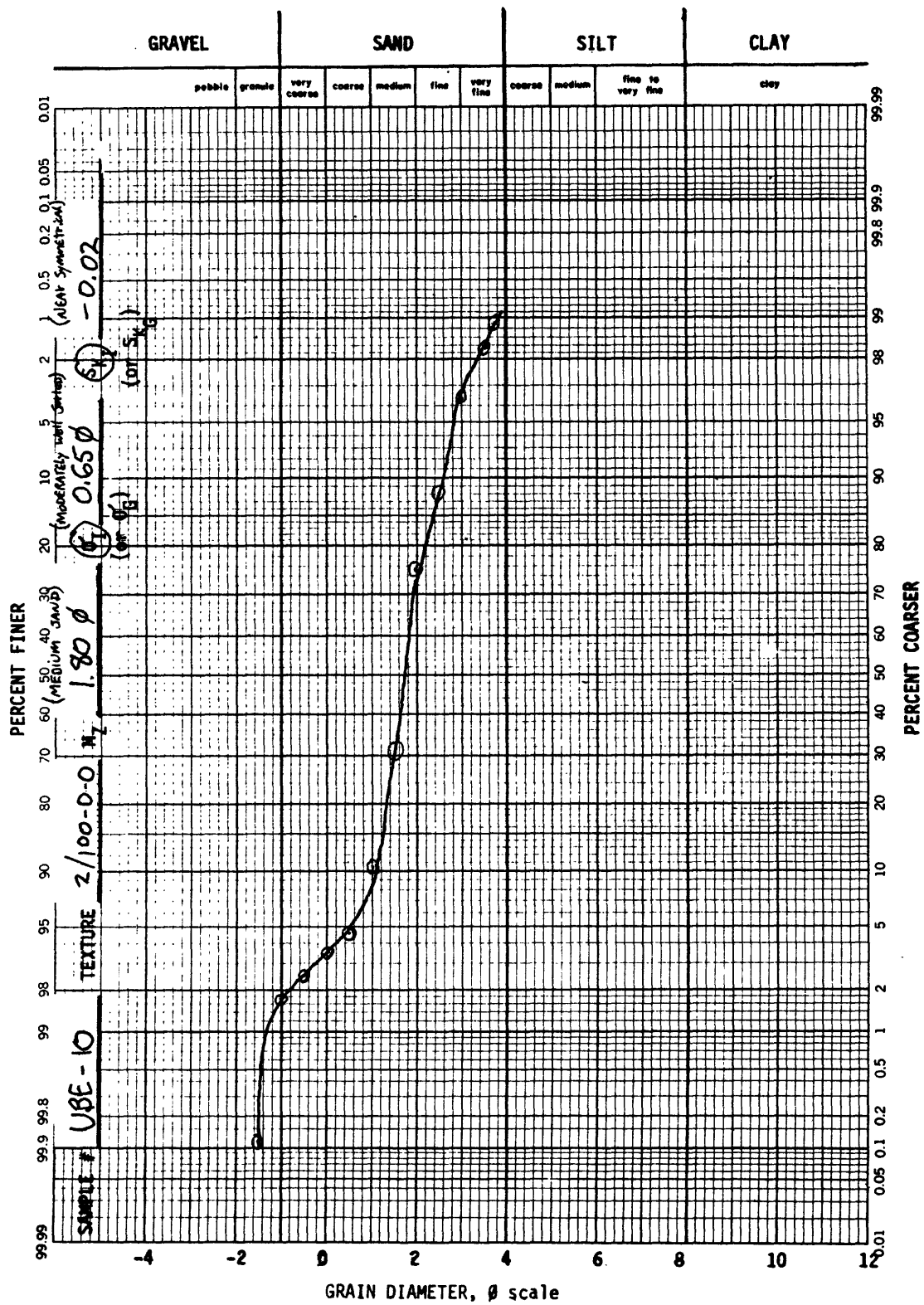


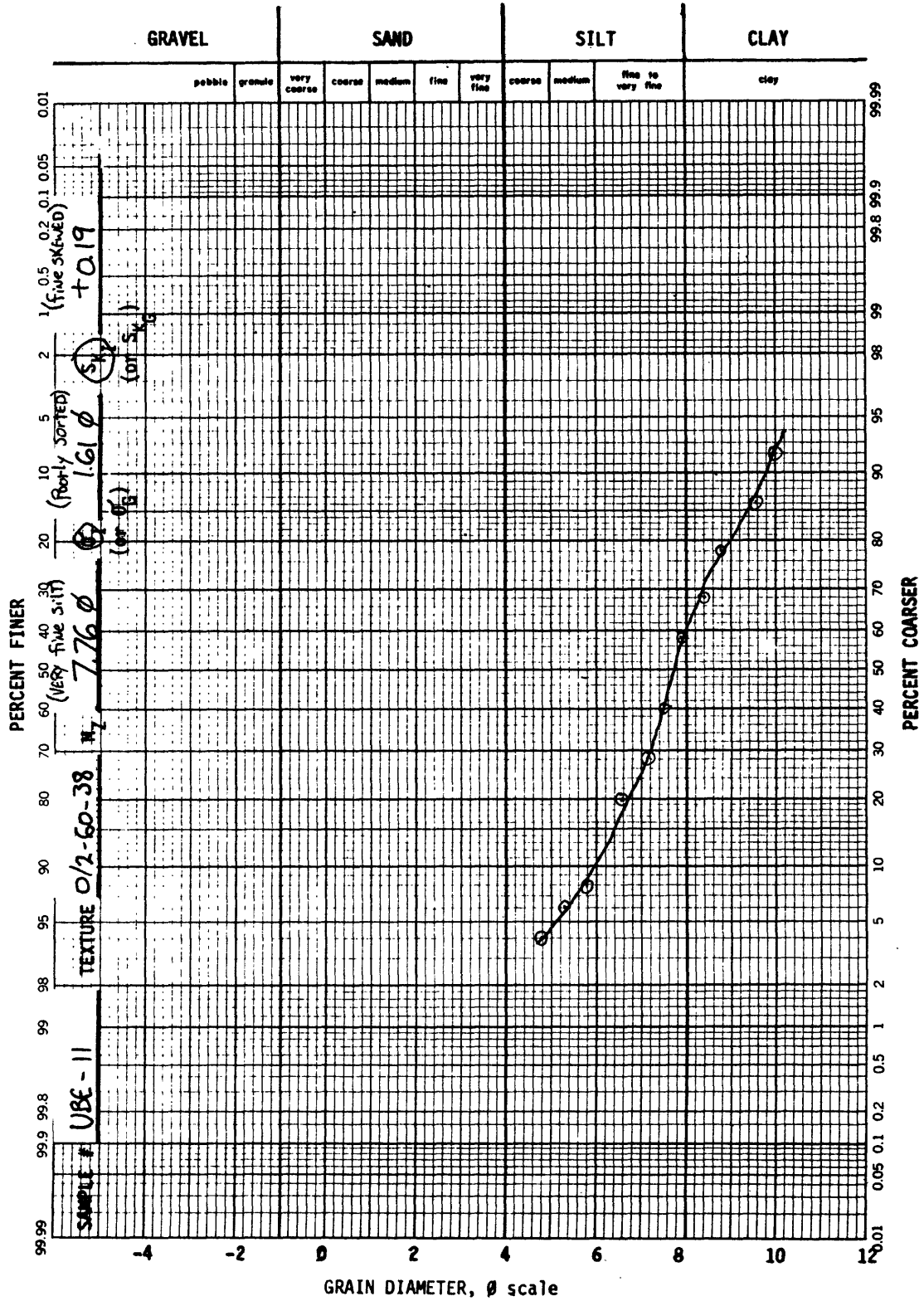




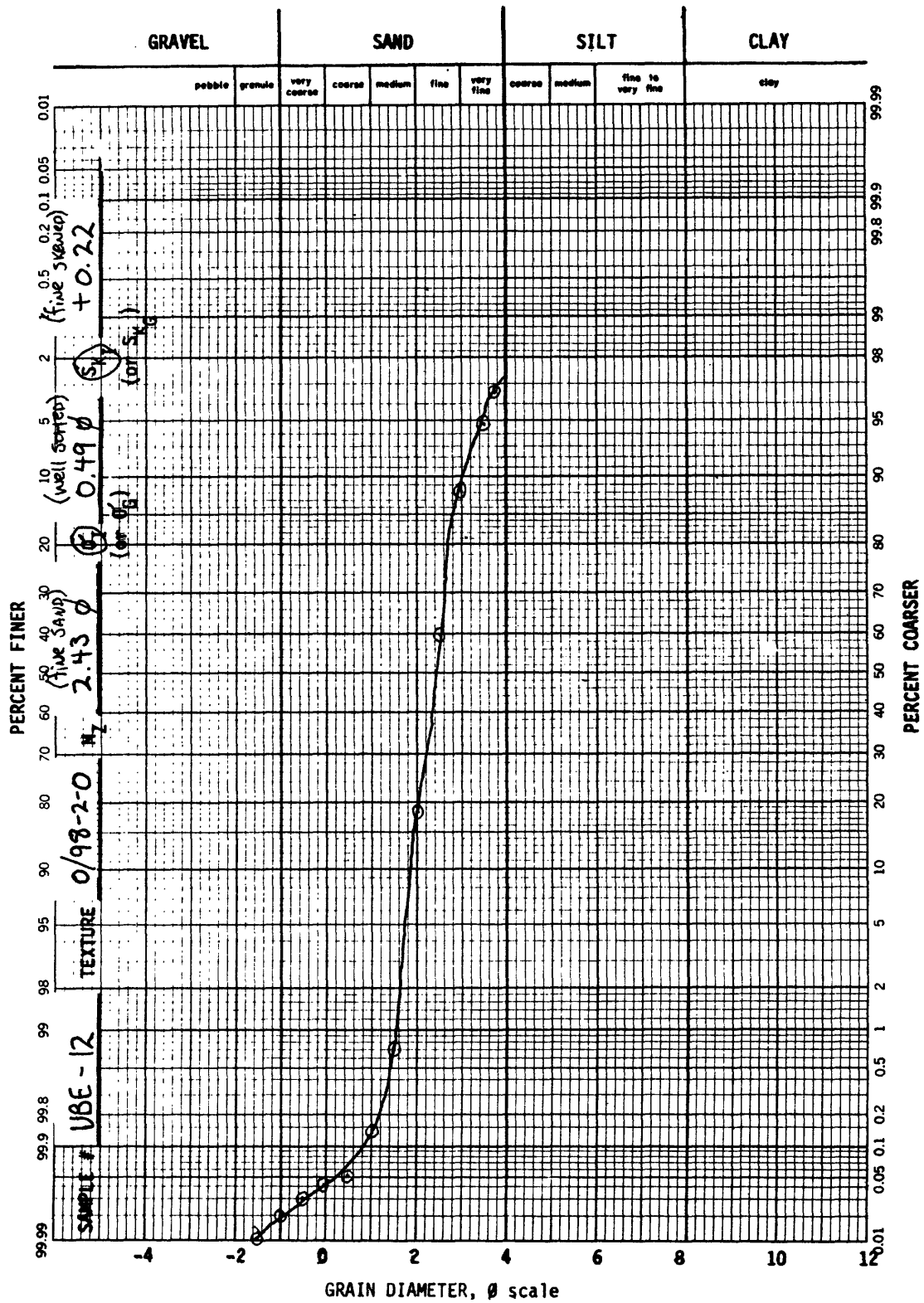


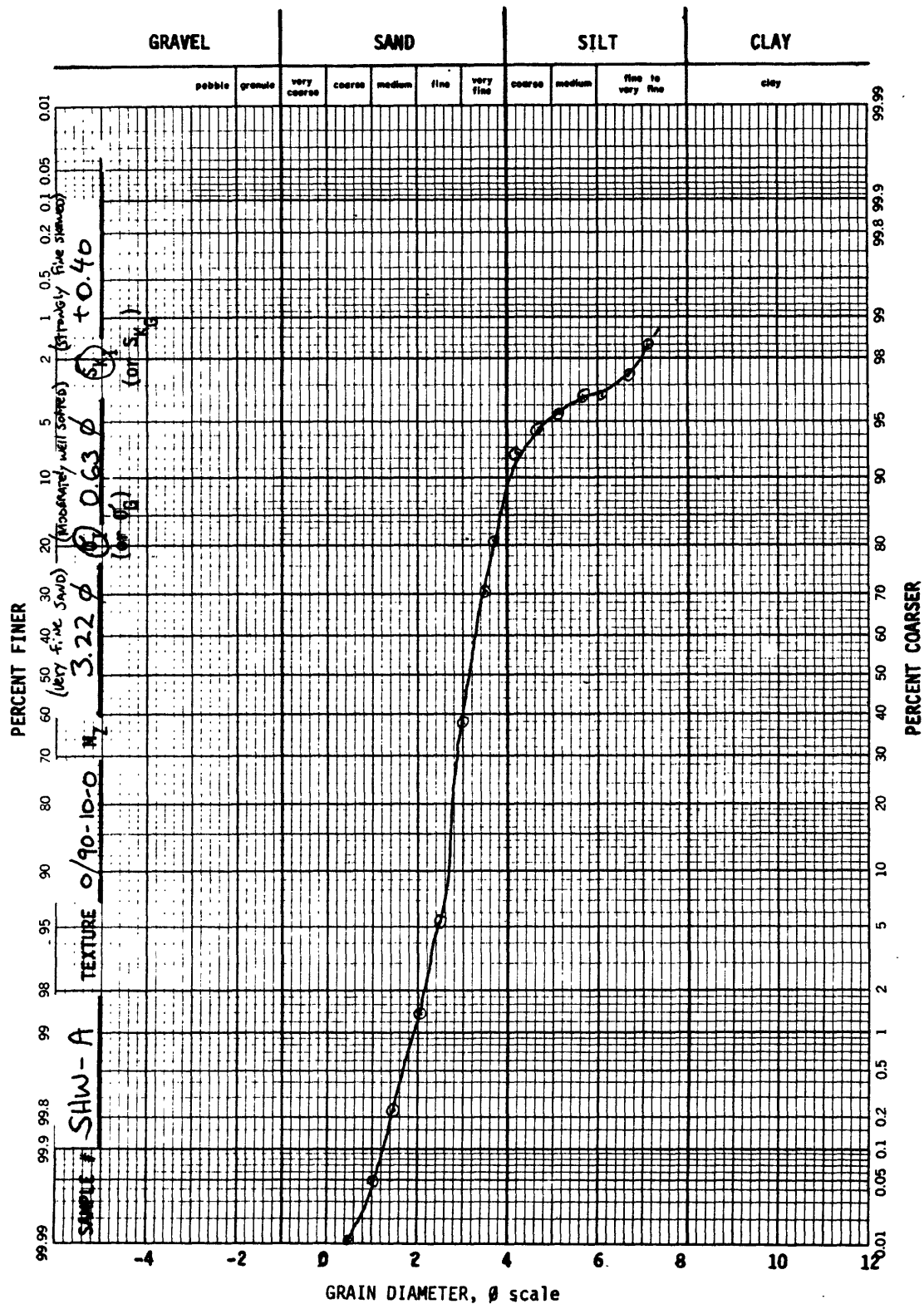


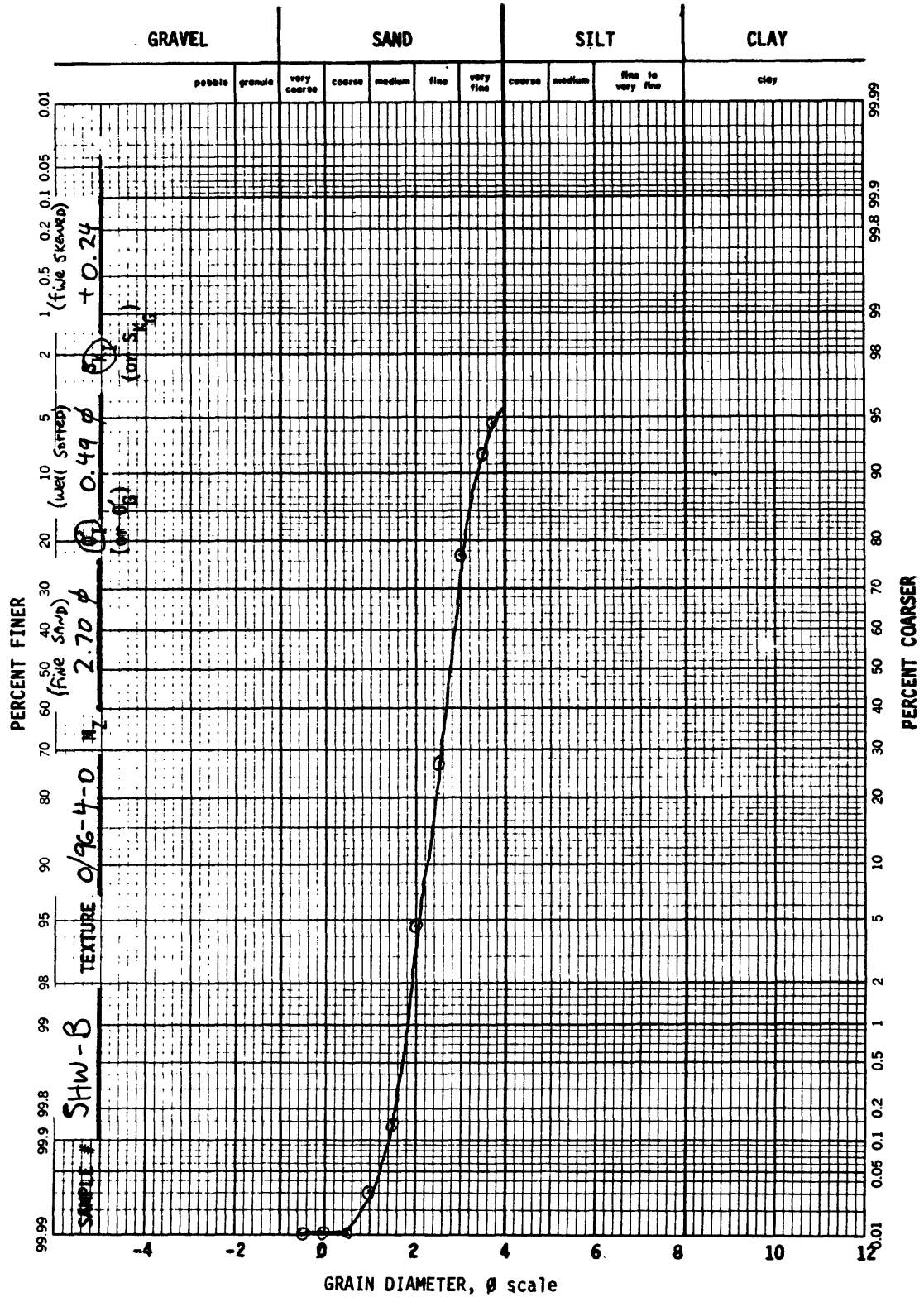


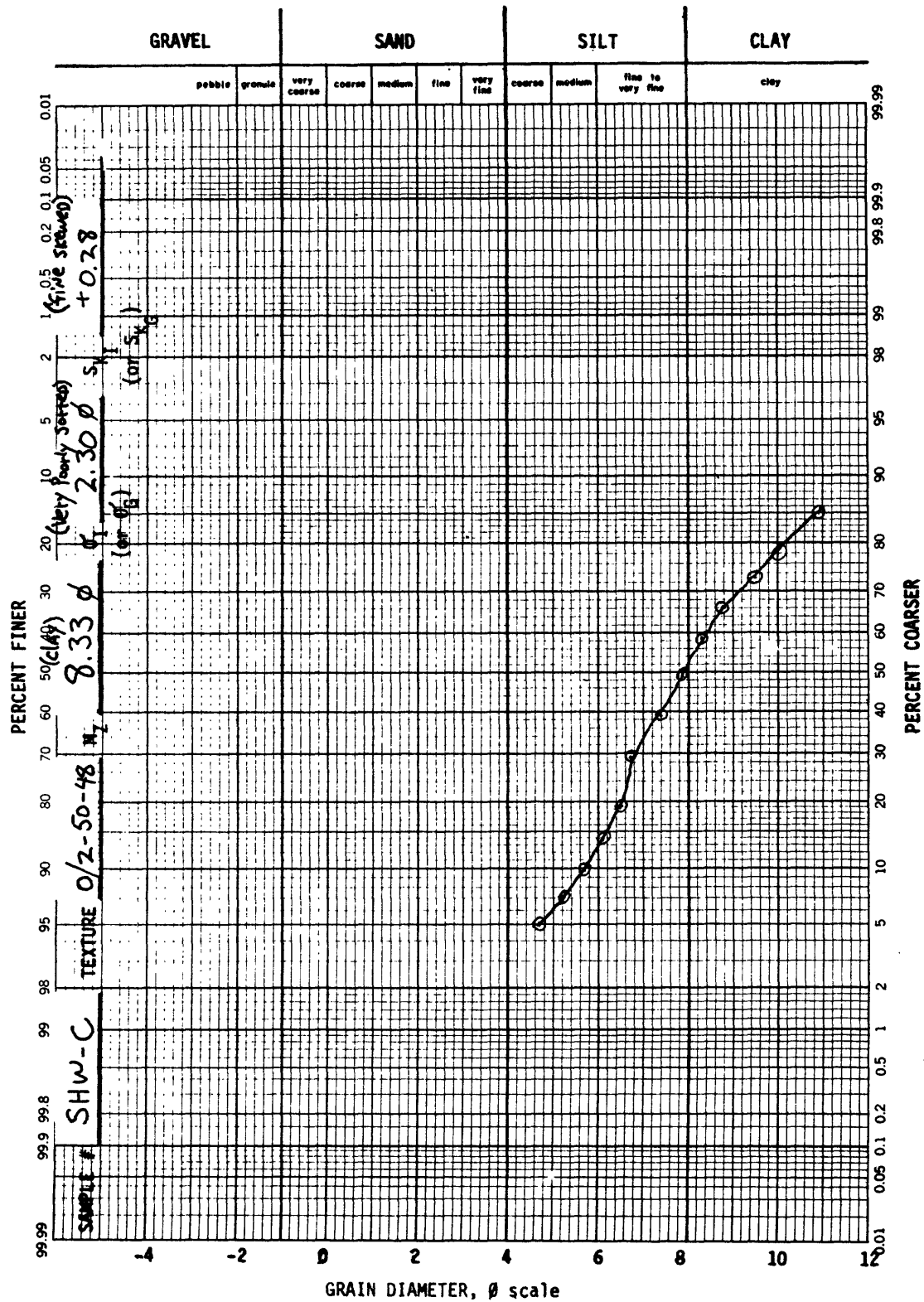


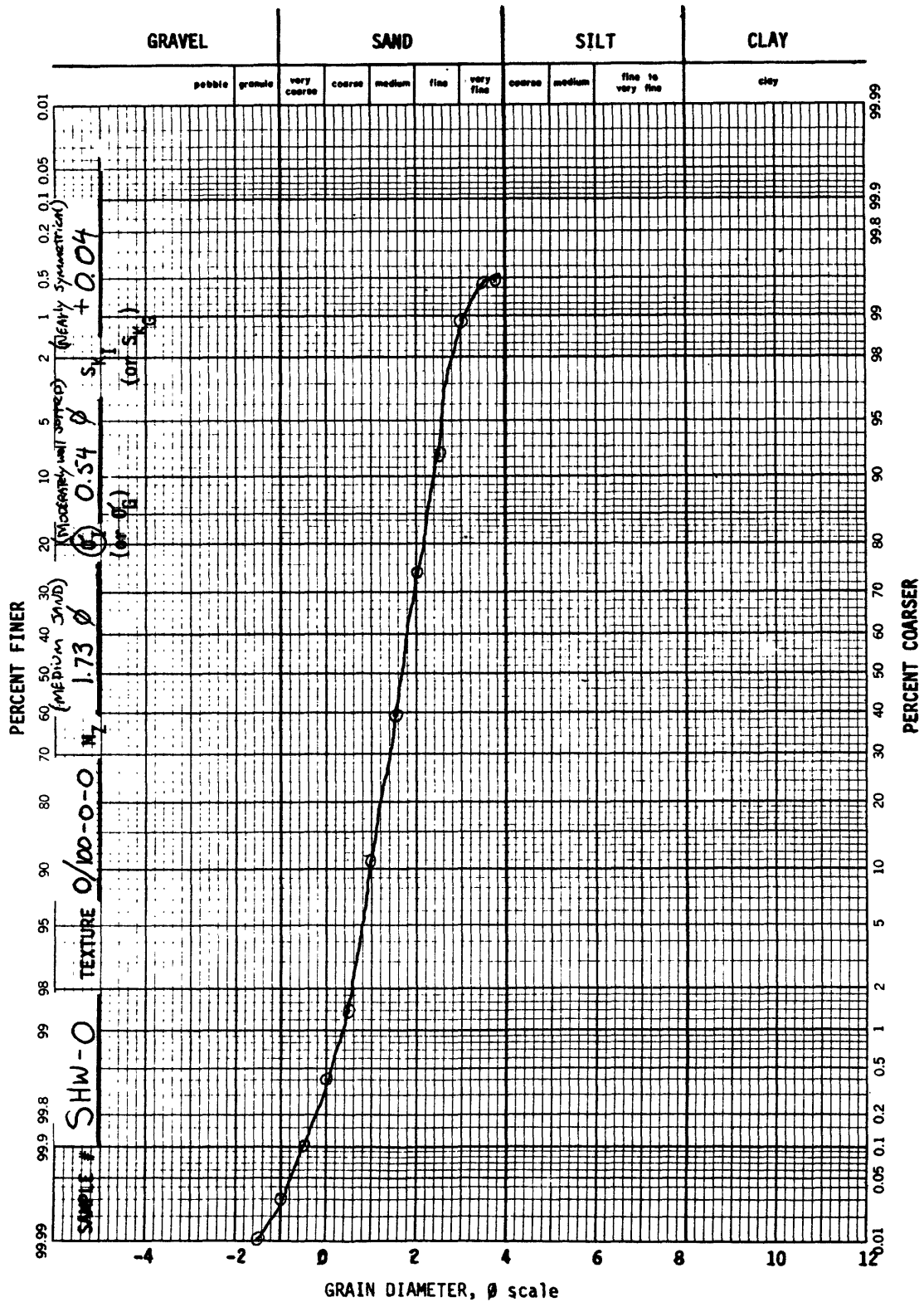


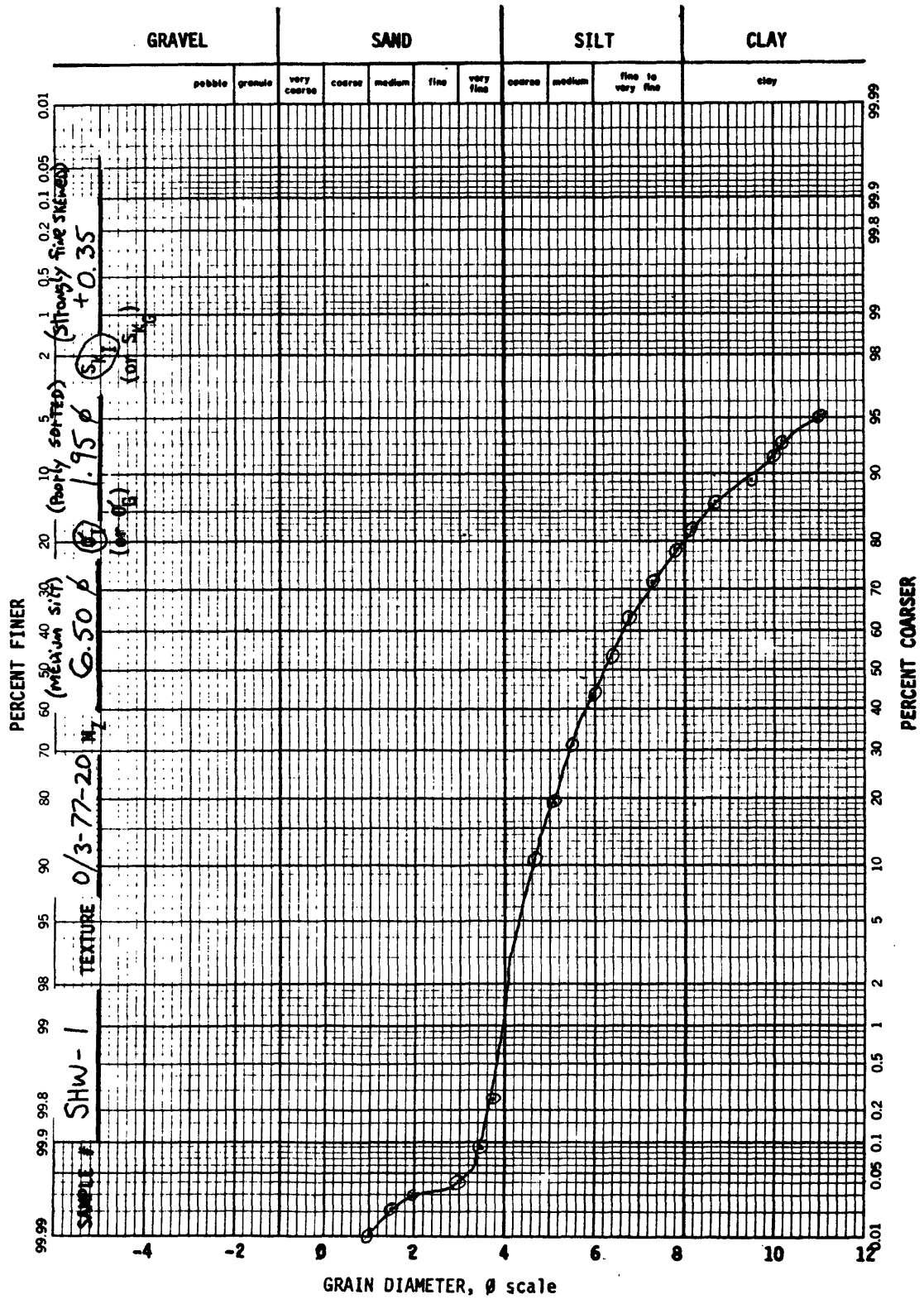


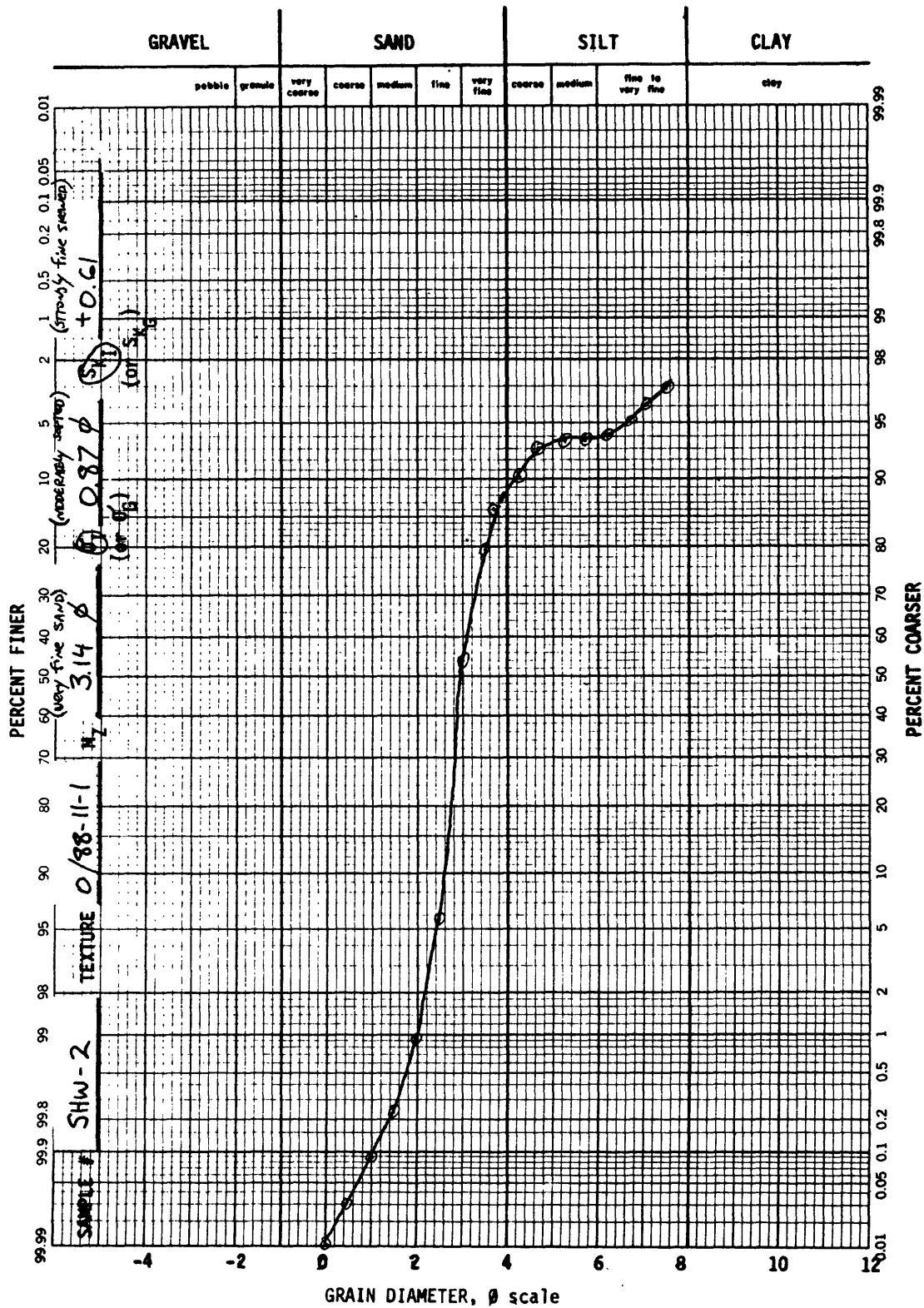


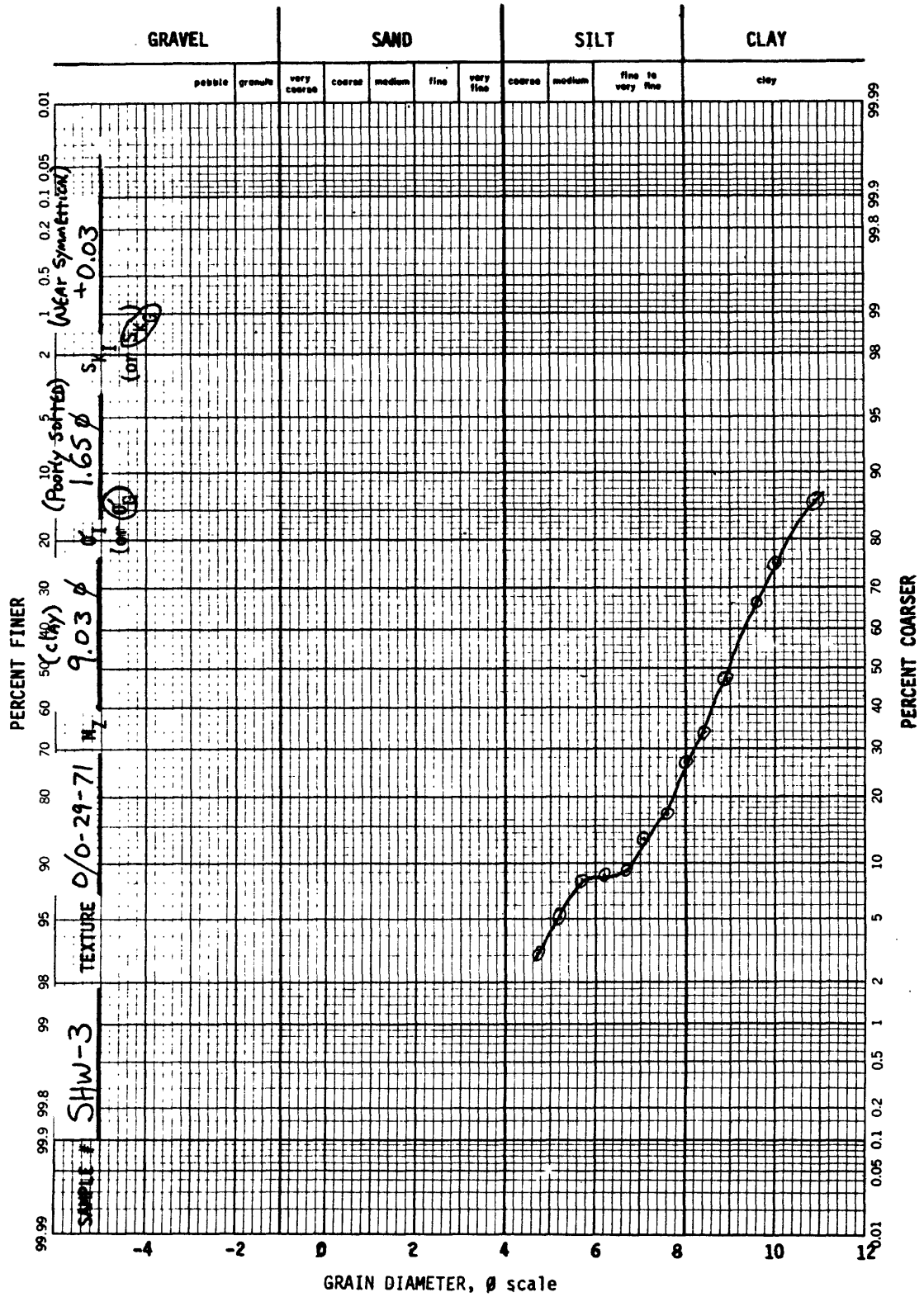




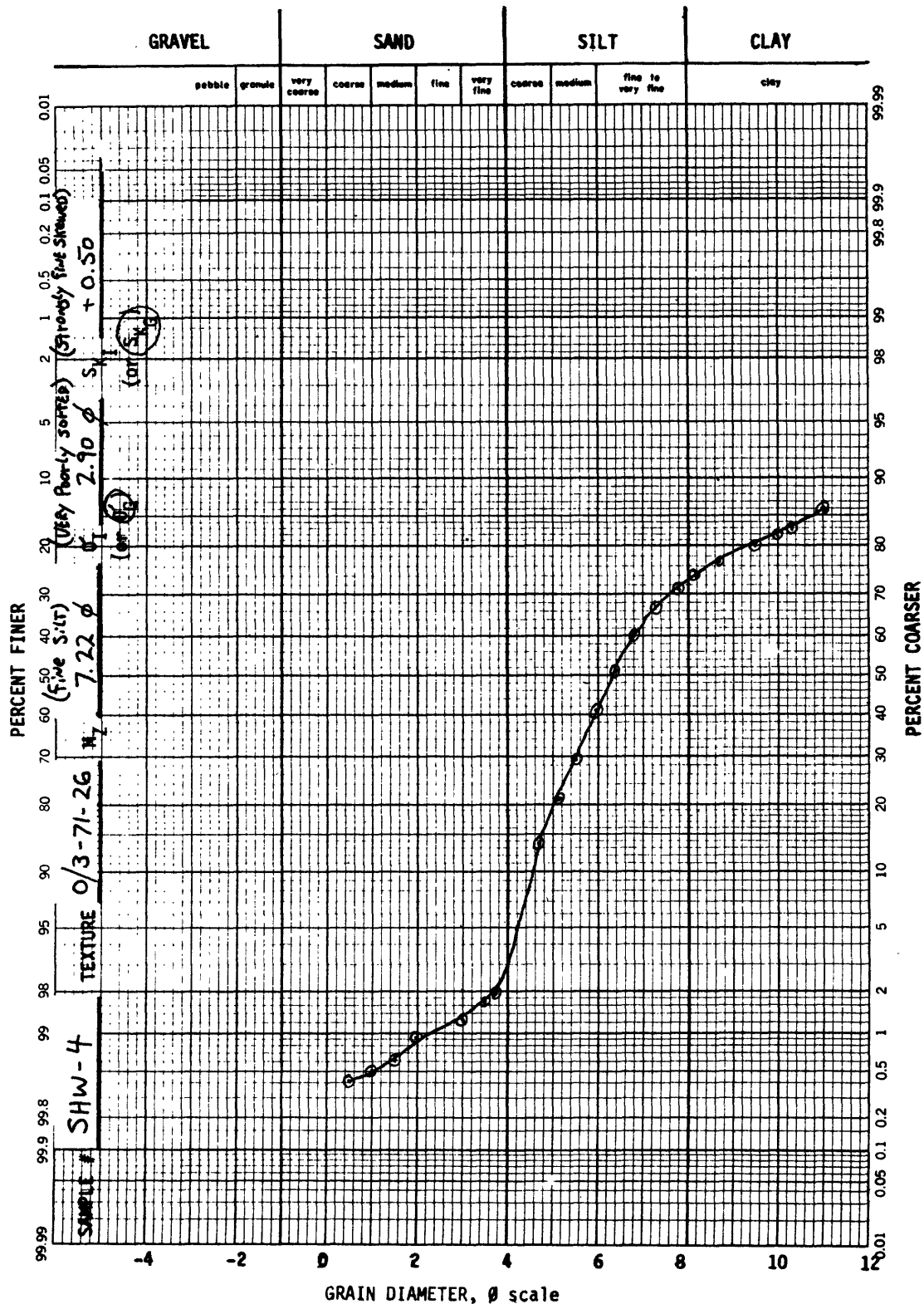


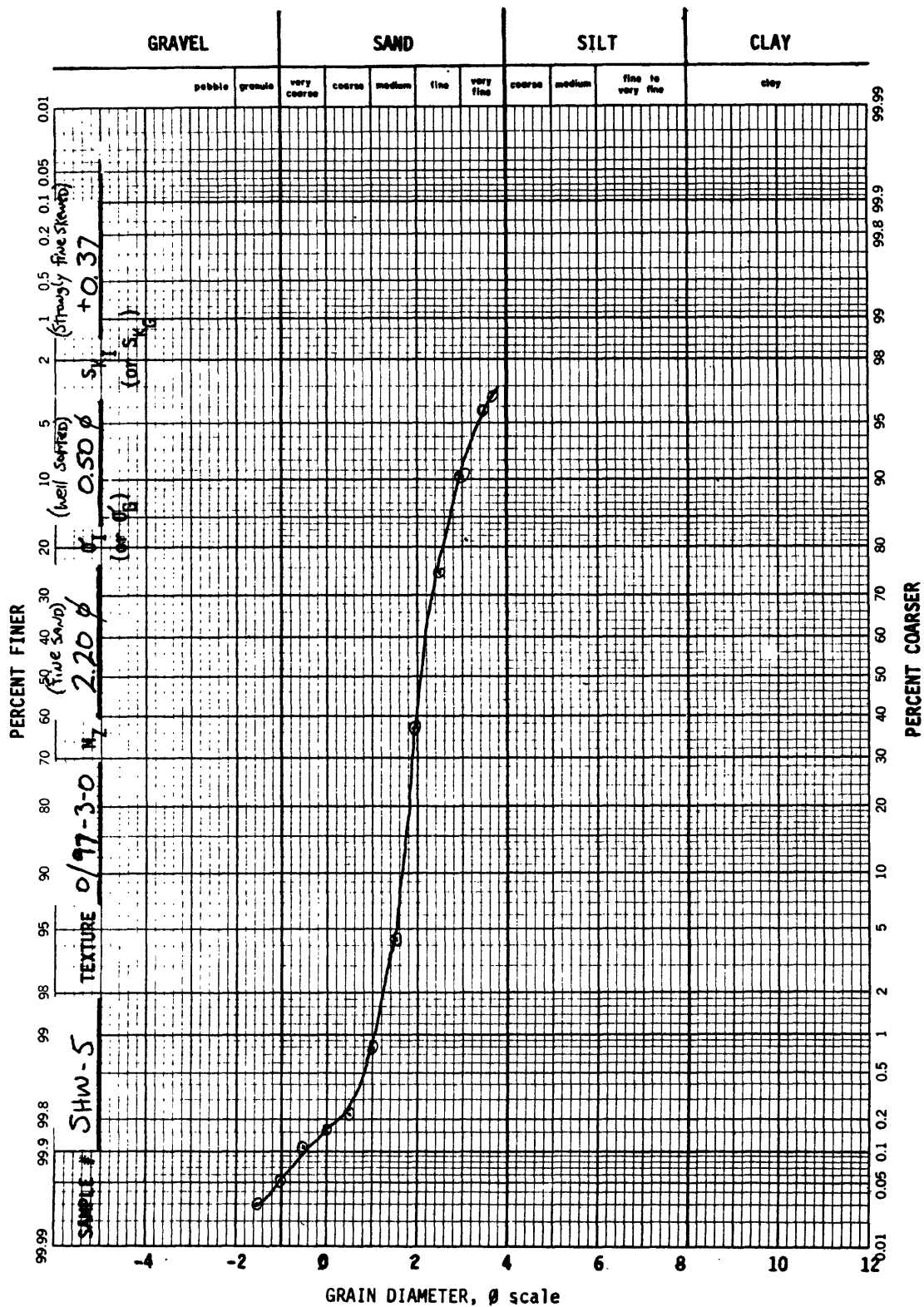


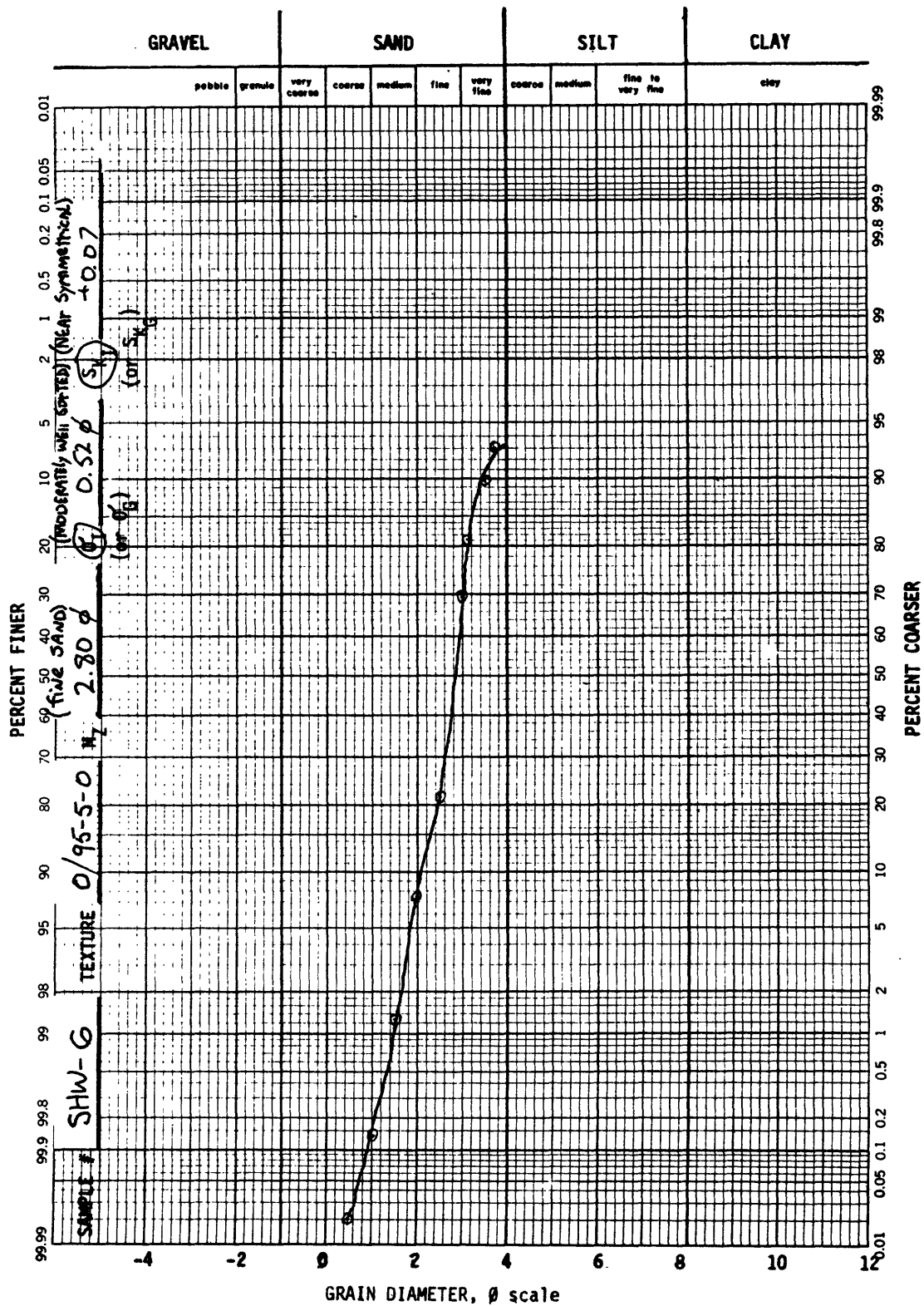


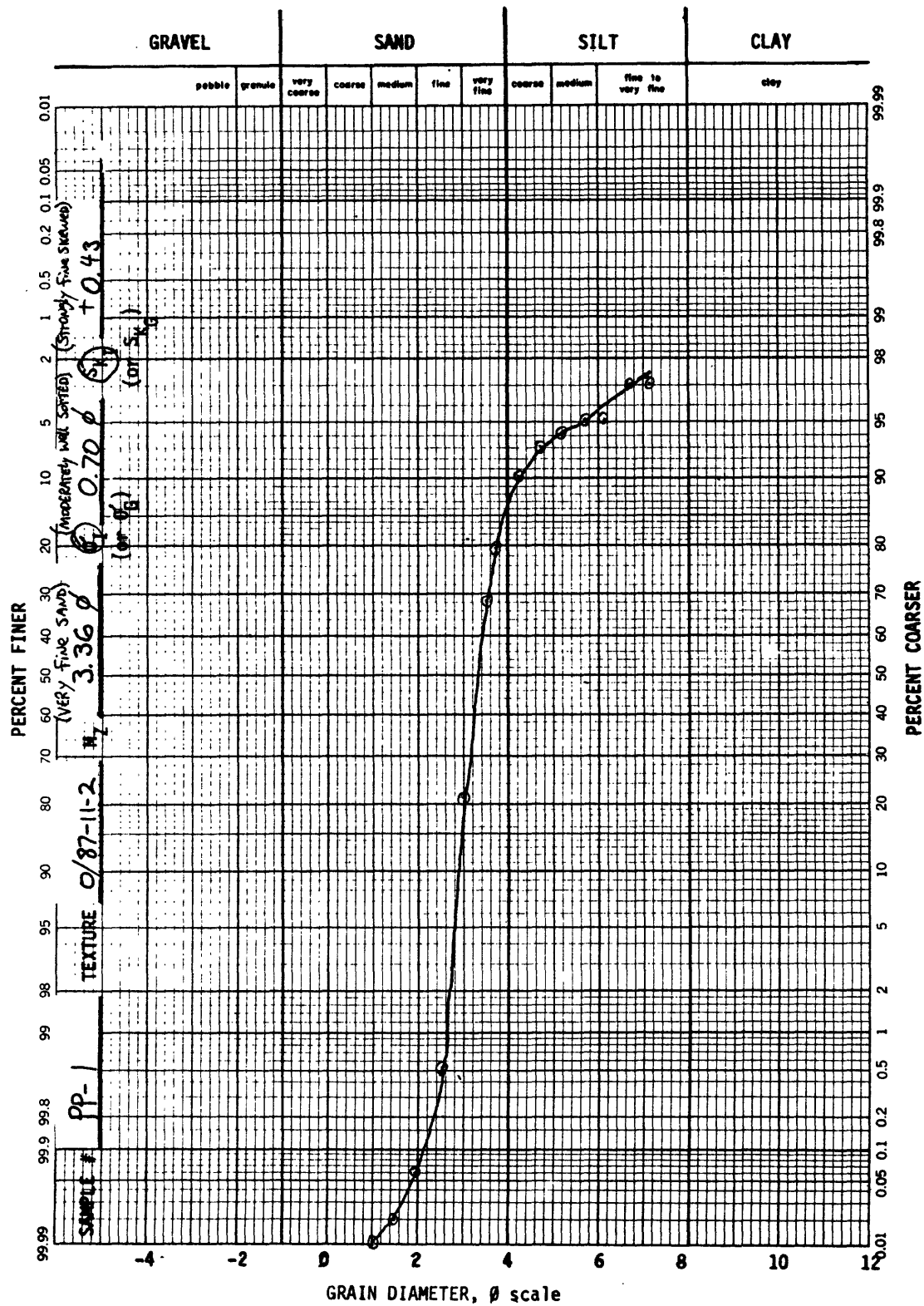




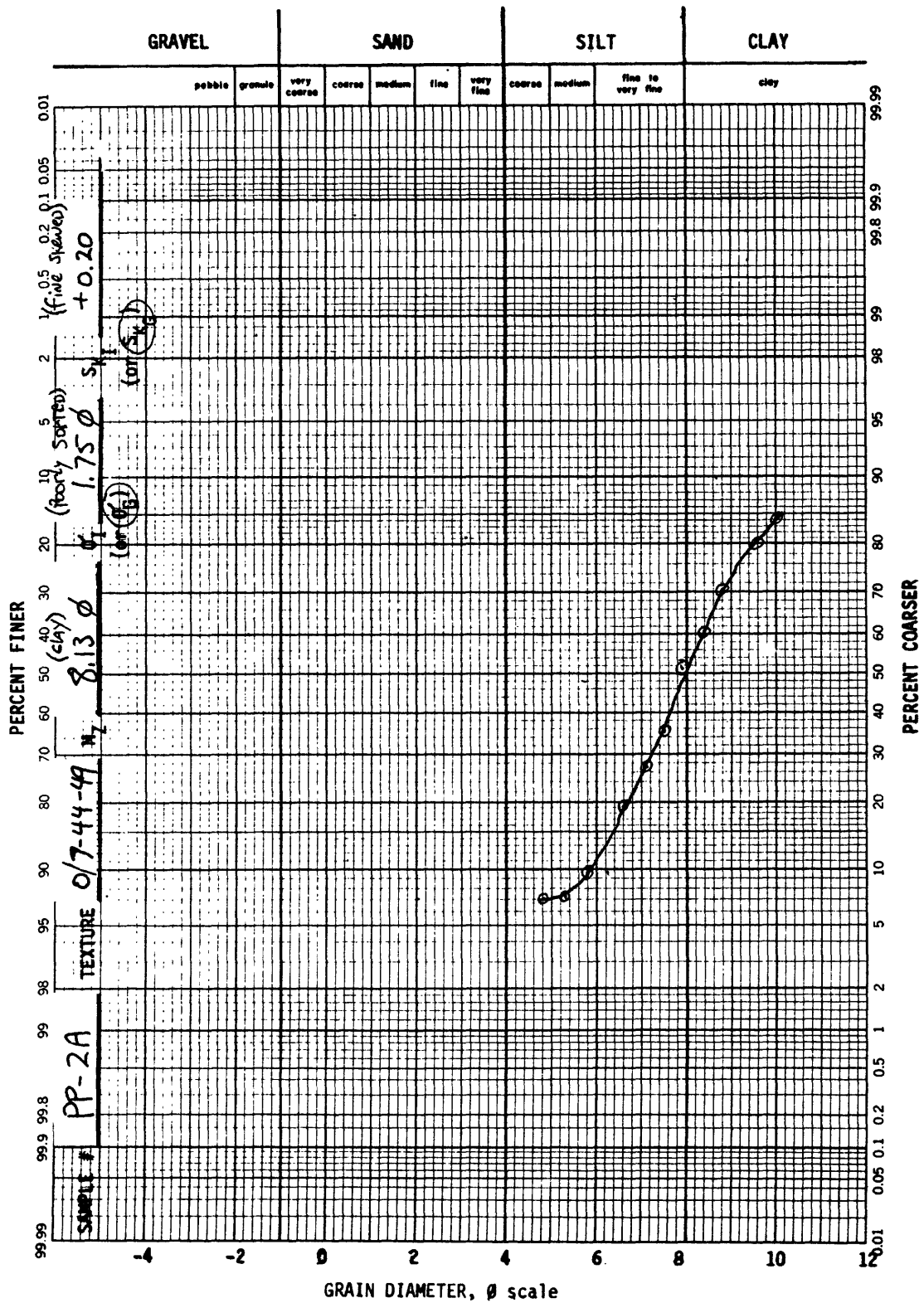


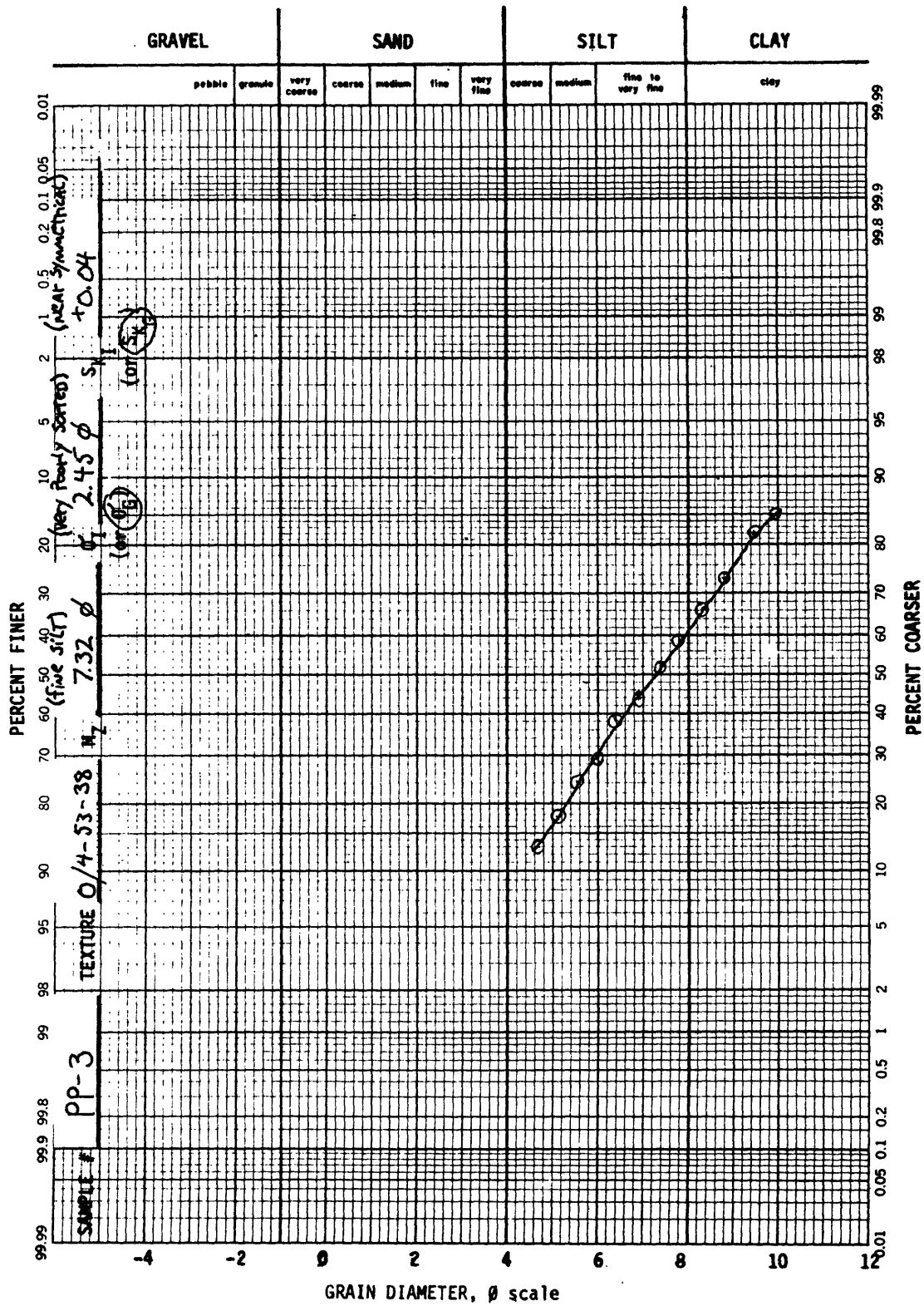


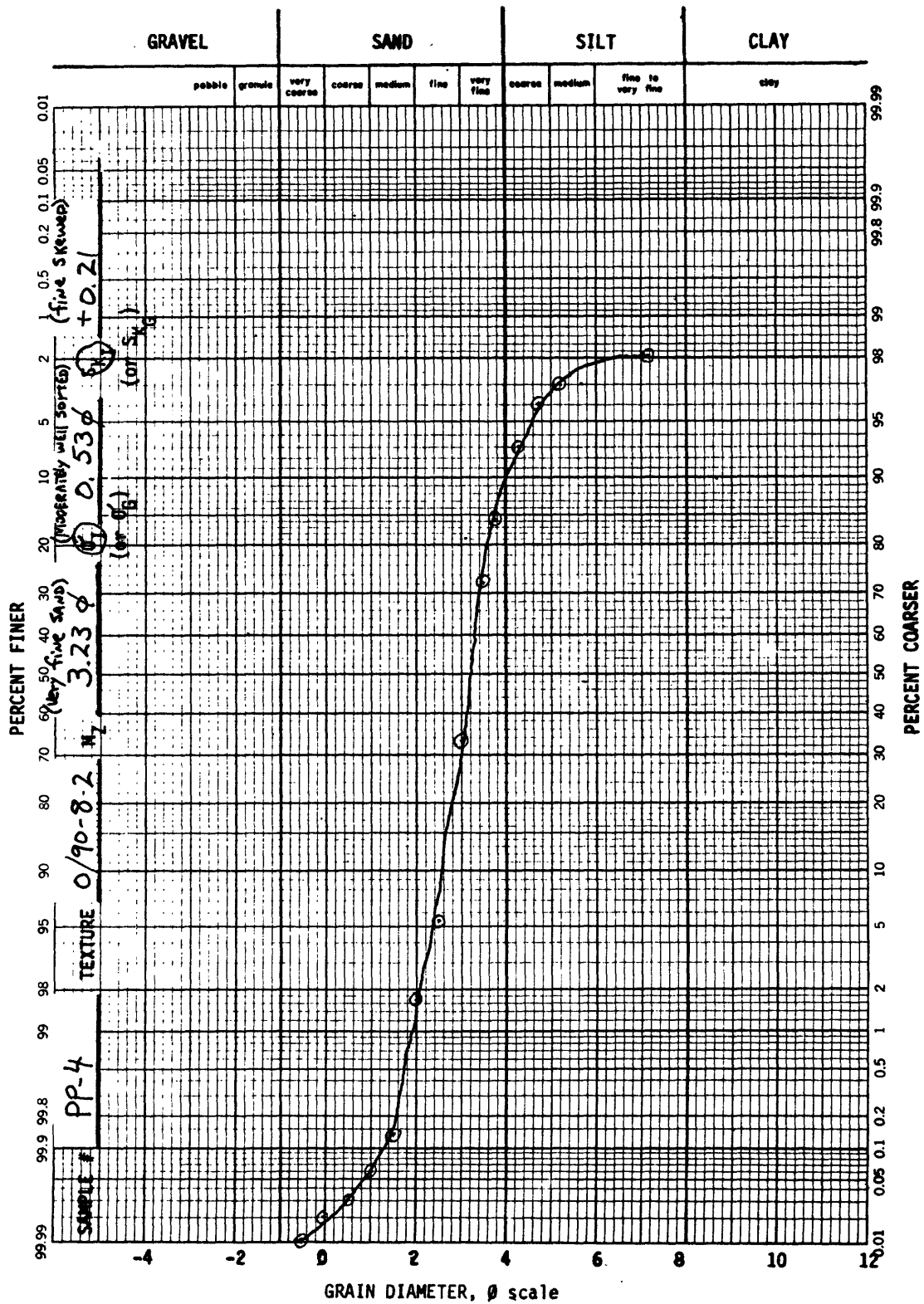




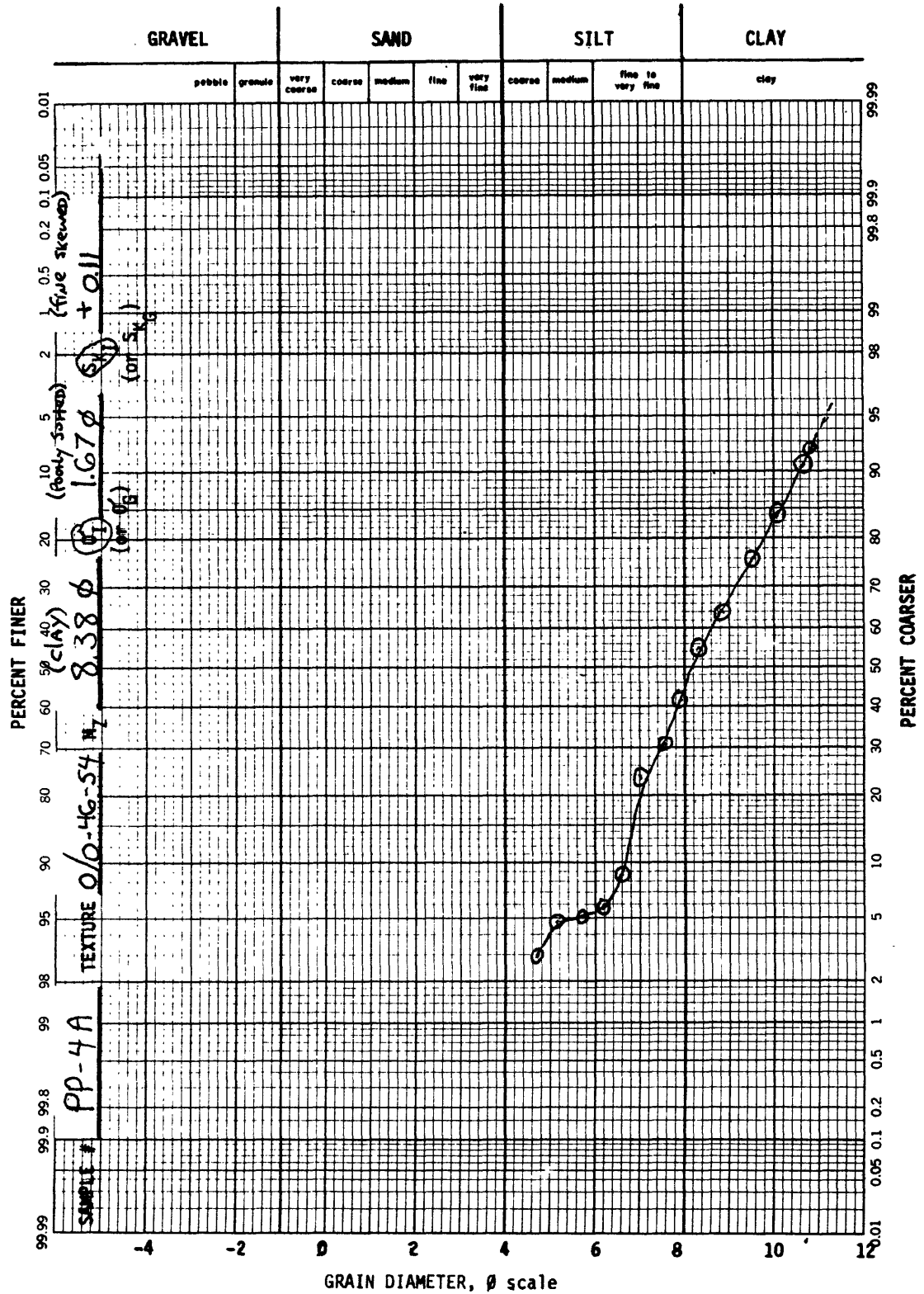


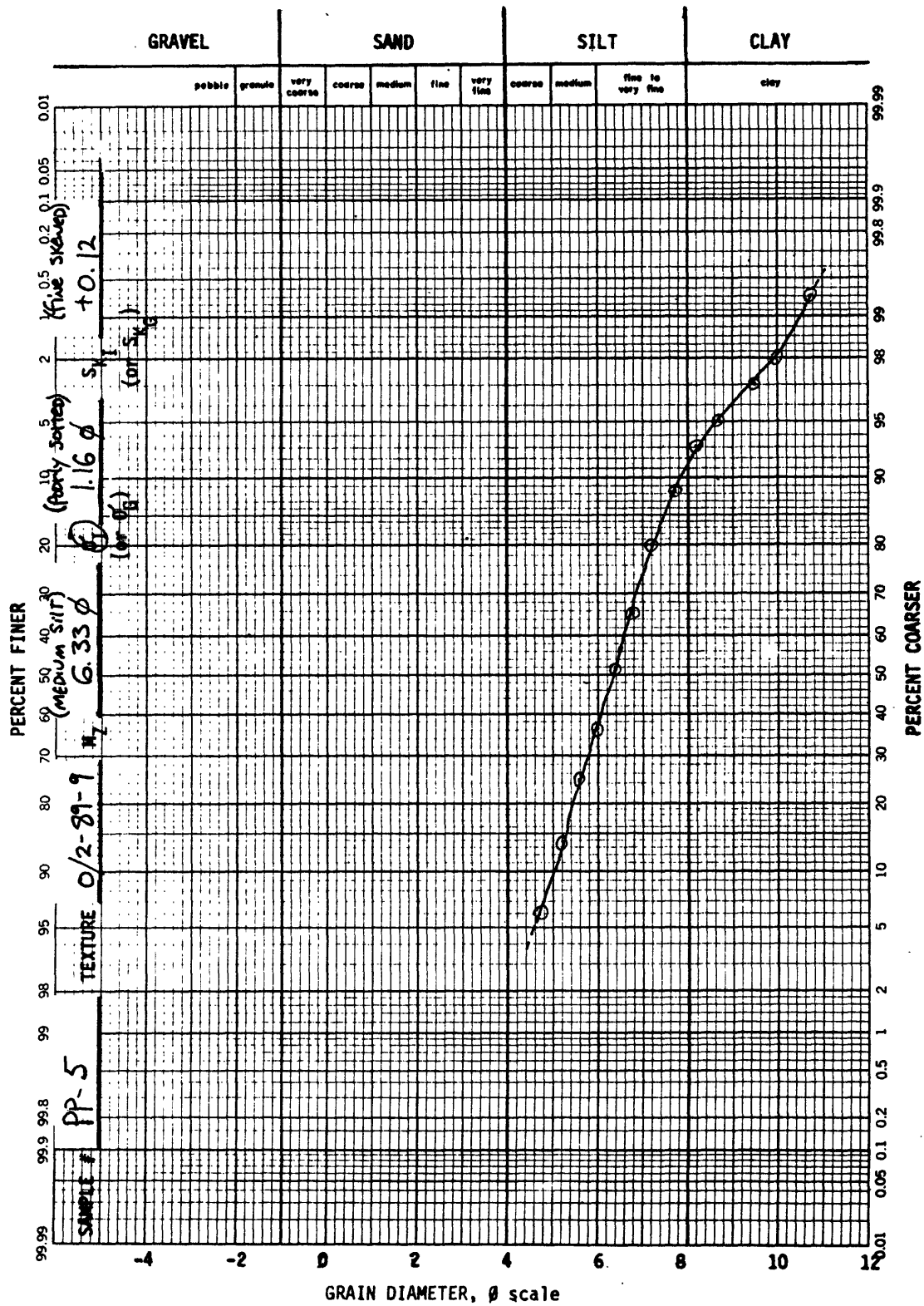


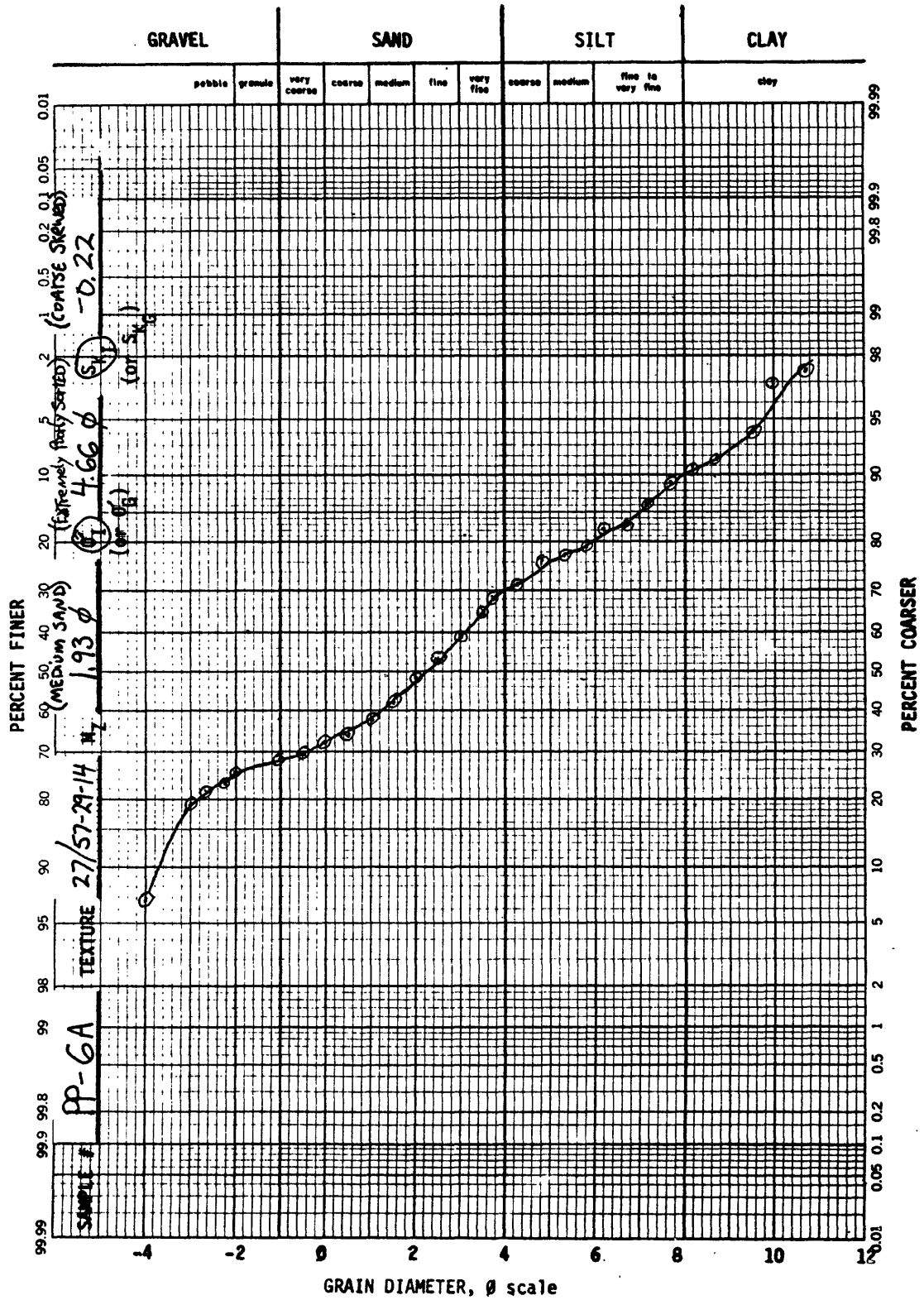












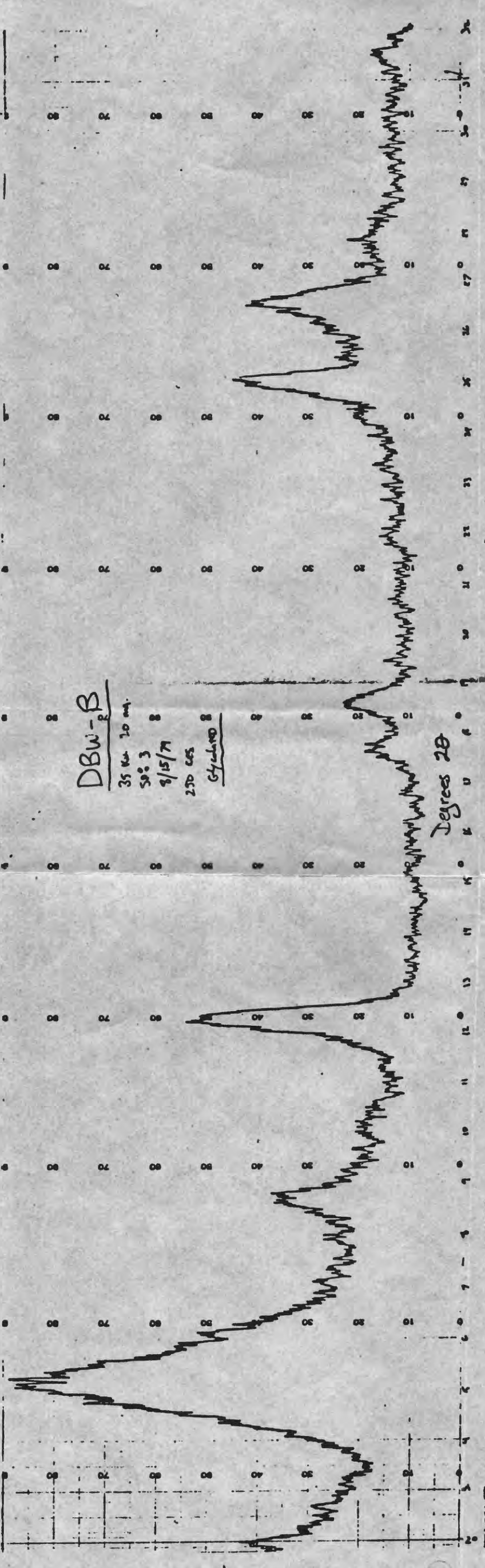
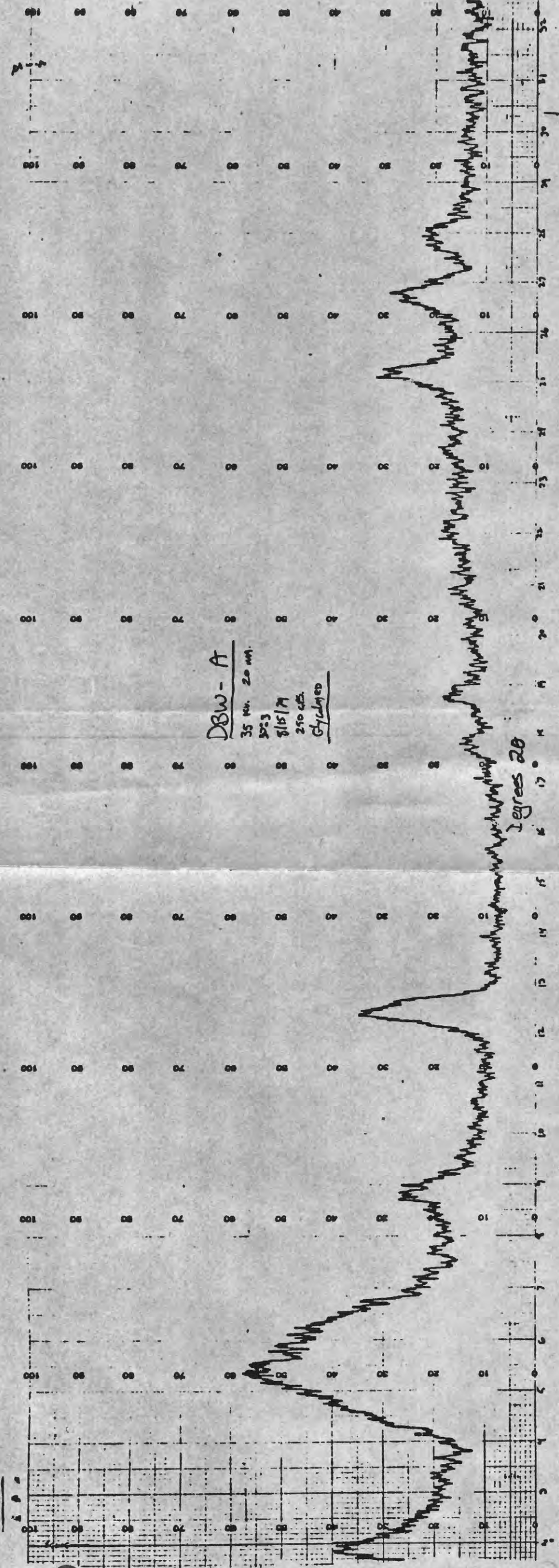
## APPENDIX C

### Clay Mineralogy

#### Procedure

The following procedure was used to obtain diffraction patterns of the sediment samples:

1. The sample was crushed with mortar and pestle.
2. The sample was placed in a centrifuge jug, and water was added to fill the jug.
3. Six to twelve drops of Calgon (sodium hexametaphosphate) were added to aid in dispersion and to prevent flocculation.
4. The solution was mechanically disaggregated in a mixer for 3 minutes.
5. The solution was centrifuged for 2 minutes at 1000 rpm, in order to obtain the less than 2 micron clay-size fraction.
6. The clay solution was eyedropped onto glass slides and allowed to dry at room temperature, producing oriented slides.
7. Once dry, a slide was placed in an ethylene glycol atmosphere for 24 hours.
8. An X-ray diffraction pattern was obtained for the glycolated slide. (Each X-ray run was from  $32^{\circ}2\theta$  to approximately  $2^{\circ}2\theta$ ).

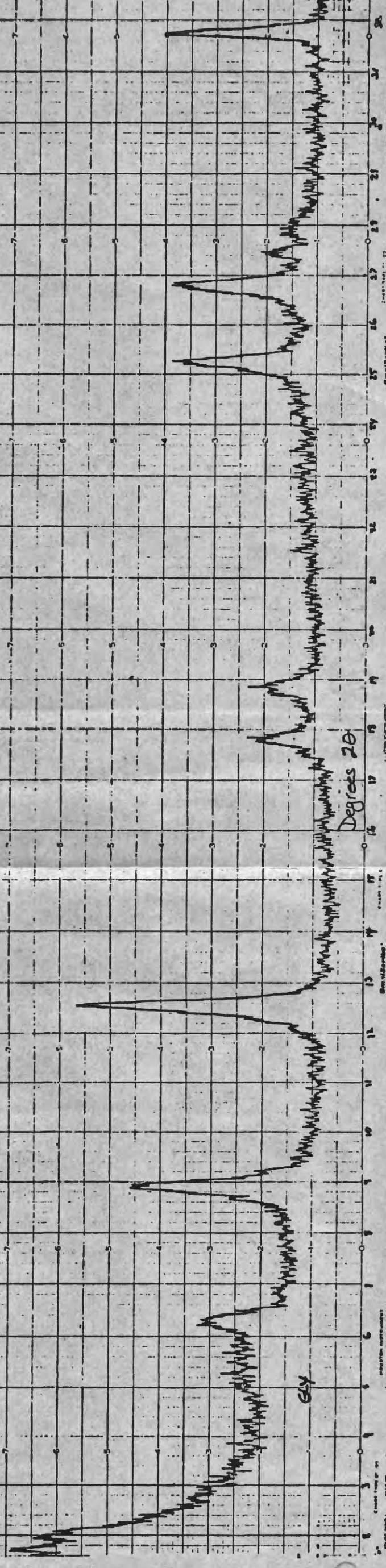




DBW-C  
500 cps  
6/17/74

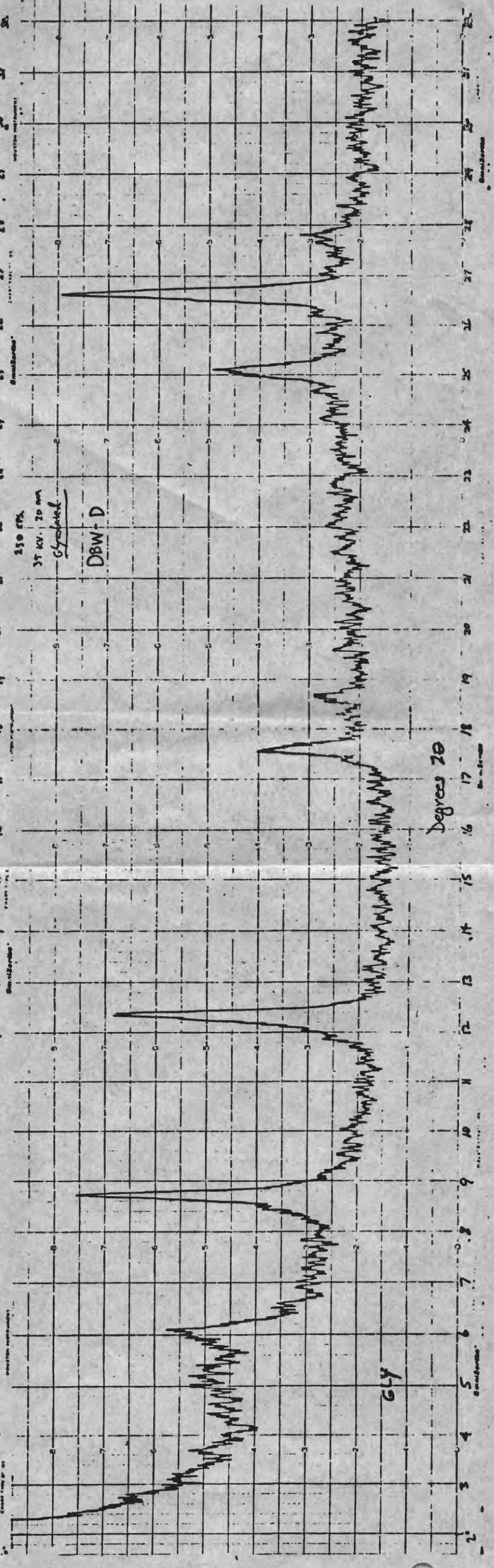
DBW-C  
500 cps  
6/17/74

DBW-C



6/17

Degrees 20



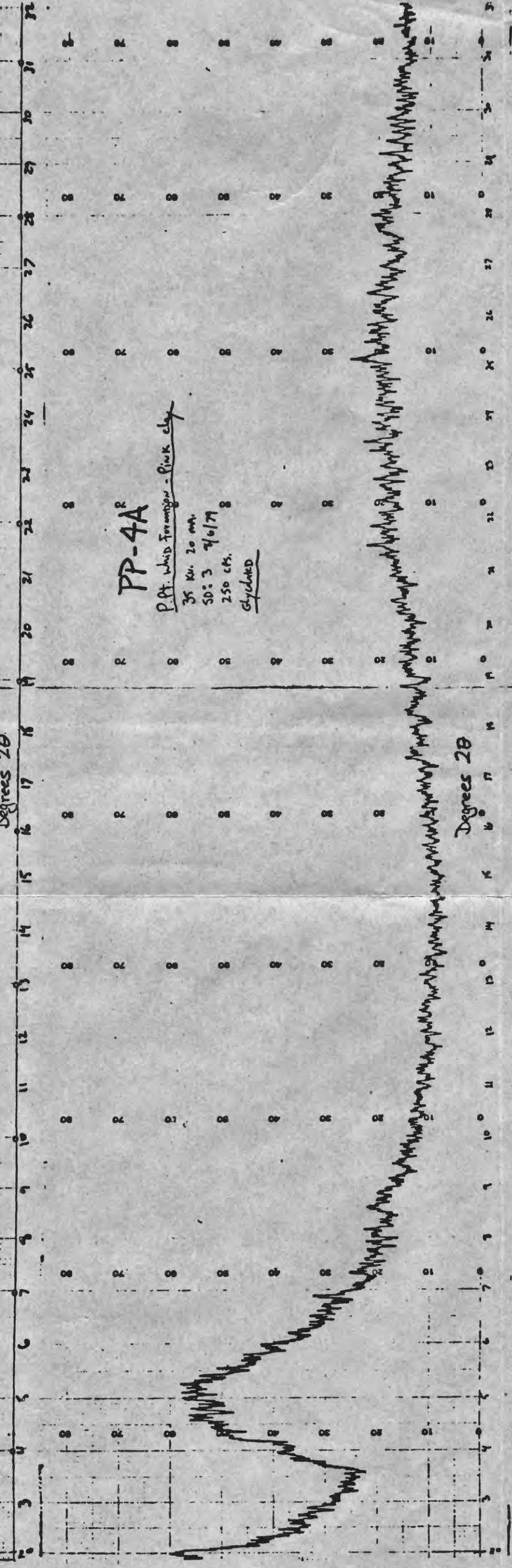
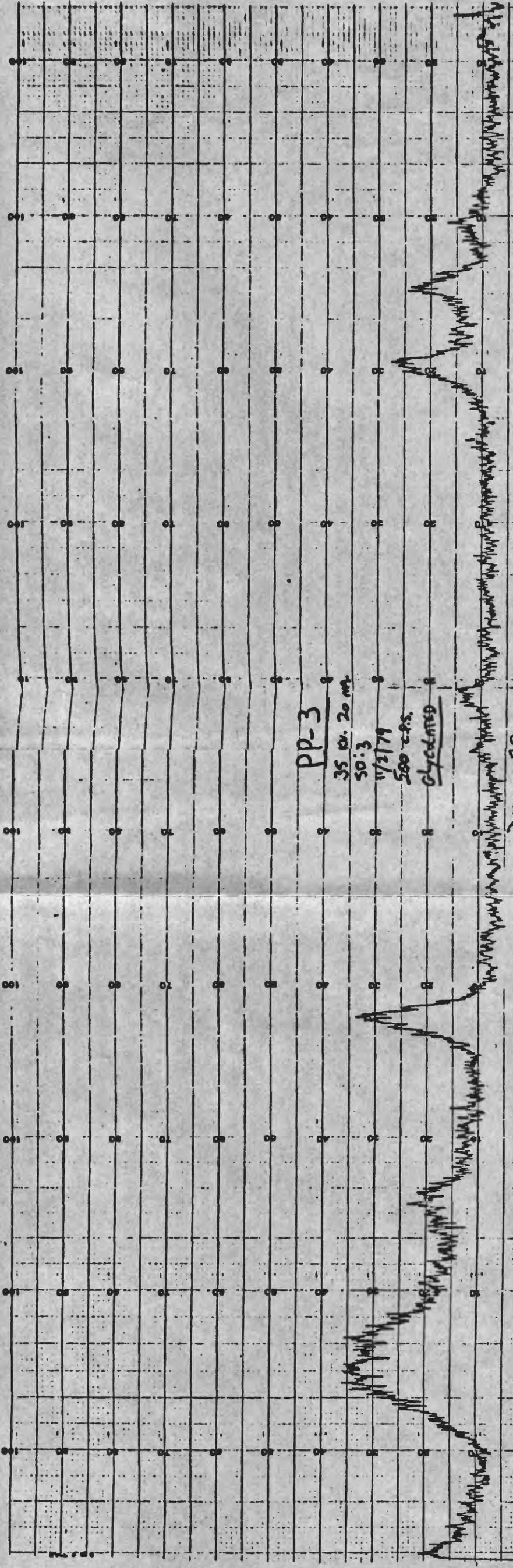
250 cps  
3500, 20 mm  
Glycol  
DBW-D

DBW-D

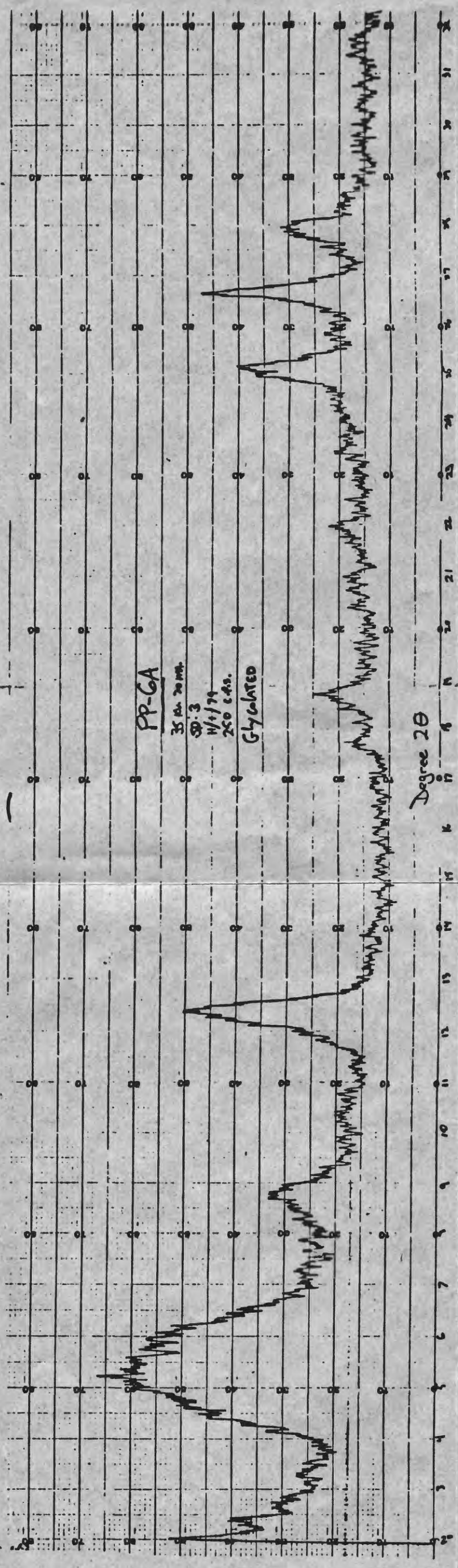
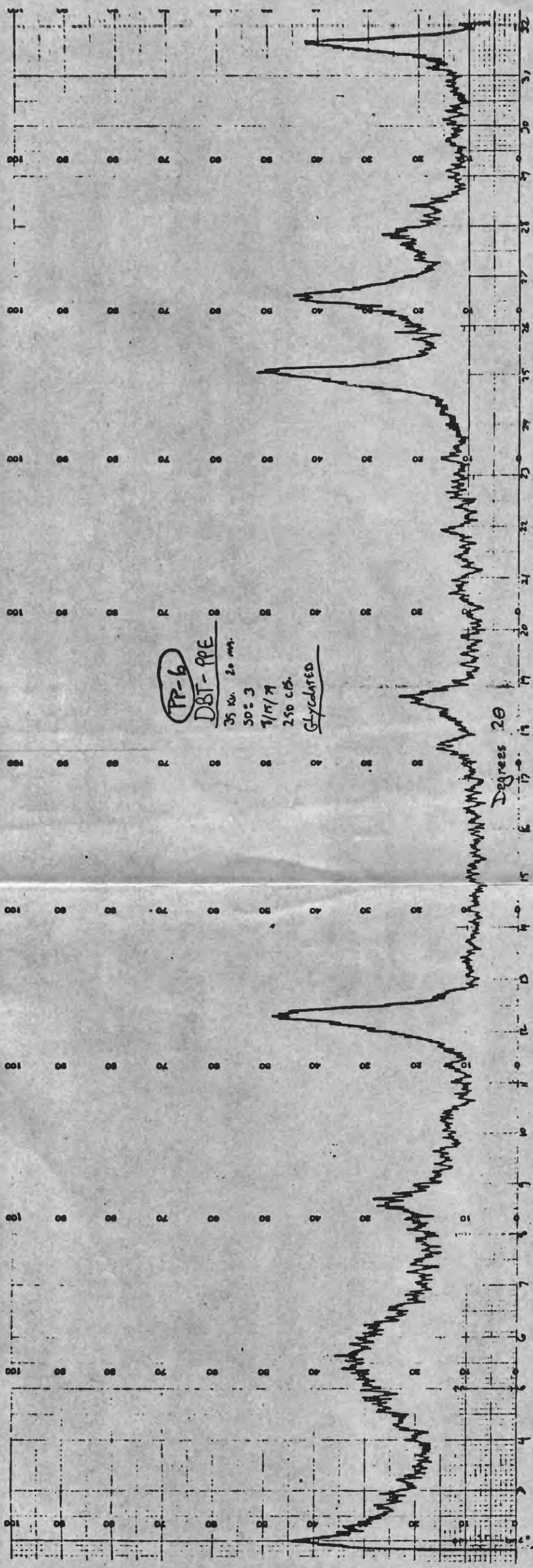
6/17

Degrees 20

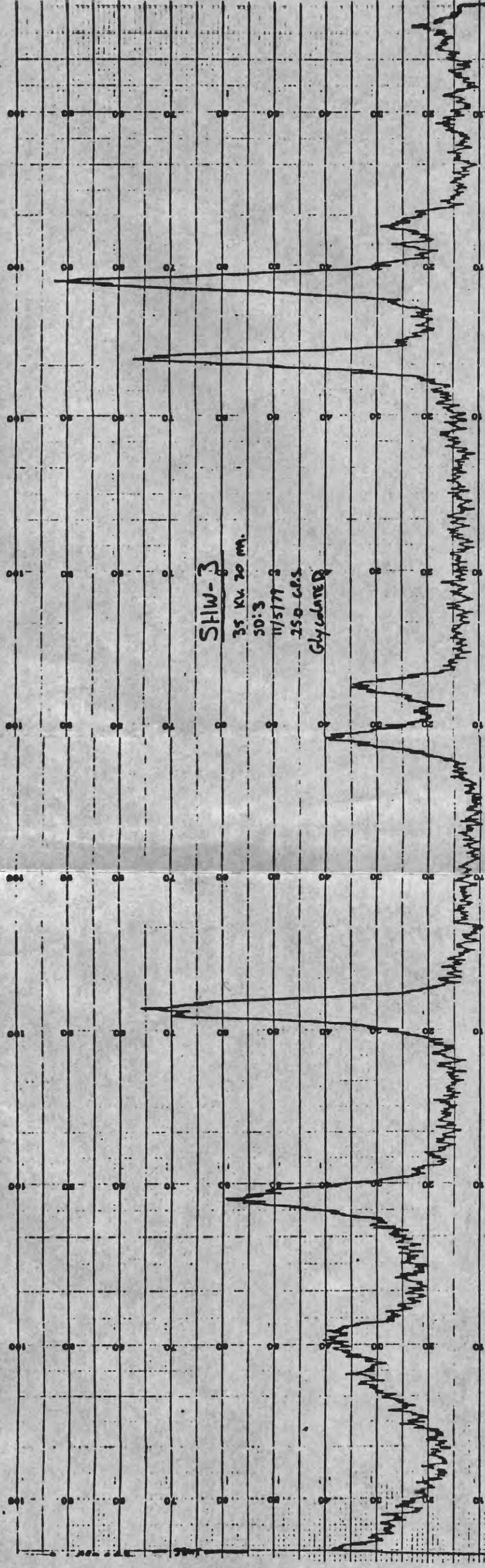






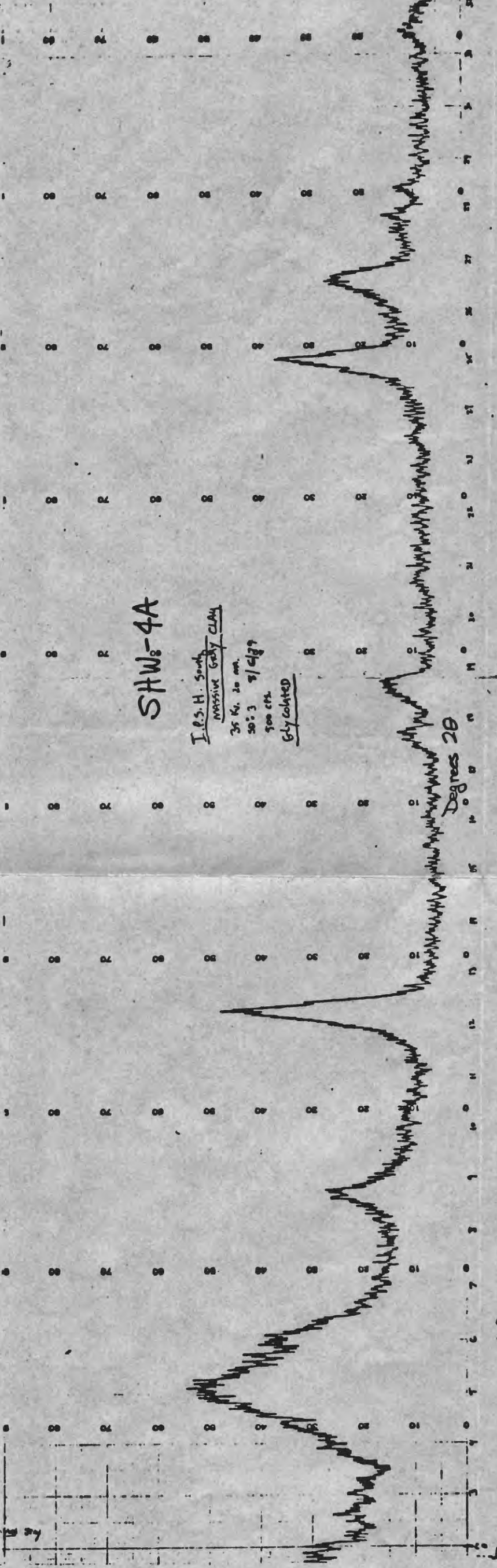






2 3 4 5 6 7 8 9 10 11 12 13 14 15 16 17 18 19 20 21 22 23 24 25 26 27 28 29 30 31 32

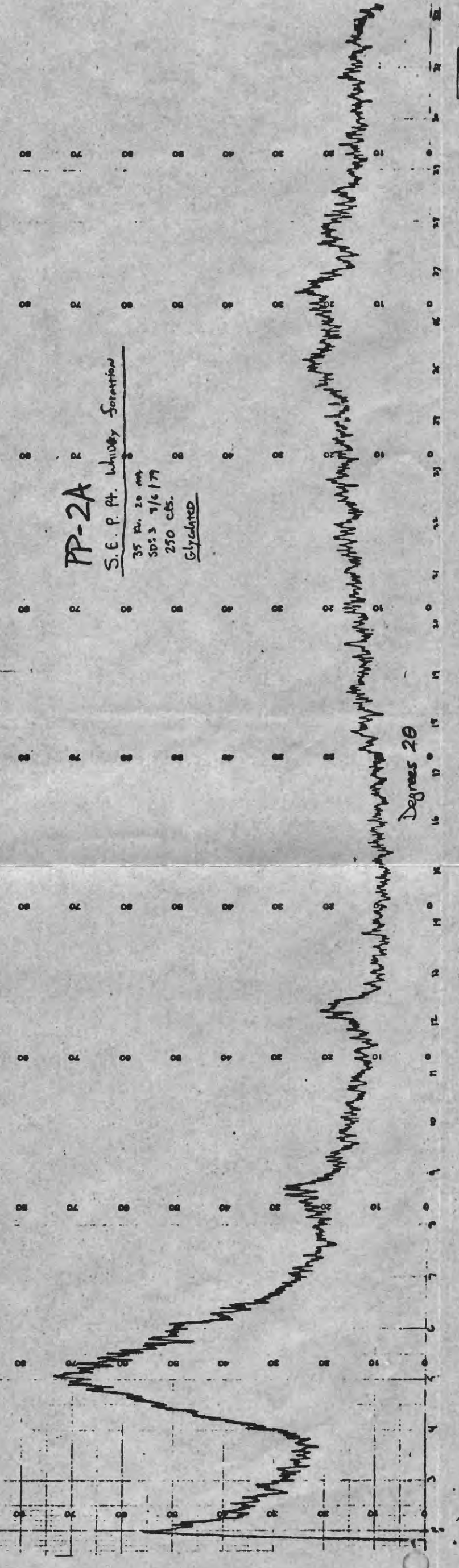
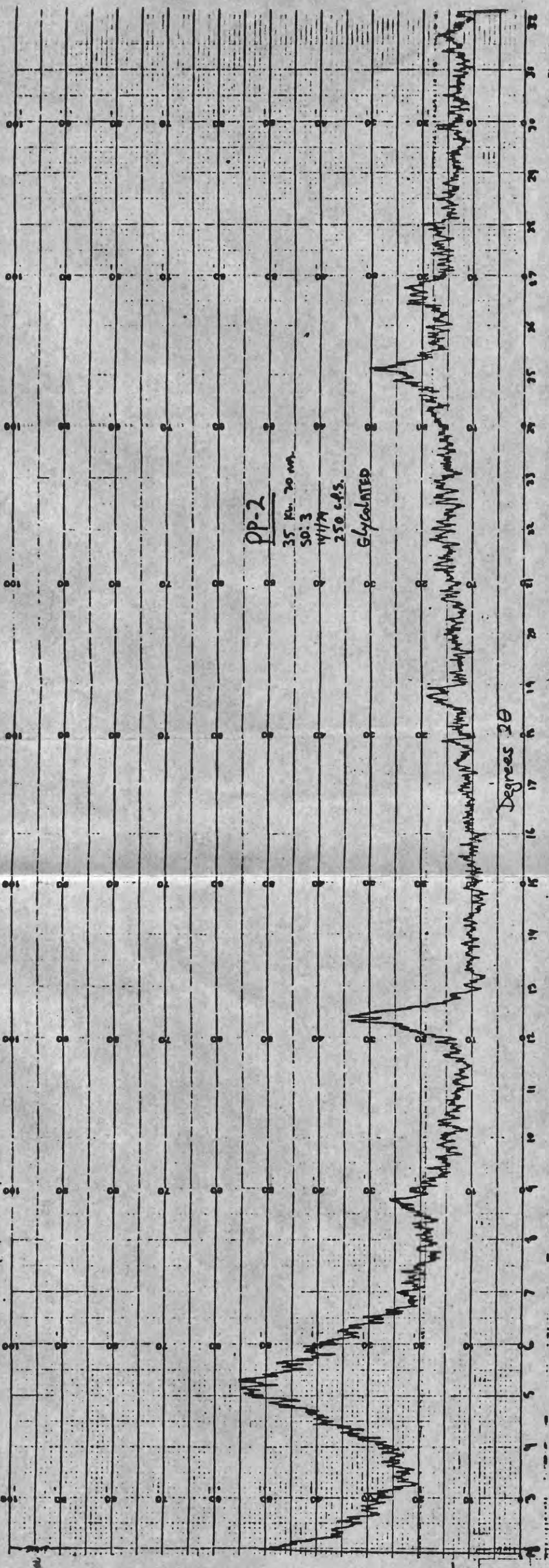
2θ



2 3 4 5 6 7 8 9 10 11 12 13 14 15 16 17 18 19 20 21 22 23 24 25 26 27 28 29 30 31 32

2θ







SHW-O

I.P.S.H. South below first #1

35 K<sub>α</sub> 2θ mm.

50:3 3/6/79

500 cm<sup>-1</sup>

Glycerol

Degrees 2θ

T-MHS

35 K<sub>α</sub> 2θ mm.

50:3

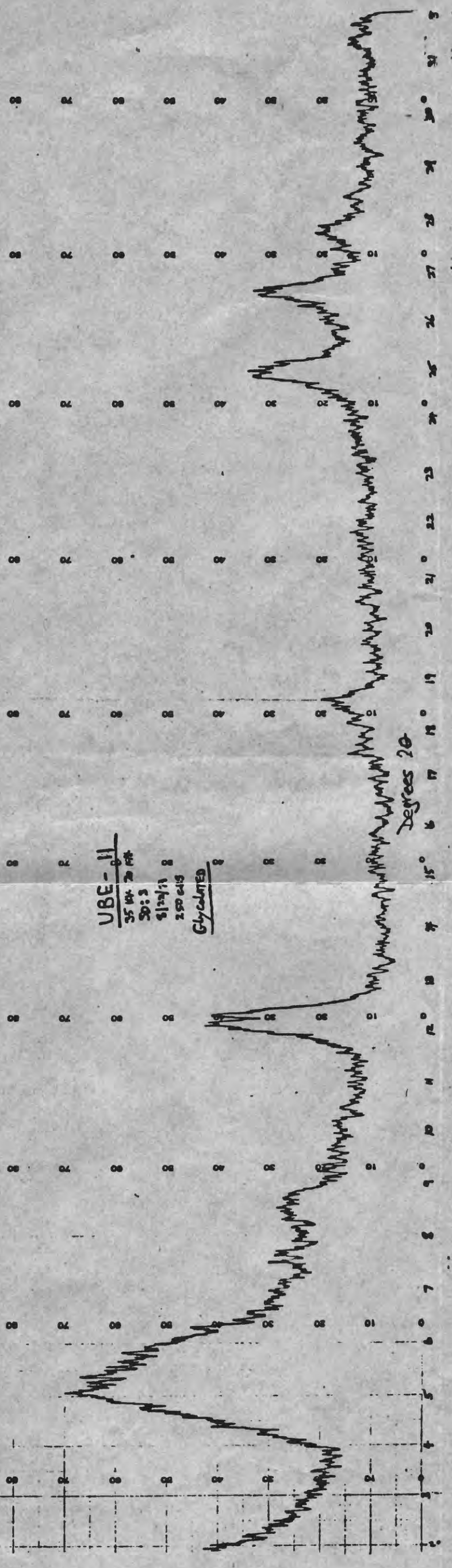
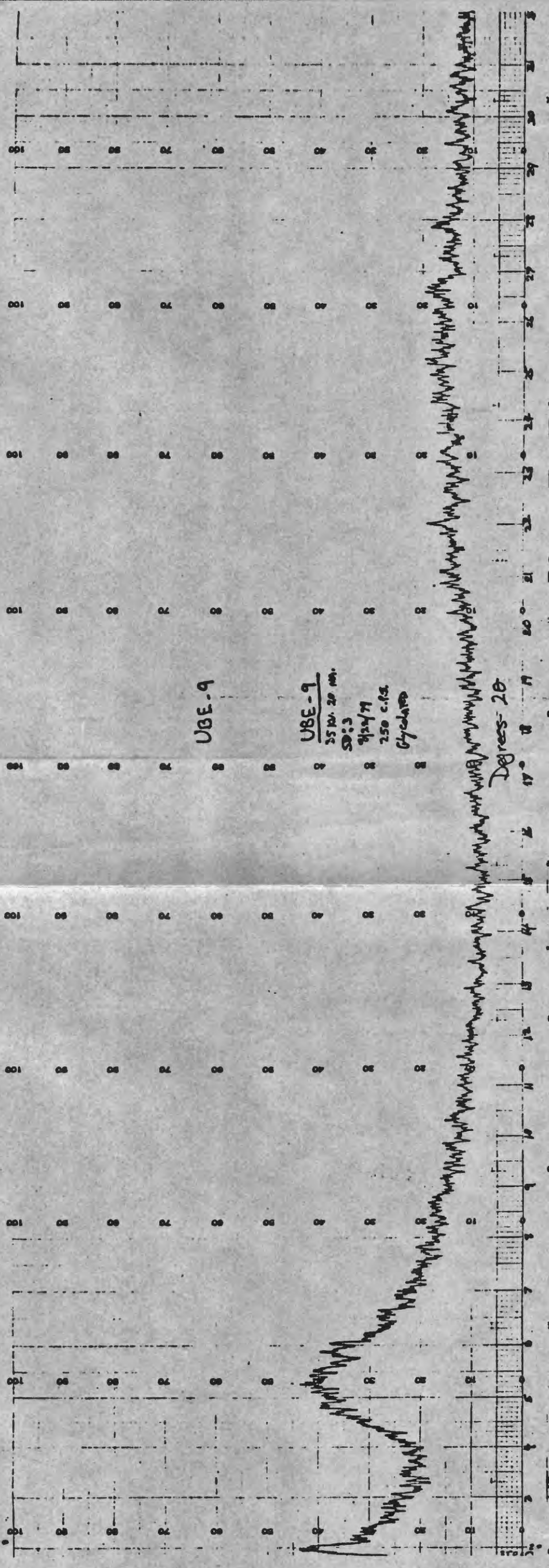
3/6/79

500 cm<sup>-1</sup>

Glycerol

Degrees 2θ







DBE-17

DBE-17

250 cfs  
35 ft. 20 m.  
Clyland

ey

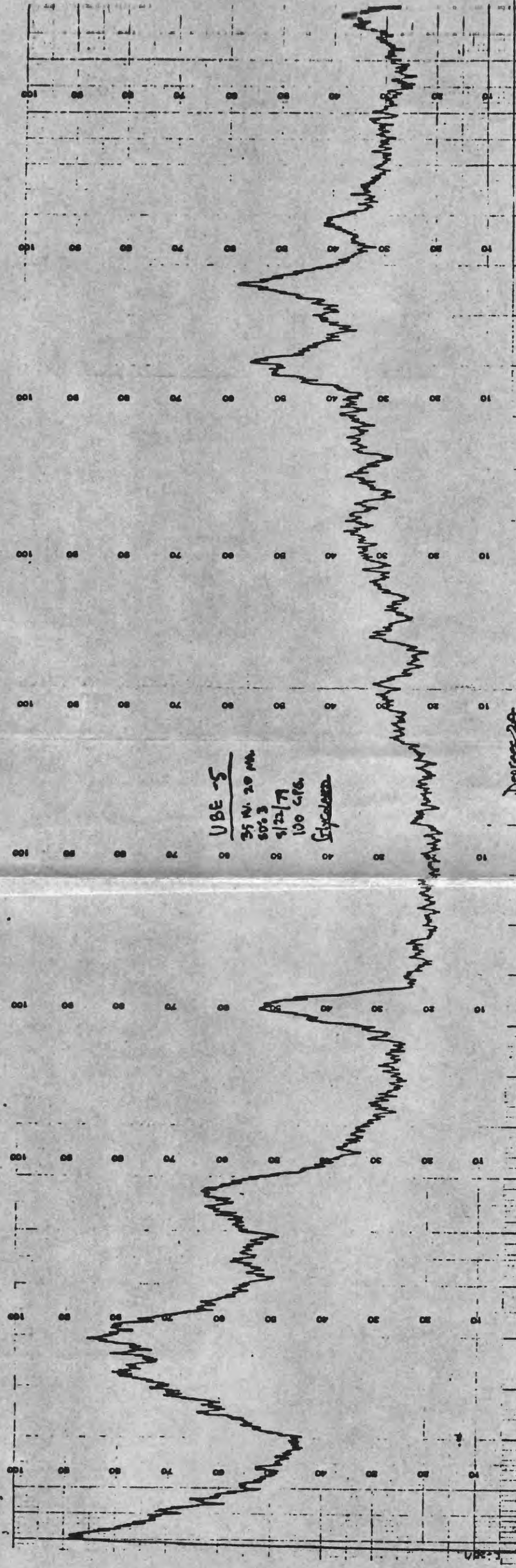
Degrees 20

UBE-2

35 ft. 20 m.  
30:3  
8/22/77  
100 cfs  
17/01/80

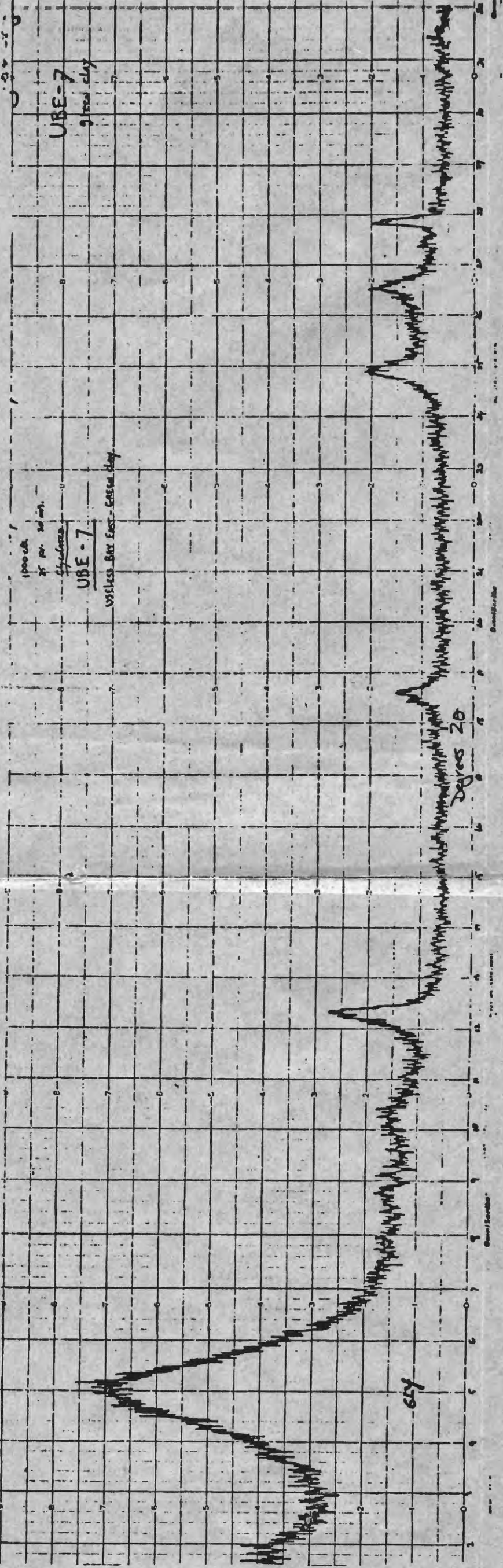
Degrees 20





UBE-5  
 35 W. 20 m.  
 50% S  
 2/22/77  
 100 GPa.  
 S. G. G. G.

Degrees 20



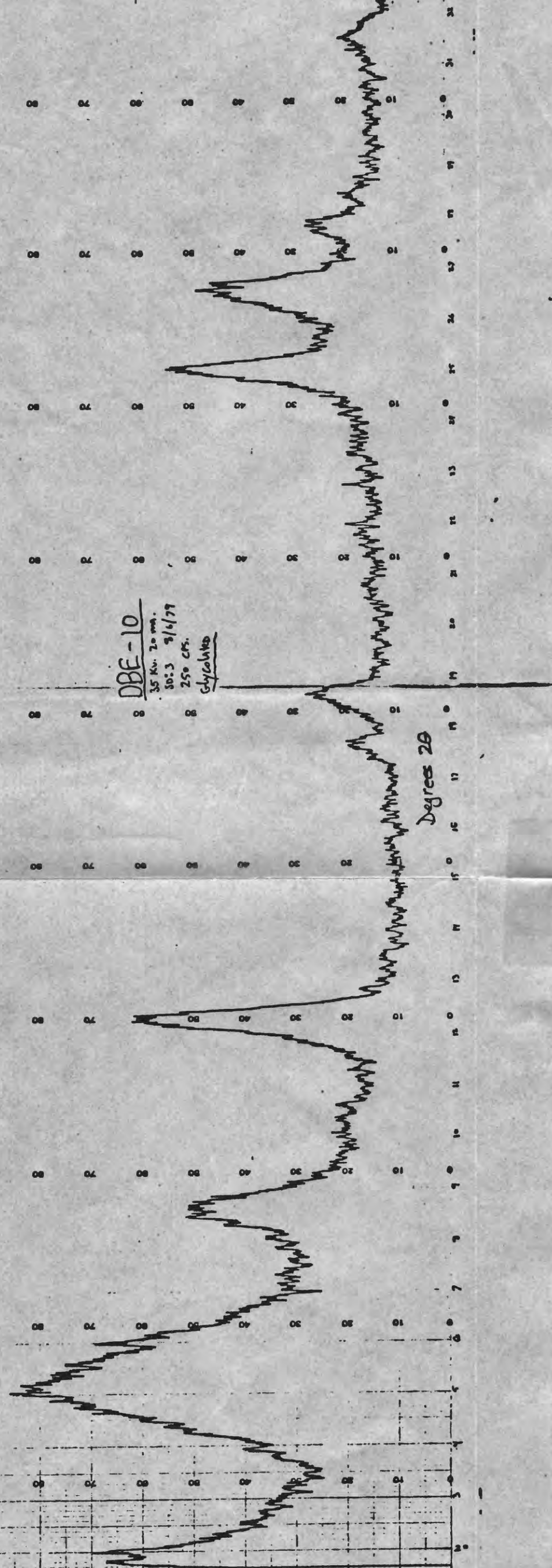
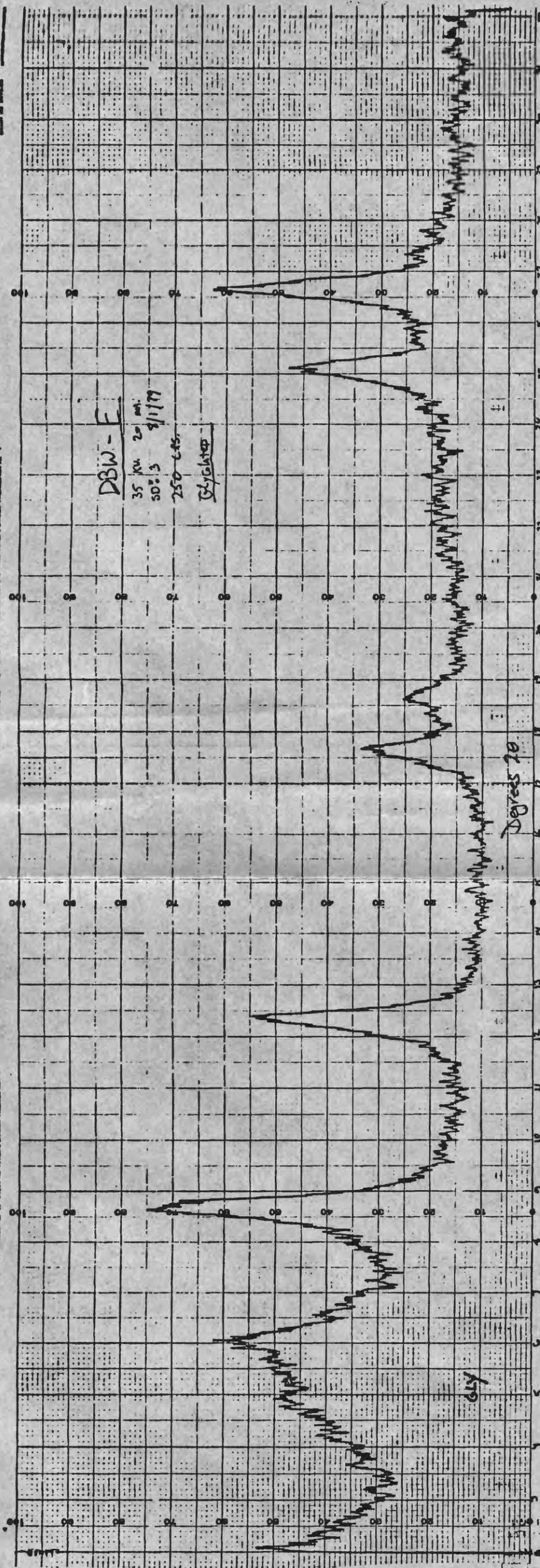
UBE-7

UBE-7

1000 m.  
35 W. 20 m.  
S. G. G. G.

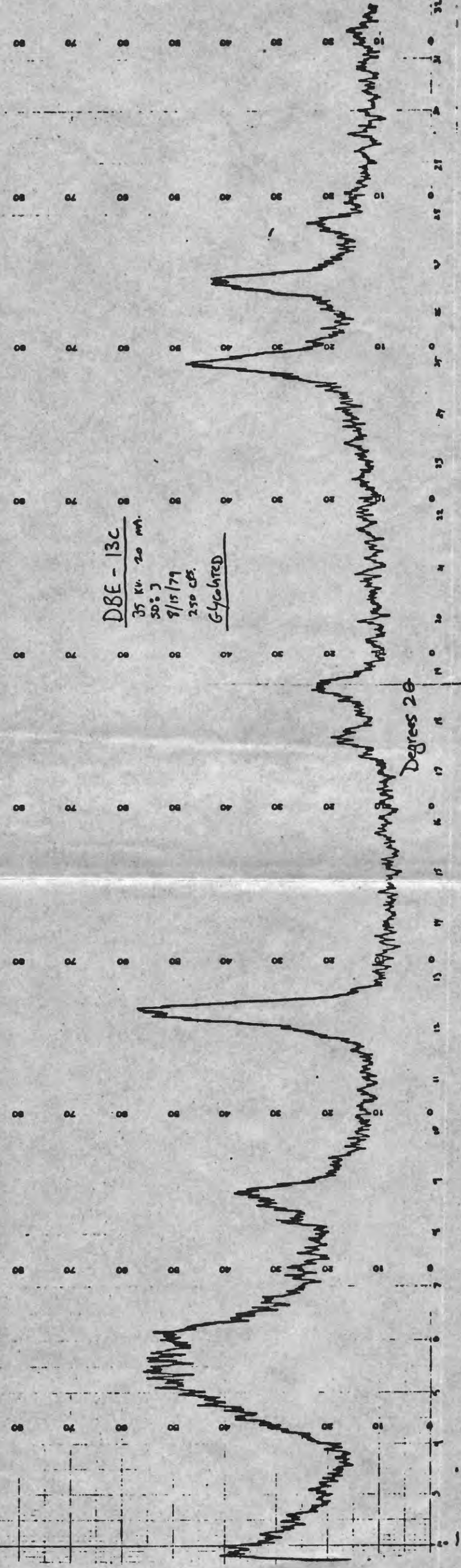
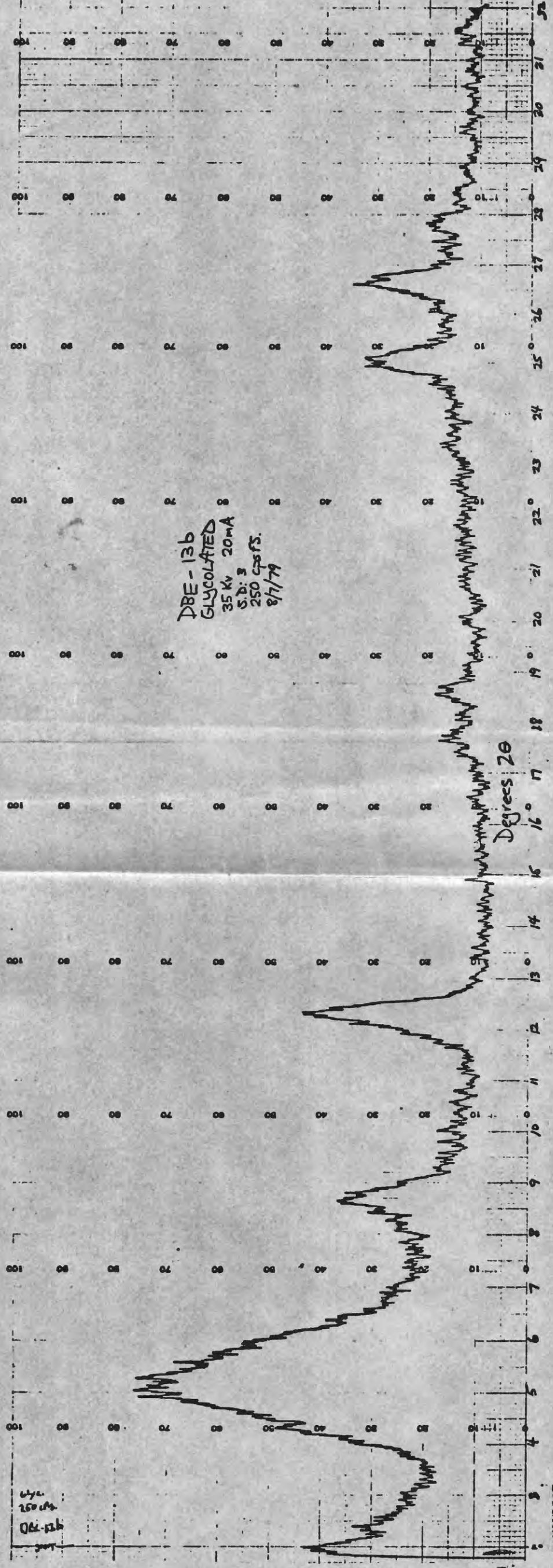
Degrees 20







Wye  
250 cps  
DBE-13b





## APPENDIX D

### Heavy Mineral Analyses

#### Procedure

##### Heavy Liquid Separation

1. A separatory funnel was secured to a ring stand, and a filtering funnel and receiving flask were placed beneath the separatory funnel.
2. 200 ml of bromoform (heavy liquid, SG=2.85) was poured into the separatory funnel.
3. The sample was slowly added, the funnel shaken vigorously, and the heavy minerals allowed to settle.
4. Heavy minerals, which had settled to the bottom of the funnel, were released to the filtering funnel, where they were rinsed with acetone and then allowed to dry.
5. Light minerals were then released to a different filtering funnel, where they were rinsed with acetone and allowed to dry.
6. The light and heavy mineral fractions were then weighed and recorded.
7. The light minerals were saved for microscopic examination.

##### Magnetic Separation

1. Prior to separation on the Franz Isodynamic Separator, magnetic minerals were removed from the heavy mineral fraction with a hand magnet, to prevent clogging of the separator.
2. Magnetic separation of the remainder of the heavy mineral fraction was performed on the Franz separator. Six settings of amperage were used to separate the heavy minerals into seven groups of various magnetic susceptibilities. These were 0.10, 0.25, 0.50, 0.75, 1.00, and 1.30 amps. For every setting a

slope of  $25^{\circ}$  and a tilt of  $15^{\circ}$  was used.

3. Each fraction was then weighed and recorded.
4. The samples were saved for mineral identification under the binocular and petrographic microscopes.

#120 Mesh - 0.10A + Magnet

NON-HEAVIES

miscellaneous

zircon

rutile (yellow-brown)

rutile (red-brown)

kyanite

black opaques	50	20	60	50	95	50	75	95	80	55
---------------	----	----	----	----	----	----	----	----	----	----

clinopyroxene	10	10	10	5			5			15
---------------	----	----	----	---	--	--	---	--	--	----

rounded blue-green

biotite + chlorite

actinolite (clear)

actinolite (brown)

actinolite (green)		20	10	5		20				
--------------------	--	----	----	---	--	----	--	--	--	--

almandine

epidote

hornblende		20		10						5
------------	--	----	--	----	--	--	--	--	--	---

idocrase	40	30	20	30	5	30	20	5	20	25
----------	----	----	----	----	---	----	----	---	----	----

SAMPLE

DBW-1

DBW-2

DBE-6

DBE-14

DBE-18

UBE-3

UBE-4

UBE-8

UBE-10

SHW-0

#120 Mesh - 0.25A

NON-HEAVIES

miscellaneous					25					
zircon										
rutile (yellow-brown)										
rutile (red-brown)										
kyanite										
black opaques		10	20		55					
clinopyroxene	10	10	20	20	10	5	5	5	10	10
rounded blue-green										
biotite + chlorite										
actinolite (clear)										
actinolite (brown)										
actinolite (green)		20	10	10	5	5	5	10	5	10
almandine										
epidote					5					
hornblende		20	30	5		20	20	20	10	10
idocrase	90	40	30	40	25	75	70	65	75	70

SAMPLE

DBW-1	DBW-2	DBE-6	DBE-14	DBE-18	UBE-3	UBE-4	UBE-8	UBE-10	SHW-0
-------	-------	-------	--------	--------	-------	-------	-------	--------	-------

#120 Mesh - 0.50A

NON-HEAVIES

miscellaneous

zircon

rutile (yellow-brown)

rutile (red-brown)

kyanite

black opaques

clinopyroxene	10				5					
rounded blue-green										
biotite + chlorite		10			5		5			
actinolite (clear)										
actinolite (brown)		5		20		20	5		10	
actinolite (green)		30	5	30	10	20	10	5	10	15
almandine	25	5	25	5	25	10	10	10	10	30
epidote				10	5	10		5		
hornblende	15	40	50	30	30	20	45	40	30	25
idocrase	50	10	20	15	20	20	25	40	40	30

SAMPLE

DBW-1

DBW-2

DBE-6

DBE-14

DBE-18

UBE-3

UBE-4

UBE-8

UBE-10

SHW-0

#120 Mesh - 0.75A

NON-HEAVIES

miscellaneous

zircon

rutile (yellow-brown)

rutile (red-brown)

kyanite

5

black opaques

clinopyroxene 20 5 5 5

rounded blue-green 10 10

biotite + chlorite 5 5 5

actinolite (clear)

actinolite (brown) 20 20 5 10 20 30 5 20 20

actinolite (green) 10 30 10 25 20 30 30 10 10 15

almandine

epidote 30 40 40 60 60 40 40 65 60 25

hornblende 25 30 10 10 25

idocrase 15

SAMPLE

DBW-1

DBW-2

DBE-6

DBE-14

DBE-18

UBE-3

UBE-4

UBE-8

UBE-10

SHW-0

#120 Mesh - 1.0A

NON-HEAVIES

X

miscellaneous

zircon

rutile (yellow-brown)

rutile (red-brown)

5

kyanite

black opaques

clinopyroxene

30

10

10

X

rounded blue-green

10

20

15

20

20

30

biotite + chlorite

10

actinolite (clear)

10

10

20

5

X

actinolite (brown)

actinolite (green)

10

30

10

10

20

almandine

epidote

50

60

70

60

70

60

80

70

70

hornblende

5

idocrase

SAMPLE

DBW-1

DBW-2

DBE-6

DBE-14

DBE-18

UBE-3

UBE-4

UBE-8

UBE-10

SHW-0

X = Heavy mineral percentage could not be estimated due to an abundant light mineral contamination. X indicates mineral present. No percentage estimate could be made.

#120 Mesh - 1.30A

<u>NON-HEAVIES</u>			X	X		X	X	X	X	X
miscellaneous	10							X		
zircon										10
rutile (yellow-brown)	20		X							
rutile (red-brown)					20	X				40
kyanite										
black opaques										
clinopyroxene					10					
rounded blue-green				X				X		
biotite + chlorite										
actinolite (clear)				X						
actinolite (brown)										
actinolite (green)		20	X			X	X			40
almandine										
epidote	70	80		X	70					10
hornblende										
idocrase										

SAMPLE

DBW-1

DBW-2

DBE-6

DBE-14

DBE-18

UBE-3

UBE-4

UBE-8

UBE-10

SHW-0

X = Heavy mineral percentage could not be estimated due to an abundant light mineral contamination. X indicates mineral present. No percentage estimate could be made



#120 Mesh - >1.30A

<u>NON-HEAVIES</u>	X	X	X	X	X	X	X	X	X	X
miscellaneous										
zircon	40		30		50					
rutile (yellow-brown)										
rutile (red-brown)	20	X	60	X	30	X	X	70		40
kyanite	10		10	X		X	X	30	X	60
black opaques										
clinopyroxene										
rounded blue-green										
biotite + chlorite										
actinolite (clear)										
actinolite (brown)										
actinolite (green)										
almandine										
epidote										
hornblende										
idocrase										

SAMPLE

DBW-1 DBW-2 DBE-6 DBE-14 DBE-18 UBE-3 UBE-4 UBE-8 UBE-10 SHW-0

X = Heavy mineral percentage could not be estimated due to an abundant light mineral contamination. X indicates mineral present. No percentage estimate could be made.